Journal of Medicinal Chemistry

Design and Synthesis of Clinical Candidate PF-06751979: A Potent, Brain Penetrant, #-site amyloid precursor protein cleaving enzyme 1 (BACE1) Inhibitor Lacking Hypopigmentation

Brian T. O'Neill, Elizabeth M. Beck, Christopher R. Butler, Charles E. Nolan, Cathleen Gonzales, Lei Zhang, Shawn D Doran, Kimberly Lapham, Leanne M Buzon, Jason K Dutra, Gabriela Barreiro, Xinjun Hou, Luis A Martinez-Alsina, Bruce N. Rogers, Anabella Villalobos, John C. Murray, Kevin Ogilvie, Erik A. LaChapelle, Cheng Chang, Lorraine F Lanyon, Claire M. Steppan, Ashley Robshaw, Katherine Hales, Germaine G. Boucher, Karamjeet Pandher, Christopher Houle, Claude W. Ambroise, David Karanian, David Riddell, Kelly R. Bales, and Michael A. Brodney

J. Med. Chem., **Just Accepted Manuscript** • DOI: 10.1021/acs.jmedchem.8b00246 • Publication Date (Web): 03 Apr 2018

Design and Synthesis of Clinical Candidate PF-06751979: A Potent, Brain Penetrant, β-site amyloid precursor protein cleaving enzyme 1 (BACE1) Inhibitor Lacking Hypopigmentation

Brian T. O'Neill,[2] Elizabeth M. Beck,[1] Christopher R. Butler,[1] Charles E. Nolan,[4] Cathleen Gonzales,[4] Lei Zhang,[1] Shawn D. Doran,[3] Kimberly Lapham,[3] Leanne M. Buzon,[2] Jason K. Dutra,[2] Gabriela Barreiro,[1] Xinjun Hou,[1] Luis A. Martinez-Alsina,[2] Bruce N. Rogers,[1] Anabella Villalobos,[1] John C. Murray,[2] Kevin Ogilvie,[2] Erik A. LaChapelle,[2] Cheng Chang,[3] Lorraine F. Lanyon,[6] Claire M. Steppan,[6] Ashley Robshaw,[4] Katherine Hales,[4] Germaine G. Boucher,[5] Karamjeet Pandher,[5] Christopher Houle,[5] Claude W. Ambroise,[4] David Karanian,[5] David Riddell,[4] Kelly R. Bales,[4] and Michael A. Brodney*[,1]

[1]Medicine Design, Medicinal Chemistry, Pfizer Inc., Cambridge, MA 02139, USA; [2]Medicine Design, Medicinal Chemistry, Pfizer Inc., Groton, CT 06340, USA; [3]Medicine Design, Pharmacokinetics, Dynamics and Metabolism, Pfizer Inc., Groton, CT 06340, USA; [4]Internal Medicine, Pfizer Inc., Cambridge, MA 02139, USA; [5]Drug Safety Research and Development, Pfizer Inc., Groton, CT 06340, USA; [6]Discovery Sciences, Primary Pharmacology, Pfizer Inc., Groton, CT 06340, USA;

RECEIVED DATE (to be automatically inserted after your manuscript is accepted if required

Keywords: BACE1, BACE2, hypopigmentation, depigmenation phenotype, PMEL17, Thiazole. PF-06751979.

ABSTRACT

A major challenge in the development of β-site amyloid precursor protein cleaving enzyme 1 (BACE1) inhibitors for the treatment of Alzheimer's disease is the alignment of potency, drug-like properties, and selectivity over related aspartyl proteases such as Cathepsin D (CatD) and BACE2. The potential liabilities of inhibiting BACE2 chronically has only recently begun to emerge as BACE2 impacts the processing of the premelanosome protein (PMEL17) and disrupts melanosome morphology resulting in a depigmentation phenotype. Herein we describe the identification of clinical candidate PF-06751979 (**64**) which displays excellent brain penetration, potent in vivo efficacy, and broad selectivity over related aspartyl proteases including BACE2. Chronic dosing of **64** for up to 9-months in dog did not reveal any observation of hair coat color (pigmentation) changes and suggests a key differentiator over current BACE1 inhibitors that are non-selective against BACE2 in later stage clinical development.

Introduction

Alzheimer's disease (AD) pathology is characterized by the presence of extracellular plaques in the hippocampal and cortical regions of the brain, accompanied by intraneuronal neurofibrillary tangles and extensive neuronal loss. Proteolytic cleavage of the amyloid precursor protein (APP) by β-site amyloid precursor protein cleaving enzyme 1 (BACE1), a

member of the aspartyl protease family of enzymes, takes place within the endosome at low pH, generating a soluble N-terminal ectodomain of APP (sAPPβ) and C-terminal fragment (C99).[1] Subsequent cleavage of the membrane-bound C99 fragment by γ-secretase liberates the various amyloid-β (Aβ) peptide species, of which $Aβ_{40}$ and $Aβ_{42}$ are the predominant forms.[2] A number of mutations in APP, near the BACE1 cleavage site have been reported that either increase Aβ generation and are associated with early-onset AD, or decrease Aβ generation and protect against late-onset AD.[3-4] Therefore, limiting the generation of Aβ through inhibition of BACE1 is an attractive approach for the treatment of Alzheimer's disease (AD) and is being intensely pursued by the pharmaceutical industry.[5-6]

Despite the considerable efforts to understand the impact of inhibiting BACE1, the physiological consequences of inhibiting BACE2 has only recently begun to emerge. The expression pattern of BACE2 is very low in brain and much greater in peripheral tissues.[7] Identifying and understanding the role of BACE2 substrates and their inhibition is important from an off-target perspective. Recently identified BACE2 substrates include transmembrane protein 27 (TMEM27) and the pigment cell-specific melanocyte protein (PMEL17). In the case of TMEM27, which is robustly expressed in pancreatic β-cells, inhibition of BACE2 may actually increase β-cell mass and improve glucose tolerance in conditions of insulin resistence.[8] On the other hand, disruption of PMEL17 processing in pigment cells, due to BACE2 knockdown, has profound effects on the formation of physiologically important, non-pathologial amyloid fibers necessary for proper sequestration of melanin and ultrastuctural integrity of melanosomes.[9-11] Genetic mutation of BACE2 in zebrafish through zinc finger nuclease-mediated genome editing generates a melanocyte migration phenotype, while failing to generate any semblance of a hypomyelination phenotype seen with BACE1 silencing.[12] Insights into the

mechanism of this melanocyte migration phenotype comes from PMEL knockdown studies in zebrafish retinal pigment epithelium, demonstrating a failure of cylindrical melanosomes to form which consequently prevents the movement of melanosomes into apical processes.[13] In addition, BACE2 KO mice display a hypopigmented phenotype[11], and several non-selective BACE1/2 inhibitors such as AZD3293 (**5**), NB-360 (**6**), and SCH1682496 have shown fur and skin pigment loss in mice or dog following chronic dosing regimens.[14-16]

In recent years, several small molecule BACE1 inhibitors including MK-8931 (**2**), AZD3293 (**5**), E2609, CNP-520, and JNJ-54861911 have advanced into late stage clinical trials (Figure 1).[17-18] This new class of amidine based inhibitors possess excellent BACE1 potency, adequate central nervous system (CNS) penetration, robust lowering of Aβ in the cerebral spinal fluid (CSF) of humans, and overcame ocular toxicity associated with earlier development candidates such as compound **1** likely due to the off-target inhibition of CatD.[19-20] However, the current cohort of clinical development candidates appear to inhibit both BACE1 and BACE2 to a similar degree. This lack of selectivity is consistent with additional inhibitors reported in the literature such as LY-2886721 (**4**), Merck (**3**), and NB-360 (**6**).[15, 21-22] Despite the lack of selectivity over BACE2, we are unaware of any potential safety concerns emerging thus far in late stage clinical trials for the current cohort of Phase 3 molecules. For instance, the dosing of healthy human volunteers for 14-day duration with AZD3293, a non-selective BACE1 inhibitor, showed no signs of hypopigmentation.[14]

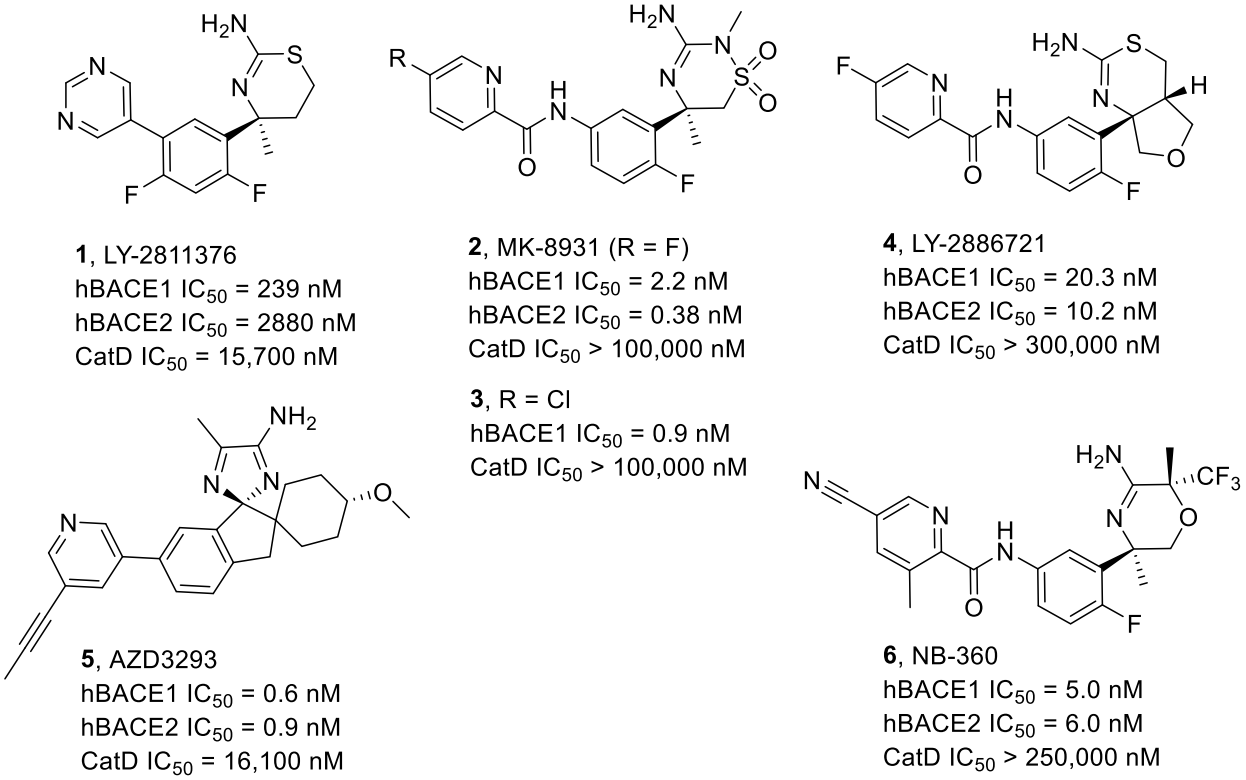

Figure 1: Representative Overview of BACE1 Inhibitors and Selectivity over BACE2

The rational design of BACE1 inhibitors with an improved balance of potency, CNS penetration and reduced safety liabilities has been a major focus within medicinal chemistry groups across the pharmaceutical industry. Balancing the compound attributes has been a direct result of optimizing the underlying physico-chemical properties (pK_a, MW, logD, hydrogen bond donors) and removing undesired structural motifs to increase the probability for compound survival.[23] As BACE1 inhibition typically requires a basic amine for interaction with the catalytic aspartic acids, the optimization of the amidine pK_a has been critical in reducing P-gp mediated efflux and driving central pharmacodynamic responses.[24-27] In addition to reducing efflux, a lower pK_a has been associated with reduced safety liabilities such as inhibition of the IKs channel (hERG) and reduction in potential drug-drug interactions (DDIs).[28-29]

A common strategy to reduce pK_a has been modification of the amidine functionality by strategic placement of an electron withdrawing group such as fluorine (Figure 2).[30] For example, we recently disclosed a novel series of thioamidine-containing BACE1 inhibitors that possess excellent overall properties such as high CNS penetration (C_{ub}/C_{up} = 1), low clearance, reduced hERG inhibition, and low projected DDI.[31] A key design element of the series was strategic incorporation of a pK_a lowering group adjacent to the thioamidine moiety (compound **7** to **8**). The addition of fluorine reduced the pK_a from 7.7 to 7.0, resulting in reduced inhibition of hERG from an IC_{50} of 2.1 μM to 10.1 μM. Janssen and Novartis have described a related strategy for a series of 1,4 oxazine-derived inhibitors that suffered from poor CNS penetration due to high transporter efflux, hERG inhibition, and a weak pharmacodynamics response in brain, as exemplified by compound **9**. Tuning the pK_a of the amidine with a trifluoromethyl group (compound **10**) reduced the pKa from 9.2 to 7.8 with a corresponding decrease in P-gp mediated efflux and an increase in brain penetration.[32] A similar strategy was taken by F. Hoffman-La Roche[30], wherein the modification of the amidine pK_a by incorporation of the fluoro group resulted in a well-balanced analog with robust central lowering of Aβ due to increased exposure in brain (compound **12** vs. **11**).

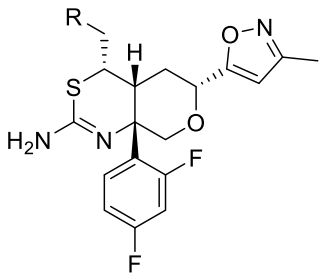

7, R = H
BACE1 IC_{50} = 74 nM
pKa = 7.7
P-gp Er = 1.7
hERG IC_{50} = 2.1 μM

8, R = F
BACE1 IC_{50} = 53 nM
pKa = 7.0
P-gp Er = 1.6
hERG IC_{50} = 10.1 μM

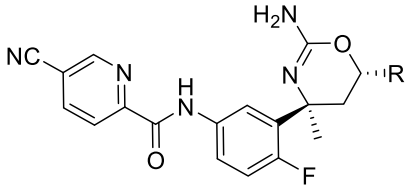

9, R= H
BACE1 IC_{50} = 51 nM
pKa = 9.7
P-gp Er = 14.8
hERG inh = 88% @ 10 uM

10, R = CF_3
BACE1 IC_{50} = 12 nM
pKa = 7.0
P-gp Er = 1.9
hERG inh = 75% @ 10 uM

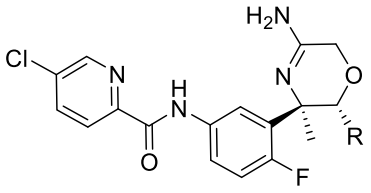

11, R = H
BACE1 IC50 =IC_{50} 22 nM
pKa = 9.2
brain/plasma Kp = 0.1

12, R = F
BACE1 IC_{50} = 12 nM
pKa = 7.8
brain/plasma Kp = 0.65

Figure 2. The Impact of Reduced pK_a on Key Properties

Despite the advances in aligning properties with potency, efforts in designing BACE1 inhibitors with selectivity over BACE2 have been minimal to date. A notable exception was the incorporation of unique substituents into the S3 pocket that take advantage of greater flexibility in the 10s loop for BACE1 over BACE2 as reported by F. Hoffman-La Roche.[30] In this paper, we describe efforts to modulate the basic pK_a of the thioamidine moiety (represented by **13**) through modification of the P1 substituent while simultaneously obtaining selectivity over BACE2 by modification of the inhibitor in the P3 and flap regions of BACE1 (represented by **14**). We had previously described a stereospecific incorporation of electron withdrawing fluoro or trifluoromethyl groups on the thioamidine backbone core that also reduced the pK_a of this functionality but that required lengthy complex synthesis and failed to deliver molecules with

improved selectivity over BACE2.[31] The present synthesis and characterization of thiazole containing inhibitors (**14**) has resulted in the identification of compound **64**, a clinical candidate with an excellent balance of BACE1 potency, CNS penetration, robust central Aβ lowering, long predicted human half-life, and selectivity over BACE2 as determined by in vitro binding, cellular/tissue pigmentation models, and long-term safety studies.

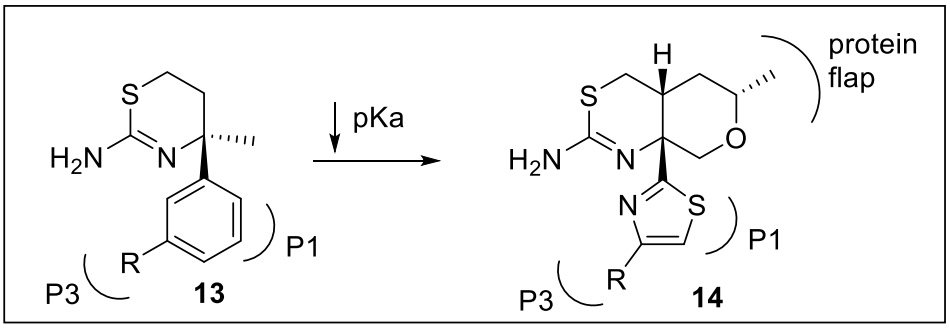

Figure 3: Design Strategy for Modulating pK_a and Selectivity over BACE2

Results

We previously described a strategy to add aryl and heteroaryl substituents by straightforward Lewis acid catalyzed anion addition to isoxazoline template **15** followed by elaboration to the thioamidines **40**-**47** (Scheme 1).[31] The chirality of the isoxazoline **15** originates from commercial propylene oxide or a commercial homoallylic alcohol (*S*)-pent-4-en-2-ol that controls the creation of two additional chiral centers. The compact ring structure contributes to the high selectivity of the anion addition to the convex face. Following addition, the isoxazoline ring **16**-**23** can be reductively cleaved to amino-alcohols **24**-**31** and the thioamidine ring formed by addition of an acylisothiocyanate followed by ring closure to thioamides **32**-**39**. Deprotection in basic methanol provided the desired analogs **40**-**47** that were assessed for potency, pK_a and physical properties.

Scheme 1. Synthesis of aryl or heteroaryl containing thioamidines

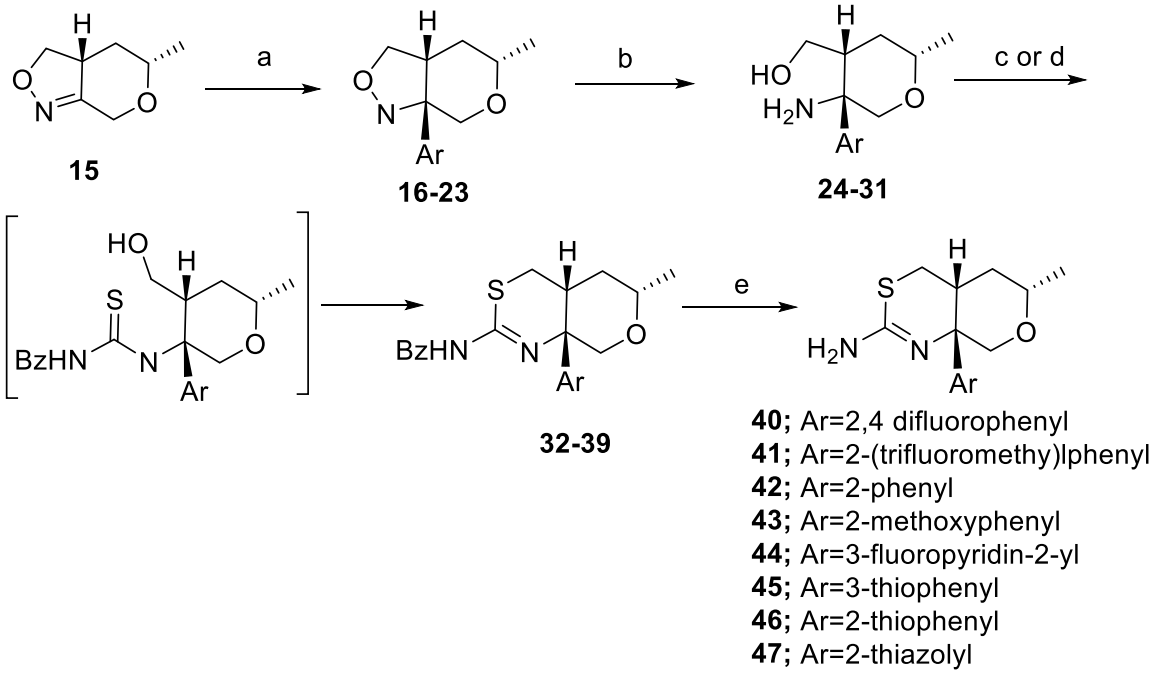

Reagents and conditions: (a) ArX, 2.5M n-BuLi in hexane, BF_3-Et_2O, toluene:THF (10:1 v:v), -70°C then add 1**5** in toluene:THF (10:1 v:v), 25-68%; (b) H_2, Raney nickel, ethanol or IPA/THF, 50 °C; (c) 2eq BzNCS, ethyl acetate, r.t. to 90 °C (no isolation of thiourea intermediate); (d) BzNCS, ethyl acetate, r.t., 2.5h (isolate thiourea), then BzNCS, ethyl acetate, 90 °C, 26-66%; (e) DBU, methanol, 70 °C, 15-74%.

In addition, we prepared an array of analogs bearing various P1 moieties in a parallel medicinal chemistry fashion illustrated in Scheme 2. Starting with a diverse set of amino alcohols **48**, that were prepared using the procedure described above, the desired analogs **50** were obtained in two distinct steps followed by high throughput purification (Scheme 2). The success rate for this parallel effort was 89% (40/45). The sum total of these efforts led us to the thiazole series with the desired pK_a and physical property profile.

Scheme 2. Array Chemistry to Generate P1 Aryl Groups

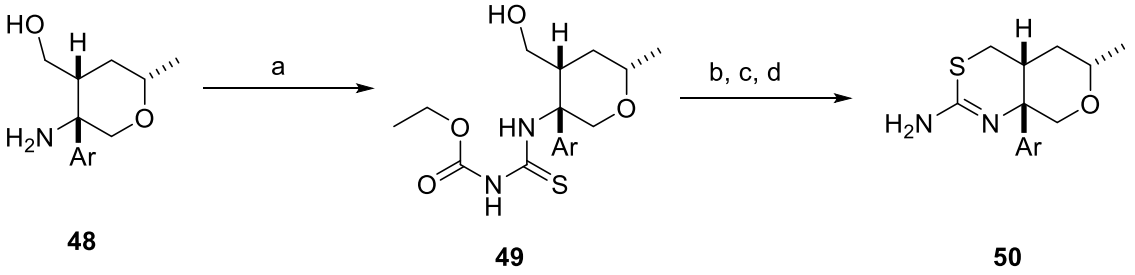

48 **49** **50**

Reagents and conditions: (a) $EtO_2CN=C=S$ / THF then Scavenging Resin; (b) MeTHF / H_2O / TFA, 60 ^oC, 1h; (c) 120 ^oC, 4h (d) high throughput purification.

In order to fully evaluate the SAR of the thiazole containing series, we desired a robust procedure to prepare the thiazole bromide **54** which could serve as a viable intermediate for exploration of the P3 subpocket (Scheme 3). Selective C-2 halogen metal exchange of 2,4-dibromothiazole followed by addition to **15** provided compound **51** which was poised for elaboration into the P3 region. Alternatively, addition of the anion from halogen metal exchange of 2-bromothiazole (or reductive removal of the previously mentioned C-4 bromide) afforded a substrate that could be metalated at C-5 directed by the proximal sulfur. Due to the presence of the bromide, an alternative method was required for selective cleavage of the N-O bond. Reduction with a Mo (0) hexacarbonyl complex followed by a reductive work up afforded the amino alcohol **52** without loss of the bromide. Addition of benzoyl isothiocyanate formed the thiourea **53**, which upon activation of the alcohol with Ghosez's reagent[33] yielded the key thioamidine intermediate **54**.

Scheme 3: Synthesis of Bromo-Thiazole 54

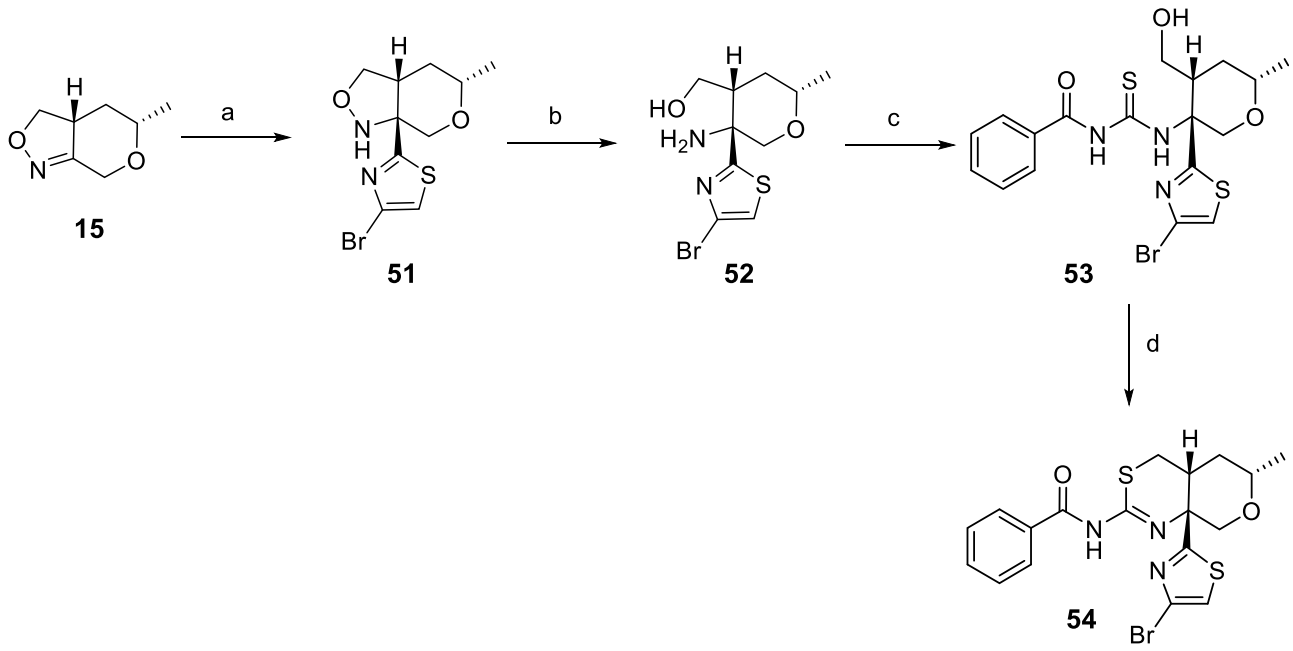

Reagents and conditions : (a) 2,4-dibromo-thiazole, 2.5M n-BuLi in hexane, BF_3-Et_2O, toluene:THF (10:1 v:v), -70 °C then add 1**5** in toluene:THF (10:1 v:v), 1h, 85%; (b) $Mo(CO)_6$, CH_3CN, H_2O, $NaBH_4$, 70 °C, 1h, 95%; (c) benzoyl isothiocyante, CH_2Cl_2, rt, 24h, 66%; (d) Ghosez's reagent, CH_2Cl_2, rt, 1h, 77%.

The elaboration of the bromide **54** into the key thiazole-amides **56**-**68** and **70**-**71** is shown in Scheme 4. The bromide was transformed to an amine and eventually to amides **55** by one of several routes described below. Our initial protocol involved a copper-catalyzed azide addition in the presence of ascorbic acid that conveniently reduced the azide *in situ* to an amine. Acylation of the amine yielded the desired amides **55** which readily deprotected in basic methanol to afford thioamidines **56**-**68**. Amides **55** were also available via direct palladium catalyzed amidation. For target **69**, the bromide of **54** was removed via zinc reduction and a new anion was then formed at C-5 with butyl lithium. The anion was then quenched with CO_2 to give the acid, which by suitable manipulation was coverted to a series of amides **69**. Deprotection afforded the C-5 amides **70** and **71** in good yield.

Scheme 4. Elaboration of Bromide 54 into Amide Analogs

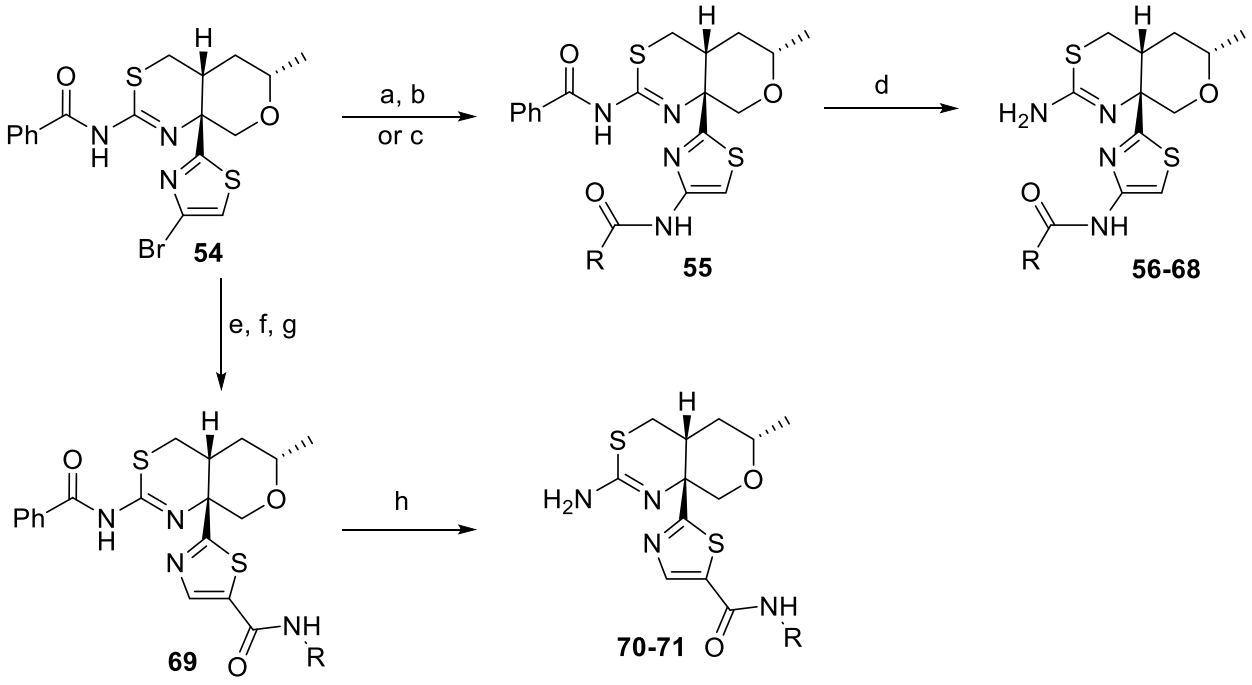

Reagents and conditions : (a) *trans*-N,N'-Dimethylcyclohexane-1,2-diamine, NaN_3, H_2O, Sodium-L-ascorbate rt then CuI, 70 ^oC, 2h, 47%; (b) HATU, R-CO_2H, DMF, rt, 1h or 2,4,6-Tripropyl-1,3,5,2,4,6-trioxatriphosphinane 2,4,6-trioxide, pyridine or Et_3N, rt, 12-24h; (c) $ArC(O)NH_2$, Pd_2dba_3, *t*BuBrettPhos, LiO-*t*-Bu, 2-MeBuOH, 95 ^oC, 1h, 61%; (d) Methoxyl-amine, HCl, pyridine, 50^oC, 16h or DBU, methanol, 70 °C; (e) Zn dust, THF, aq NaOH, 40 ^oC, 16h, 86%; (f) *n*-BuLi, THF, CO_2, -78 ^oC, 1h, 95%; (g) HATU, R-NH_2, DMF; (h) $MeNH_2$, EtOH, rt, 2-4h.

A synthesis of **64** on intermediate scale (25 g) is illustrated in Scheme 5. The Buchwald coupling conditions arose from the need to replace the azide coupling on scale and provided for a mild, selective deprotection with HCl. Amide formation with **72** was easily accomplished through coupling with a variety of agents such as HATU or T_3P. The final debenzoylation of **73** was delicate due to interference from the thioamidine. This was achieved in high yield using basic methanol.

Scheme 5. Synthesis of Compound 64

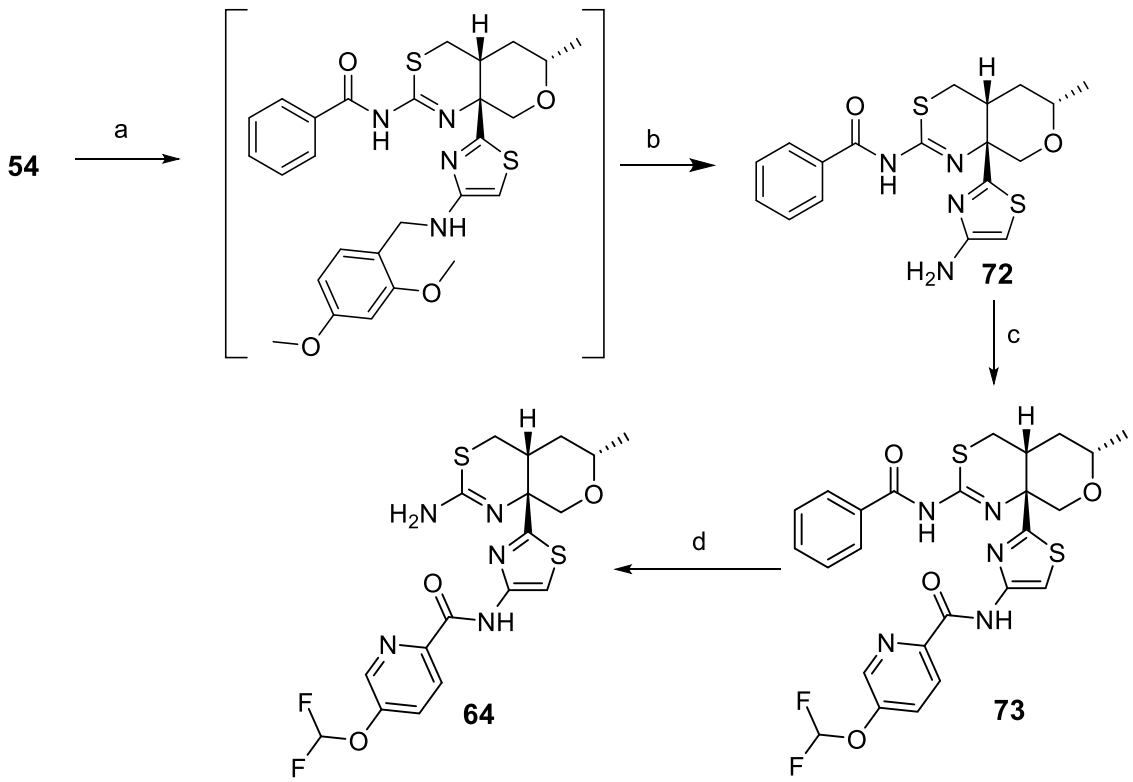

Reagents and conditions : (a) 2,4-dimethoxy benzyl amine, $Pd_2(dba)_3$, *t*-BuONa, *t*-BuXPhos, 70 °C, 1h then HCl, H_2O, rt, 1h, 70%; (c) HATU, $iPrNEt_2$, CH_3CN, 5-(difluoromethoxy)picolinic acid, rt, 4h, 81%; (d) DBU, methanol, 70 °C, 1.5h, 55%.

Discussion and Conclusions

Our primary strategy to modulate the basic pK_a of the amidine was accomplished by a systematic exploration of the P1 region (Table 1). Our goal was to identify those aromatic substituents or heteroaryl replacements that inherently reduced pK_a to an optimal range of 6.5-7, an optimal range to balance BACE1 potency with overall alignment of properties. This strategy would obviate the need to fluorinate the core and reduce synthetic complexity. In previous SAR, we had optimized the fluorination pattern on the P1 substituent for BACE1 potency and the optimal substitution pattern was the 2,4 difluoro analog **40** which had a basic pK_a of 8.1.[31] As

anticipated, removal of the fluorines produced analog **42** with weaker BACE1 potency in a fluorescent polarization (FP) assay and a higher pK_a (8.8). Attempts to further reduce the pK_a with an ortho substituted aryl group (**41** or **43**) resulted in a similar potency and pK_a relative to unsubstituted phenyl analog **42**. We next investigated installation of a 2-pyridyl group **(44**) in P1 and were surprised that the pK_a increased to 8.6 relative to analog **40**. Further modification to 5-membered ring heteroaryls such as thiophenes **45** or **46** resulted in reasonable BACE1 potency but only the 2-thienyl analog **46** reduced the pK_a to the desired range. This raised the possibility that a thiazole in P1 would further reduce the pK_a of the amidine due to the greater electron withdrawing nature relative to thiophene. We were gratified to find that thiazole **47** resulted in a BACE1 inhibitor with a pK_a of 7 and displayed reasonable cellular activity (IC_{50} = 2.05 μM), low P-gp mediated efflux, high passive permeability, and low clearance from human liver microsomes. Despite the drop in potency for thiazole **47**, we anticipated that appropriate substitution on the thiazole ring would make favorable interactions with protein residues to improve potency without increasing pK_a. Across the P1 variations prepared in Table 1, each analog displayed weak activity against CatD and the hERG channel.

Table 1. Modification of the P1 Aryl Group

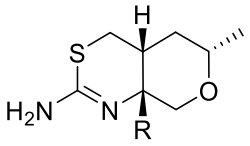

Cpd	R	BACE1 FP IC_{50} (μM)[a]	CatD FP IC_{50} (μM)[b]	BACE1 WCA IC_{50} (μM)[c]	MDR Er[d]	RRCK ($x10^{-6}$ cm/s)[e]	HLM (mL/min/kg)[f]	pK_a (hERG IC_{50}, μM)

40	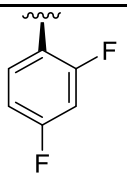	0.704	> 72	0.039	1.19	17.5	< 8	8.1 (15.8)
41	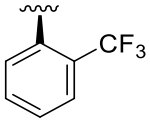	> 79.3	> 100	2.92	1.62	17.9	< 8	8.8 (55.4)
42	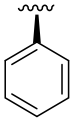	1.33	> 100	0.82	1.64	19.7	< 8	8.8 (85.7)
43	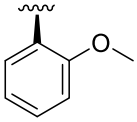	6.06	>100	0.85	4.3	8.5	<8	9.1 (85.6)
44	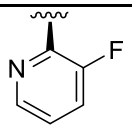	9.16	> 100	0.25	2.4	7.6	< 8	8.6 (> 100)
45	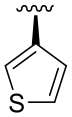	5.17	> 100	0.17	1.4	13.2	< 8	8.4 (39.9)
46	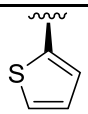	1.92	> 98	0.11	1.1	24.1	< 8	7.9 (>100)
47	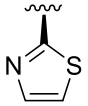	23.9	> 64	2.05	1.2	13.6	< 8	7.0 (> 100)

[a]IC_{50} values obtained from BACE1 Fluorescent Polarization (FP) Assay. [b]IC_{50} values obtained from CatD FP Assay. [c]IC_{50} values obtained from BACE1 Whole-Cell Assay (WCA). [d]Ratio from the MS-based quantification of apical/basal and basal/apical transfer rates of a test compound at 2 μM across contiguous monolayers from MDR1-transfected MDCK cells. [e]RRCK–MDCK cells used to evaluate passive permeability [f]Hepatic clearance predicted from in vitro human microsomal stability study.

A key strategy to improve potency of thiazole **47** was installation of an aryl amide moiety to engage the back-bone carbonyl of Gly230 while simultaneously placing an aryl substitutent into the lipophilic S3 pocket. To guide the optimal placement of the amide group, we modeled thiazole **47** using a co-crystal structure (PDB Code: 5CLM) (Figure 4a and 4b). Because of a wider bond angle (150^o vs 131^o) induced by the sulfur atom in the thiazole ring, the vector off the 5-position of the thiazole is not ideal for aligning the amide functionality within the P1-P3

region of the protein (Figure 4a). On the other hand, the 4-position of the thiazole afforded a more favorable angle for amide introduction (Figure 4b). Structural optimizations of the two proposed phenyl amides demonstrated that 5-substituted phenyl amide would not make the key hydrogen bond (Figure 4C), yet the 4-substituted phenyl amide would occupy the S3 pocket nicely and make the desired hydrogen bond interaction to Gly230 (Figure 4d).

Figure 4. Molecular Modeling of Thiazole Regioisomers

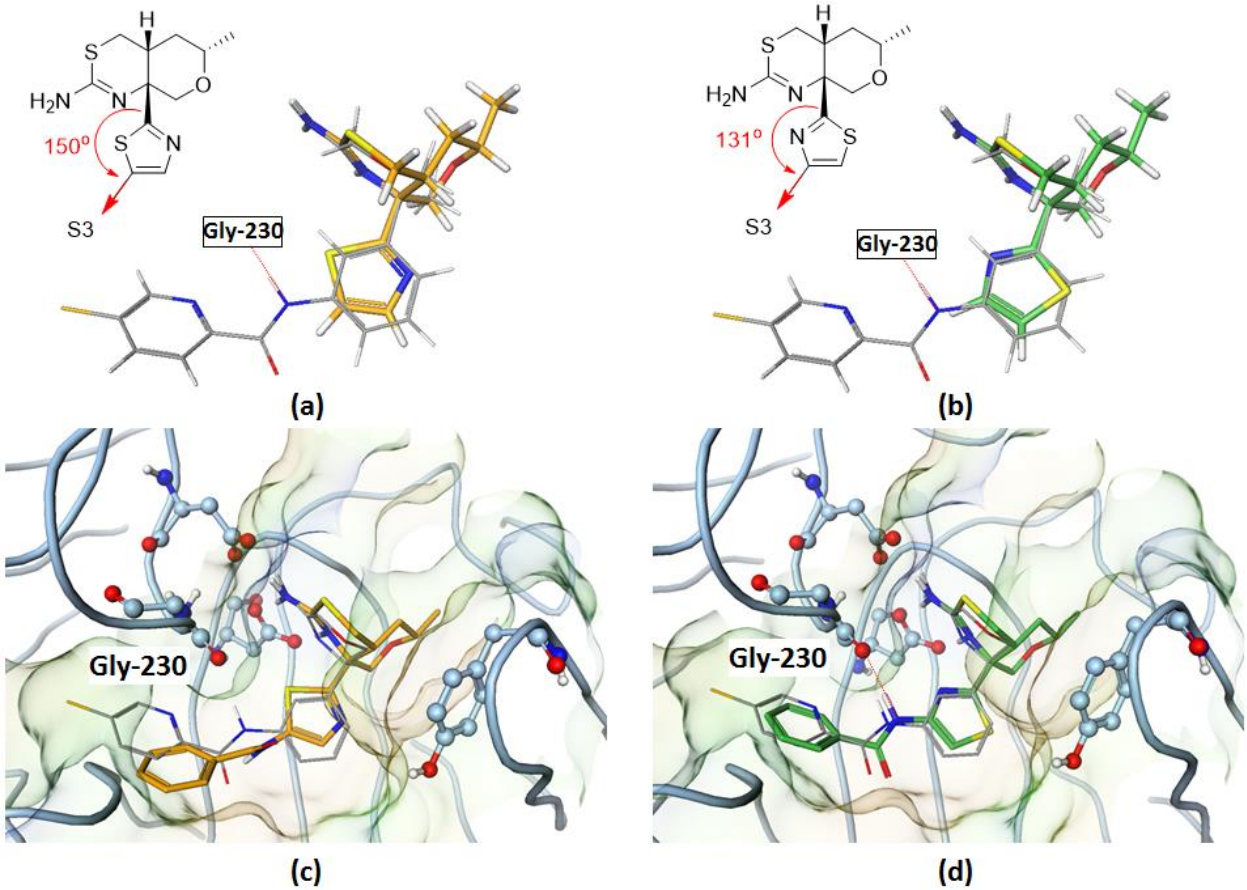

Vectors to reach S3 pocket from 4 or 5-position of thiazole **40** aligned in co-crystal structure (thin grey, PDB: 5CLM). Panels a and b: the initial vector of 4- or 5-substitutions and Panels c and d: the modeled phenyl amides reaching S3 pockets.

We also evaluated the conformational energy profile of the thiazole orientation of thiazole **47** to assess the potential energy penalty as different substitutions were introducted into

P3. The torsion of amidine and thiazole bond was subjected to a conformational analysis using TetraChem with B3LYP/6-31G** in gas phase.[34] We noticed that the "trans" conformation (corresponding to Figure 4a) is at the lowest energy potential well, whereas the "cis" conformation (corresponding to Figure 4b) is only at a slightly higher energy state (Figure 5), giving us assurance that any conformational penalty of 4- vs. 5- substituted thiazoles would be tolerated without a significant loss of potency.

Figure 5. Energy Confirmations for Thiazole 47

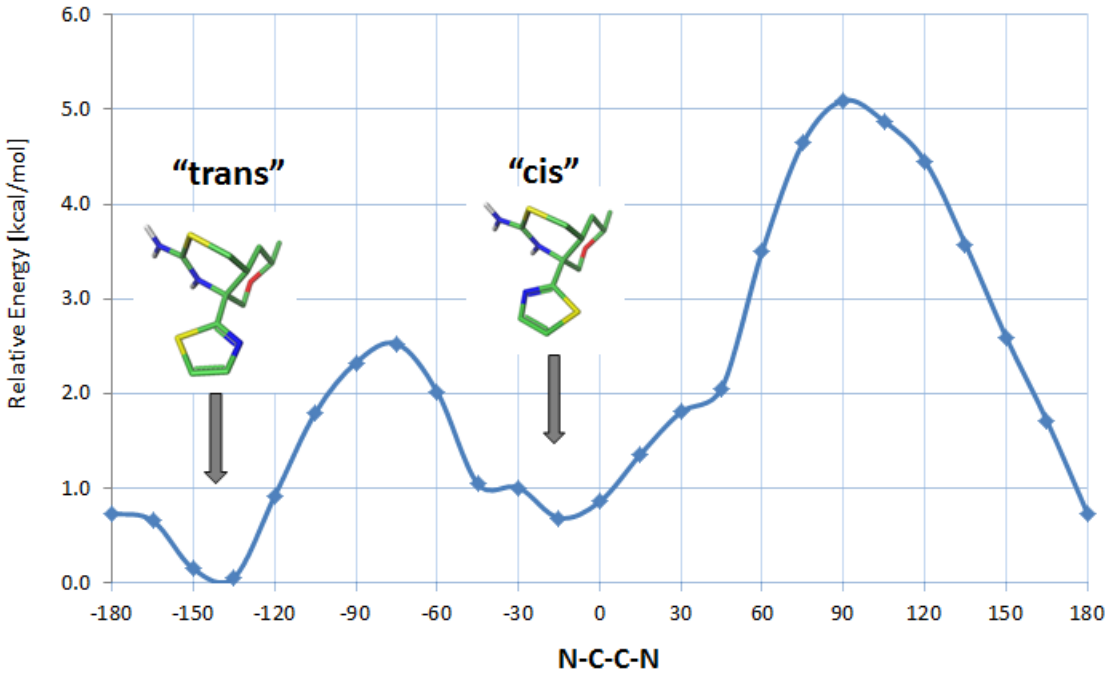

Since the conformational energies for thiazole **47** were relatively comparable, we modeled four variations of aryl-amide linkers (**74**-**77**) to asses and rank-order their potential binding to BACE1 (Figure 6, Panel A). Structure minimization using a variant of MM-GB/SA calculations (PLIERS[35]) showed that 4-pheny amide **76** and 5-phenyl reversed amide **75** bound preferably based on intermolecular energy, desolvation, and ligand strain energy components (Figure 6, Panel B). An important consideration is the angle between the bicyclic core and the amide group on the thiazole ring. The requirement to reverse the amide confirmation from **74** to

75 allowed for the optimization of the amide vector to P3 and alignment of a hydrogen bond between Gly230 and the amide.

Figure 6 (Panel A-B). Aryl-amide linkers designed to reach S3 pocket with potential to make H-bond to Gly230 backbone carbonyl.

Panel A: Amide regioisomers on the Thiazole Ring

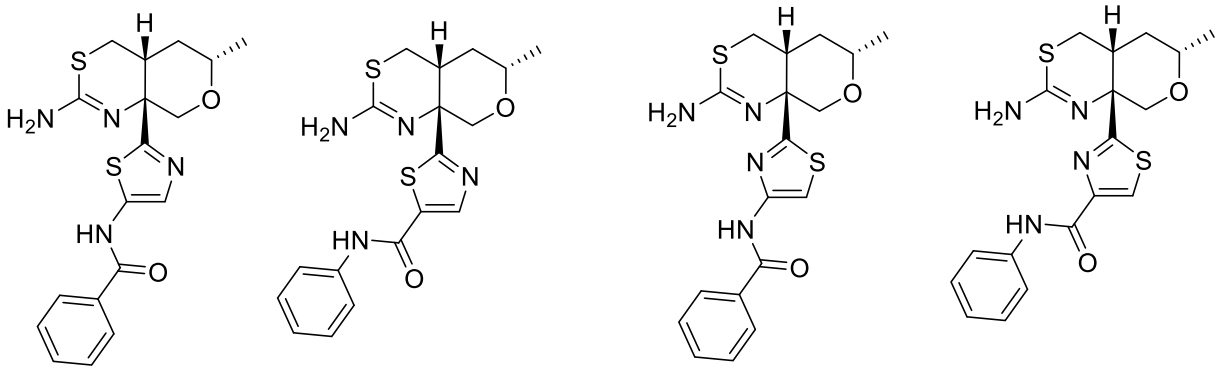

74 **75** **76** **77**

Panel B: PLIERS calculations for analogs **74-77**. Total energy (dE, kcal/mol) is the sum of all components in the table. Only relative dE are are significant for rank ordering of these molecules.

Molecule	Electrostatic Interaction (kcal/mol)	van der Waals Interaction (kcal/mol)	GB/SA Desolvation (kcal/mol)	Ligand Conformational Strain (kcal/mol)	Total dE (kcal/mol)
74	-104.6	-33.1	76.9	8.3	-52.5
75	-109.4	-33.7	76.1	3.2	-63.8
76	-124.1	-37.0	93.4	2.6	-65.1
77	-123.4	-35.7	94.0	4.1	-61.0

As the amido-thiazoles **75** and **76** both appeared to satisfy the key parameters for binding, synthesis and profiling of analogs **70-71** and **56-57** was initiated which contained a methoxy group for additional potency (Table 2). For each case, molecular modeling suggested that a meta or para substituted aryl group was optimal for BACE1 activity. We were gratified to find that

both analogs **56** and **70** showed considerable binding and cellular potency improvement relative to the parent thiazole **47** while maintaining a similar pK_a (6.8 and 6.5 respectively). Both analogs exhibited low clearance in human liver microsomes and high passive permeability. Unfortunately, the increase in hydrogen bond donor (HBD) count and molecular weight increased the P-gp mediated efflux liability. Modification of the P3 aryl ring to a pyridine ring has been previously demonstrated to reduce P-gp mediated efflux due to the potential for an intramolecular hydrogen bond between the amide NH with nitrogen of the pyridine ring.[31] In an attempt to understand the impact of the pyridine ring on efflux and lower logD, we designed and profiled analogs **71** and **57**. For each matched molecular pair, the modification from phenyl to pyridine improved potency, lowered P-gp mediated efflux, and reduced hERG binding without negatively impacting clearance in human microsomes relative to the phenyl analogs **56** and **70**. Unfortunately, cross-species plasma instability with 5-amido substituted thiazoles **70** and **71** precluded further evaluation for efficacy or safety due to rapid turnover in rodent plasma. Fortunately, thiazole-amides **56** and **57** were stable in cross species plasma stability assays.

Table 2: Profile for Aryl-Amides 52-55

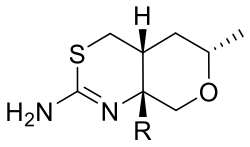

Molecule	R	BACE1 FP IC_{50} (μM)[a]	CatD FP IC_{50} (μM)[b]	BACE1 WCA IC_{50} (nM)[c]	MDR Er[d]	RRCK ($x10^{-6}$ cm/s)[e]	HLM (mL/ min /kg)[f]	pK_a; (hERG IC_{50} μM)	Rat; Human Plasma stability T1/2 (min)

70	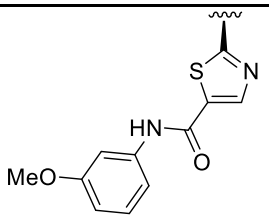	0.27	> 100	0.11	8.9	14.7	<11.1	6.5, 6.2	20; >360
71	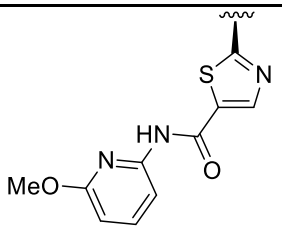	0.11	> 100	0.033	6.4	13.5	< 11.3	6.5; 4.8	2; >360
56	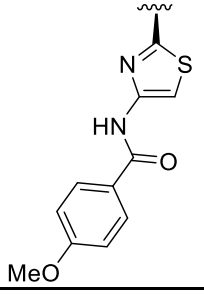	0.99	> 97	0.034	4.4	12.9	< 8	6.9; 18.4	>360; >360
57	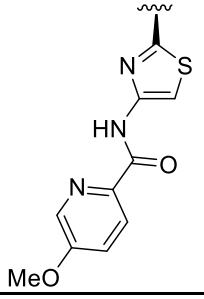	0.26	> 95	0.014	1.8	15.7	< 8	6.9; 13.1	>360; >360

[a]IC_{50} values obtained from BACE1 FP Assay. [b]IC_{50} values obtained from CatD FP Assay. [c]IC_{50} values obtained from BACE1 Whole-Cell Assay (WCA). [d]Ratio from the MS-based quantification of apical/basal and basal/apical transfer rates of a test compound at 2 μM across contiguous monolayers from MDR1-transfected MDCK cells. [e]RRCK–MDCK cells used to evaluate passive permeability [f]Hepatic clearance predicted from in vitro human microsomal stability study.

With the 4-amido subsitutent on the thiazole ring providing a vector to probe potency and selectivity by filling the P3 pocket, we profiled a range of 6-membered ring heteroaryl groups such as pyridines and pyrazines containing a substituent in the 5-position (Table 4). In each case, the regiochemistry of the heteroaryl ring placed a nitrogen atom *ortho* to carbonyl of the

amide as this was previously reported to both lock the confirmation of the amide and reduce P-gp mediated efflux. With suitable binding assays in place, pyridine **58** gave comparable potency and selectivity over CatD to the methoxy analog **56** while maintaining the low clearance, plasma stability, and low P-pg efflux ratio (Table 3). As further potency improvements were needed, we modified the fluoro substituent to a variety of analogs **60**-**64**. We were gratified to identify chloro, cyano, and difluoromethoxy substitutents improved potency in binding and whole cell (IC_{50} < 10 nM) BACE1 assays relative to fluoro analog **58**. In all cases, clearance was reduced and the compounds showed high passive permeability. A second strategy to improve potency was incorporation of an ortho methyl group resulting in analogs **59** and **65**. Substitued pyrazines (**66-67**) were well tolerated along with a 5-membered ring in P3 such as pyrazole **68**. Using BACE1 and BACE2 FP assays, compounds **60**, **62**, **64**, and **67** displayed the highest levels of selectivity over BACE2 of 5.6, 10, 6.4, and 5-fold respectively. The improved selectivity with larger substituents in the P3 region may be explained by the greater flexibility in this region of the protein relative to the rigid confirmation observed in BACE2. Unfortunately, poor plasma stability was observed with compounds **60** and **66**-**68** which precluded further development.

Table 3

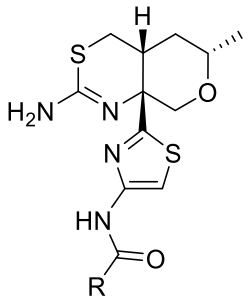

Cpd	**R**	**BACE1; BACE2 FP IC_{50} (nM)[a]**	**CatD FP IC_{50} (µM)[b]**	**BACE1 WCA IC_{50} (nM)[c]**	**MDR Er**	**Rat;Human Plasma stability (min)**	**RRCK (x10^{-6} cm/s)[e]**	**HLM** (mL/min /kg)[f]	**hERG IC_{50} (µM)**

58	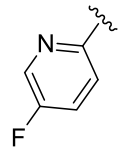	229; 233	>43	23.7	2.5	>360; >360	17.4	< 8	10.7
59	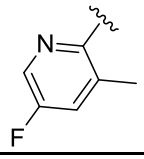	178; 38.9	34.8	26.9	2.8	ND	14.9	<8	17.9
60	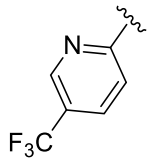	60.2; 338	>300	4.8	2.3	189/360	8.5	9.5	11.7
61	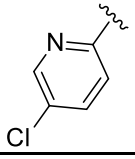	29.1; 21.6	>97	3.8	2.3	>360; >360	19.3	< 11.6	9.0
62	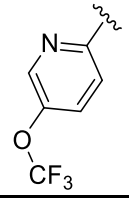	107; 1072	163.6	12.5	2.8	>360; >360	7.4	20.7	10.1
63	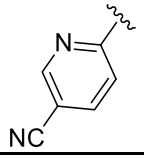	21.8; 60.7	197.6	3.9	2.3	>360; >360	14.4	<8	12.1
64	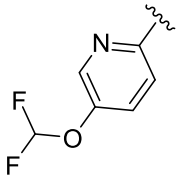	36.9; 238	>95.3	5.1	2.2	>360; >360	12.6	<8	9.9
65	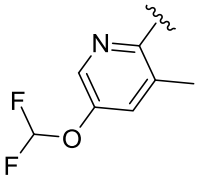	22.8; 70.5	>70.3	2.9	3.0	>360; >360	12.8	<8	9.6
66	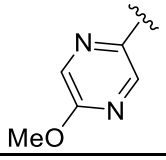	536; 1709	>96.7	47.6	2.1	225; >360	19.5	<8	43

67		72.5; 367	>300	7.2	1.8	45; >360	14.4	<8	23.6
68	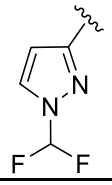	9.3; 3.9	>300	0.64	5.8	250; >360	16.3	< 8	9.3

[a]IC_{50} values obtained from BACE1 FP Assay. [b]IC_{50} values obtained from CatD FP Assay. [c]IC_{50} values obtained from BACE1 Whole-Cell Assay (WCA). [d]Ratio from the MS-based quantification of apical/basal and basal/apical transfer rates of a test compound at 2 μM across contiguous monolayers from MDR1-transfected MDCK cells. [e]RRCK–MDCK cells used to evaluate passive permeability [f]Hepatic clearance predicted from in vitro human microsomal stability study. ND = not determined.

A select group of compounds (**61**, **64**, **65**, **67**) displayed an excellent alignment of properties, potency, and were predicted to have good brain penetration due to the low P-gp mediated efflux as measured in the Borst Cell Line. However, *in vivo* neuro-pharmacokinetics in mouse suggested that all four analogs were brain impaired with C_{ub}/C_{up} values ranging from 0.06 to 0.10 (Table 4). To build a more comprehensive understanding of the transporters limiting brain penetration in rodent, we incorporated a higher expressing P-gp assay from the National Institute of Health (NIH) along with a breast cancer resistant protein (BCRP) assay, an additional transporter highly expressed at the blood-brain barrier. These analogs now displayed a range of P-gp and BCRP mediated efflux which helped to explain the apparent *in vitro* to *in vivo* disconnect. Since the expression of P-gp is highest in rodents and lower in NHP and humans, we anticipated that NHP neuroPK would more accurately reflect brain penetration in humans.[36] In contrast to P-gp, BCRP expression in rodents is lower than NHP and unlikely to contribute to differences in brain penetration when comparing mouse to NHP. To this end, brain penetration studies in NHP were conducted and resulted in much improved C_{ub}/C_{up} values ranging from 0.28 to 0.62 and CSF/C_{up} ranging from 0.39 to 0.76.

Table 4; Mouse vs NHP NeuroPK

Cpd	R^1	Mouse NeuroPK[a] Cub/Cup; CSF/Cup	NHP NeuroPK[a] Cub/Cup; CSF/Cup	Borst MDR Er[b]	NIH MDR Er[b]	BCRP Er[b]
61	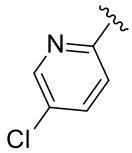	0.06;0.02	0.28;0.39	2.3	11.0	2.75
64	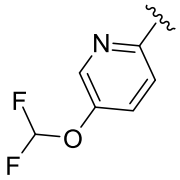	0.10;0.13	0.36;0.47	2.2	20.3	1.4
65	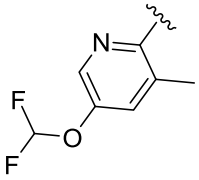	0.07;0.08	0.62; 0.76	3.0	17.7	9.4
67	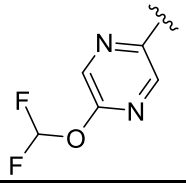	0.06;ND	0.32;0.52	1.8	11.2	4.3

[a]Unbound brain to unbound plasma and CSF to unbound plasma area under the curve (AUC) ratios in mice and non-human primates [b]Ratio from the MS-based quantification of apical/basal and basal/apical transfer rates of a test compound at 2 μM across contiguous monolayers from MDR1or BCRP-transfected MDCK cells.

The in vitro and in vivo PK properties for compounds (**61**, **64**, **65**) are shown in Table 5. All three compounds were characterized by low in vitro clearance in rat, dog and human microsomal systems. As expected based on the low in vitro clearance, compounds **61**, **64** and **65** all exhibited low in vivo clearance in both rats and dogs. All three analogs were predicted to have a long half-life in human (>12 h).

Table 5. In Vitro and in Vivo PK Properties of Representative Compounds

PK Properties	**64**	**61**	**65**

In vitro *h*-Cl_h (mL min^{-1} kg^{-1})[a]	<8	<8	<8
In vitro *r*-Cl_h (mL min^{-1} kg^{-1})[b]	<25	<25	<25
In vitro *d*-Cl_h (mL min^{-1} kg^{-1})[c]	<18	<18	<18
Rat CL (mL/min/kg)[d]	31	10	2.9
Dog CL (mL/min/kg)[e]	1.8	5.5	1.2
Rat bioavailability (%)[f]	33	43	100
Dog bioavailability (%)[g]	49	34	60

[a]Hepatic clearance predicted from in vitro human microsomal stability study. [b]Hepatic clearance predicted from in vitro rat microsomal stability study. [c]Hepatic clearance predicted from in vitro dog microsomal stability study. [cd]Rat plasma clearance determined following a single intravenous bolus dose of 1 mg/kg; [e]Dog plasma clearance determined following a single intravenous bolus dose of 1 mg/kg. [f]Rat bioavailability determined following a single oral dose of either 3 or 5 mg/kg; [g]Dog bioavailabilty determined following a single oral dose of either 1 or 3 mg/kg.

Several compounds satisfied our criteria for advancement but only compound **64** combined excellent potency, modest selectivity (~5.6-fold) over BACE2, weak hERG inhibition, stability in plasma, and high predicted brain penetration. To understand the *in vivo* potency of compound **64**, we assessed the compound against a panel of Aβ endpoints in brain, CSF and plasma in 129/sve mice and dog. The exposure was also measured in these biological compartments in order to understand PK/PD and predict efficacious concentrations (C_{eff}). For mouse studies we used sensitive immunoassays to measure Aβx-42 in brain homogenates, as well as Aβx-40 in CSF (Figure 7, Panel A and B). Acutely, robust lowering of brain Aβ42 persisted in a dose and time dependent manner with maximum inhibition of 56%, peaking at 5 to 7 h post dose. The 80 mg/kg dose did not produce any further reduction beyond the 50 mg/kg dose, but did demonstrate a delayed return to baseline at 14 hours. Acute administration of **64** yielded a robust dose-responsive and time-dependent reduction of CSF Aβx-40 with peak inhibition at 3 hours of >77%. To determine if the reduction in brain and CSF Aβ was

maintained during sustained exposure to **64**, a 5-day sub-chronic study was executed, dosing once daily by subcutaneous (SC) administration (10 or 50 mg/kg/day). Brain and CSF samples were collected on day 5, following the last dose. Compound **64** produced a dose-responsive and time-dependent inhibition of Aβ42 in mouse brain. At the 50 mg/kg/day dose, maximal brain lowering was 63% at 7 to 9 hours (see SI, Figure 1). Administration of **64** (10 or 50 mg/kg/day for 5 days) produced a dose-responsive and time-dependent inhibition of Aβx-40 in mouse CSF resulting in 77% inhibition of CSF at 3 hours post final 50 mg/kg dose.

Using cisterna magna cannulated Beagle dogs, the Aβx-42 lowering by **64** was evaluated in serial CSF samples collected over a 72 h period post-dose following oral doses of 1 or 3 mg/kg (Figure 7, Panel D). The results for each analyte measured in the CSF over a time course of 72 h are expressed as absolute levels in picograms per milliliter. Following administration of **64**, the 3 mg/kg dose showed a long-lasting reduction in CSF levels of Aβx-42, with a maximum decrease of 74% versus baseline at 11 h post dose.

Figure 7: Effect of Compound 64 on Brain and CSF Amyloid-Beta Following Administration in Mouse and Dog

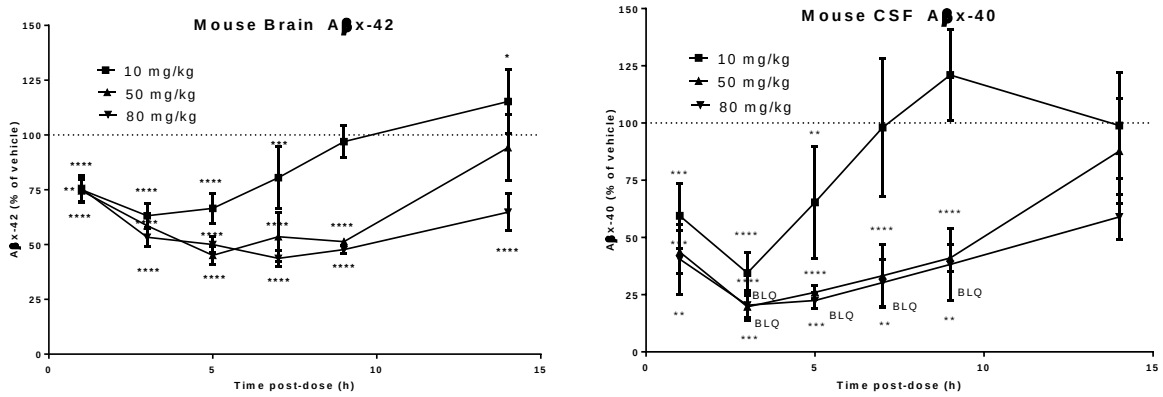

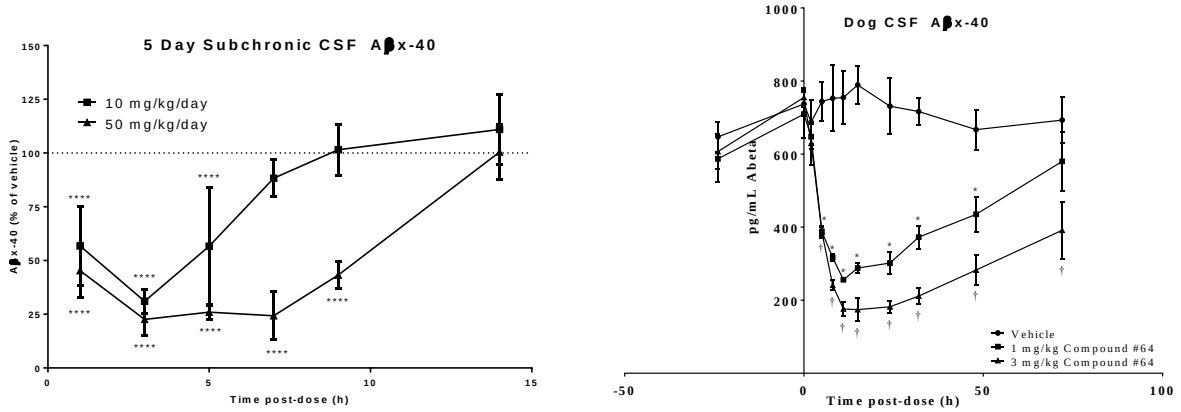

A) Compound **64** (10, 50 or 80 mg/kg) and vehicle were administered subcutaneously to male 129/sve mice. Brain Aβx-42 was assessed at 1, 3, 5, 7, 9 and 14 h post-dose. Data are expressed as the mean of % of vehicle of n = 5 animals per group ± SEM. **** p <0.0001. *** p <0.001. ** p <0.01. * p <0.05. B) Compound **64** (10, 50, or 80 mg/kg) and vehicle were administered subcutaneously to male 129/sve mice. CSF Aβx-40 was assessed at 1, 3, 5, 7, 9 and 14 h post-dose. Data are expressed as the mean of % of vehicle of n = 5 animals per group ± SEM. **** p <0.0001. *** p <0.001. ** p <0.01. All values for the 50 mg/kg dose at 3 h were below BLQ which is defined as <23 % of vehicle. All values for the 80 mg/kg dose groups at 3, 5, 7 and 9 h where BLQ which is defined as <36.3 % of vehicle. BLQ data points were interpolated from the standard curve and are represented in the graph. C) Male 129/sve mice were dosed subcutaneously once a day for 5 days with **64** (10 or 50 mg/kg/day) or vehicle. CSF Aβx-40 was assessed at 1, 3, 5, 7, 9 and 14 h after the last dose. Data are expressed as the mean percent of vehicle of n = 5 animals per group ± SEM. **** p <0.0001; *** p <0.001; ** p <0.01; * p <0.05. D) Time course data for the effect of **64** on CSF Aβx-42 levels in dog. Compound **64** was orally dosed at 1 or 3 mg/kg at time = 0 h. Data are the mean ± SEM, n = 3 per group, * = p<0.05 for the 1 mg/kg group, † = p<0.05 for the 3 mg/kg group; Aβx-40 = Amyloid-β isoform containing amino acids 17-24 and ending in carboxy-terminal amino acid 40; Aβx-42 = Amyloid-β isoform containing amino acids 17-24 and ending in carboxy-terminal amino acid 42; BLQ = Below limit of quantitation; CSF = Cerebrospinal fluid; h = hour; mg/kg = Milligram per kilogram; SEM = Standard error of the mean.

Our first goal was to establish a link between BACE2 inhibition in vitro and accumulation of full length PMEL17 in primary melonocytes. To this end, we assessed two non-selective BACE1 inhibitors (**3** and **4**) in primary human melanocytes from darkly pigmented donors after overnight incubation with a dose response of inhibitor from 10 μM to 1 nM. Accumulation of full length PMEL17 is apparent for both compounds (see SI, Figure 2) consistent with inhibition of PMEL17 processing.

Furthermore, we were concerned that the measurements in the standard fluorescent polarization (FP) assays which utilize an artificial substrate, truncated enzyme, and a non-

physiological relevant pH (4.5) may not accurately reflect the selectivity for BACE1 over BACE2 in a native environment. Due to these limitations, we established BACE1 and BACE2 binding assays using using full length human recombinant enzymes overexpressed in HEK293 cells where inhibition is determined by competition binding in cell paste at physiological pH (6.0). Table 6 compares the selectivity for literature molecules **3** and **4** relative to thiazoles **61**, **64**, and **65**. All inhibitors have excellent potency at BACE1 in binding or FP assay formats along with cellular activity looking at production of sAPPβ in H4 cells. Remarkably, thiazole **64** showed improved selectivity over BACE2 in binding (27-fold) relative to the literature examplars and across multiple chemical series in our BACE1 program (see SI, Figure 3). We hypothesized that the improved selectivity over BACE2 was due to subtle non-binding interactions in BACE1 in the P3 and flap region of the enzyme that were less tolerated in BACE2.

Table 6: Selectivity Profile for Analogs 3, 4, 61, 64, and 65

Compound	BACE1 Binding (nM)[a]	BACE2 Binding (nM)[a]	B2/B1 Binding ratio	BACE1 FP (nM)[b]	BACE2 FP (nM)[b]	sAPPβ (nM)[c]	3D-Skin Model (nM)[d]
3	6.4	3.3	0.5	<2.2	4.5	< 0.54	2.44
4	25.7	17.8	0.7	42.0	42.9	38.4	38.5
61	8.2	20	2.4	29.1	21.6	4	234
64	7.3	194	26.6	36.9	238	5	2860
65	8.7	57	6.5	22.8	70.5	3	372

[a]IC_{50} values obtained from BACE1or BACE2 binding assay. [b]IC_{50} values obtained from BACE1 or BACE2 FP assay. [c]IC_{50} values obtained from whole cell assay measuring sAPPβ. [d]Spectrophotometric

quantitation (L value) showing full dose response curves of the 3D skin model surface pigmentation using a hand held Minolta CR-700D spectrophotometer following 9 days of treatment with compounds indicated. The change in L value compared to DMSO control was plotted against a dose response of compound in duplicate using a 4-parameter curve fit with variable slope. The concentration showing a change in L value of 2 points (delta 2) was used to rank order compounds.

In order to further understand and refine the apparent cell-free selectivity of thiazole **64**, we sought a cellular assay providing a more physiologically relevant end-point of pigmentation changes. Reconstituted human epidermis models are increasingly being used to evaluate potential therapeutics.[37] To this end, we utilized a three-dimensional (3D) reconstructed skin model.[38-39] This model uses melanocytes from African American donors that are devoid of pigmentation at the start of treatment. Following 9 days in culture, untreated melanocytes will demonstrate surface pigmentation therefore providing a model in which BACE inhibitors could be compared with regard to their inhibitory effects on pigmentation. The surface pigmentation was quantified spectrophotometrically using a hand held Minolta CR-700D spectrophotometer, generating an L value which is an objective measure of skin pigmentation. Loss of pigmentation is accompanied by an increase in L value. The concentration accompanying a change in L value of 2.0 was used to rank order compounds. Dose response curves for **3**, **4**, and **64** are shown in Figure 8, panel A. Thiazole **39** is clearly more selective in the reconstructed skin model with an L value of 2.86 μM relative to non-selective literatures compound **3** or **4** as well as closely related analogs **61** and **65** (Table 7).

In order to validate the degree in surface pigmentation change of the melanocytes with a structural change in melanosomes as has been reported with BACE2 depletion[11], the ultrastructure of the treated melanocytes was examined by electron microscopy for **3** and **4** relative to control (Figure 8, Panel B). This blinded evaluation demonstrated altered melanosome morphology as well a qualitative reduction in number of melanosomes in groups

treated with a non-selective BACE inhibitor (positive control) albeit at relatively high concentrations of 100 nM and 161 nM, respectively. These ultrastructural changes in melanosomes were reflected in the higher L value scores in these groups indicative of reduced surface pigmentation.

Figure 8: Human 3-D skin model surface pigmentation following 9 days in culture; Images and L value quantitation and representative EM.

Panel A

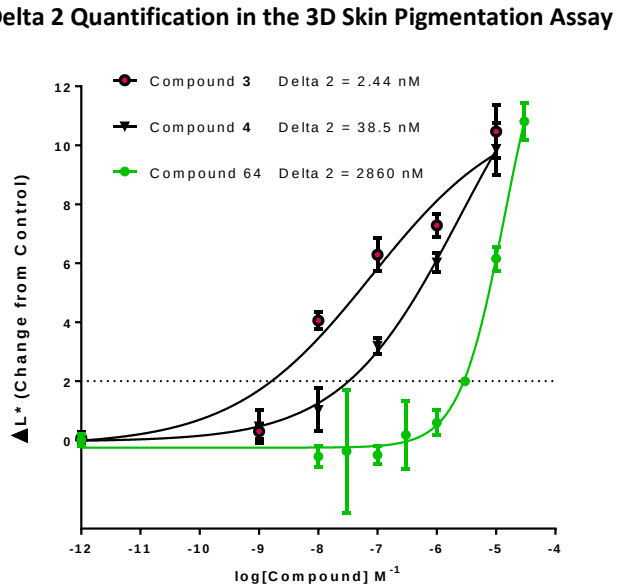

Panel B

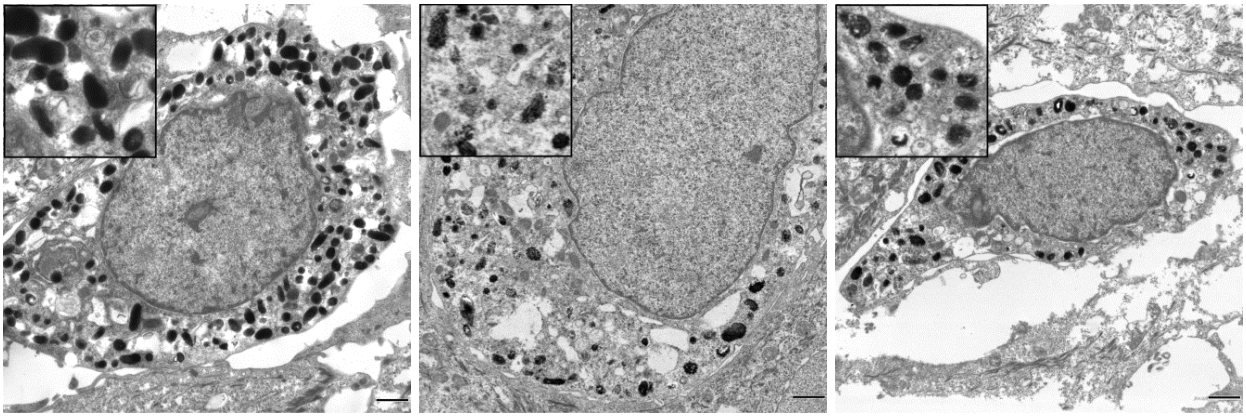

Control 100 nM Compound **3** 161 nM Compound **4**

(A) Spectrophotometric quantitation (L value) showing full dose response curves of the melanocytes surface pigmentation using a hand held Minolta CR-700D spectrophotometer following 9 days of treatment with the compounds indicated. The change in L value compared to DMSO control was plotted against a dose response of compound in duplicate using a 4-parameter curve fit with variable slope. The concentration showing a change in L value of 2 points (delta 2) was used to rank order compounds. The plotted delta L data is a compilation of 2-5 separate full dose response experiments. The dotted line designates the concentration of compound required for a change in L value of 2 units. (B) Representative transmission electron microscopic images (4000x) of melanocytes demonstrating a qualitative reduction in number of melanosomes in the 100 nM compound **3** and 161 nM compound **4** melanocytes from 3D skin model as compared with DMSO control. Inset images demonstrate alteration in melanosome morphology characterized by irregular shape and indistinct borders in the BACE inhibitor treated groups as compared with control. Bar equals one micron.

In order to translate the in vitro binding and phenotypic cellular assays to coat color changes invivo, pigmented C57BL/6J mice were selected for chronic dosing studies. Initially we sought to reproduce findings of hypopigmentation changes with extended dosing of SCH1682496 as reported, where loss of fur pigmentation occurred following 16 days of dosing with 100 mg/kg (BID).[16] Upon repeat of this study design, we observed a similar hypopigmentation phenotype with the changes in ventral fur having a heterogenous and random pattern making quantification difficult. This was mostly likely due to the the regional differences in phases of hair growth known to occur in mice. In order to have a more homogenous pigmenation response, we sought to synchronize hair growth with depilation prior to the start of dosing. In a time-course in control mice, a three-week time frame was sufficient to observe hair regrowth equivalent to pre-depilation conditions (see SI, Figure 4). To this end, we treated mice for 3-weeks using **3** and **4** in a dose reponsive manner achieving projected C_{avg} of 7-144 nM for **3** and 103-5190 nM for **4** (SI, Figure 6). Relative to control and low dose group, the higher doses of the non-selective BACE inhibitors produced a homogenous change in fur pigmentation (lighter color) at multiples of the BACE2 binding IC_{50} unbound in plasma (Figure 9 Panel A and B; SI, Figure 6).

In order to compare selectivity across different BACE inhibitors, we sought to achieve a free plasma exposure on average relative to their projected efficacy as measured by Aβ lowering in brain (Figure 9, Panel C). Using the above chronic dosing paradigm, we compared compound **64** to **3** at concentrations targeting a projected 50% Aβ lowering in brain. The actual observed C_{avg} (unbound plasma) exposure was 31 nM and 42 nM for compound **64** and compound **3**, respectively which projected an Aβ lowering in human CSF of 55% and 40%, respectively (see SI, Figure 6). The lack of a pigmentation change in the **64** treated mice is consistent with the improved selectivity indicated by both the binding and the 3D skin model cellular assays.

Figure 9: Effect of Chronic Dosing at Multiples of the BACE2 Binding IC_{50} on Pigmentation in C57BL/6J Mice After Synchronization of Fur Growth

Panel A

Compound **3**	Dose mg/kg (BID)	C_{avg}, $C_{u,p}$ (nM)	Fold above BACE2 IC_{50}
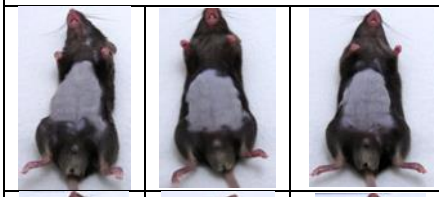	21.5	144	48
	5.5	42	14
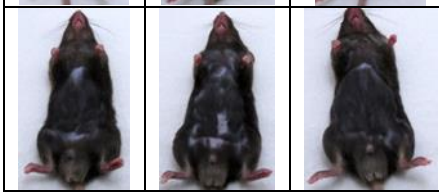	1	7	2

Panel B

Compound **4**	Dose mg/kg (BID)	C_{avg}, $C_{u,p}$ (nM)	Fold above BACE2 IC_{50}

			135	5190	291
	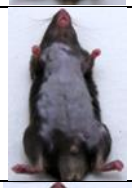	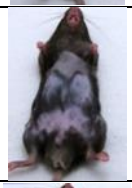	34	953	54
	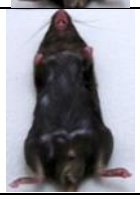		7	103	6

Panel C

Compounds	Dose mg/kg (BID)	C_{avg}, $C_{u,p}$ (nM)	Projected Aβ lowering in human
64			
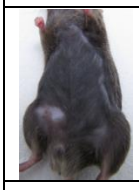 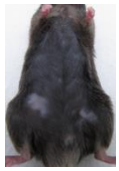 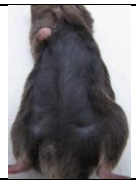	5	31	55%
3			
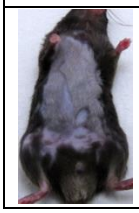 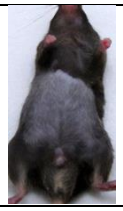 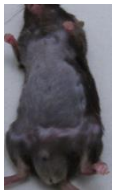	5.5	42	40%

(A) Representative images from chronic dosing of compound **3** at observed plasma Exposures of 2, 14, and 48 fold the BACE2 IC_{50} (B) Representative images from chronic dosing of compound **4** at observec plasma exposures of 6, 54, and 291 fold the BACE2 IC_{50} (C) Representative images from chronic dosing of compound **64** and **3** at comparable projected Aβ lowering in human.

Ultrastructural evaluation of follicular epithelial melanosomes from depigmentated areas of skin in these chronic mouse studies (Supplemental Figure 7) demonstrated similar morphological alterations as those noted in BACE inhibitor treated melanosomes in the 3D skin model preparation (Figure 7, insets). BACE inhibitor treatment in both the in vitro (3D skin model) and

in vivo systems (mouse) resulted in melanosomes with irregular shape and indistinct borders as compared with controls indicating that the 3D skin model system was accurately recapitulating an in vivo effect despite the differences in species and melanosome localization. This in vitro to in vivo correlation helped validate the 3D skin model system and provided confidence in its use for screening BACE inhibitor compounds and potentially for predicting the likelihood of BACE inhibitor induced skin depigmentation in humans. With clear indicators of an improved selectivity profile, compound **64** was advanced into nonclinical toxicology studies. Dog toxicology studies that included daily cage side clinical observations and weekly detailed clinical observations showed no evidence of hair coat color (pigmentation) change. The dog studies included dosing **64** for up to 9-months at 26 mg/kg/day and achieved robust systemic exposure (C_{avg} 6791 ng/mL total; 2326 nM unbound) that was approximately 10-fold above the BACE2 IC_{50}. This lack of pigmentation effect in the chronic (9-month) dog study validated the selectivity over BACE2 in large animal species and further implicated the relationship to avoiding potential hypopigmentation. The lack of a hypopigmenation in dog after treatment of **64** is a potential differentiator compared to **AZD3293** which showed reversible hypopigmentation in dog.[14] Furthermore, dosing of MK-8931 did not show hypopigmentation in chronic NHP studies which suggests that species differences may impact the translatability of these findings to human.[17]

In conclusion, a novel series of selective, brain permeable, small molecule inhibitors of BACE1 were identified for the treatment of AD. By installing a thiazole group in P1, the amidine pK_a was reduced to an optimal range while minimizing synthetic complexity. Optimization of the heteroaryl group off of the amido-thiazole resulted in compounds with an excellent balance of potency and properties. To further understand the selectivity of the lead

compounds, we incorporated a 3D skin model and utilized electron micrscopy to understand the impact of BACE2 inhibition on melanogenesis. To build a translation to an *in vivo* outcome, a unique depilation study design to understand the coat color changes in mice was implemented. Compound **64** emerged as a clinical candidate with excellent potency, overall alignment of properties including selectivity over BACE2, as well as a lack of hypopigmentation change in dog after 9-months of dosing which suggests a key differentiator over existing unselective BACE1 inhibitors. However, the safety and tolerability data from longer duration clinical trials with the current cohort of BACE1 inhibitors will establish the impact of chronic inhibition of BACE2. Recently compound **64** recently completed phase 1 clinical trials and demonstrated potent and dose-dependent Aβ lowering in human CSF.[40]

Experimental Section

In Vivo Experiments: All procedures were carried out in compliance with the National Institutes of Health Guide for the Care and Use of Laboratory Animals (1985), under approval of an Institutional Animal Care and Use Committee (IACUC).

Acute Treatment in Mice: Male 129/SVE wild-type mice (20–25 g) were in a non-fasted state prior to subcutaneous dosing with vehicle, or compound **64** using a dosing volume of 10 mL/kg in 5:5:90 DMSO:Cremophor:saline vehicle. The mice (n = 5 per group) were then sacrificed at 1, 3, 5, 7, 14, 20 and 30 h post-dose. Following cardiac puncture into ethylenediaminetetraacetic acid (EDTA)-containing tubes, whole blood samples (0.5–1.0 mL) were collected, and plasma was separated by centrifugation (1500 × g for 10 min at 4 °C). The generated plasma was distributed into separate tubes on wet ice for exposure measurements (50 μL) and Aβ analysis (remainder). CSF samples (8–12 μL) were obtained by cisterna magna puncture using a sterile

25 gauge needle and collected with a P-20 Eppendorff pipette. CSF samples were distributed into separate tubes on dry ice for exposure measurements (3 μL) and Aβ analysis (remainder). Whole brain was removed and divided for exposure measurements (cerebellum) and Aβ analysis (left and right hemispheres), weighed, and frozen on dry ice. Prior to the assay, all samples were stored at –80 °C.

Measurement of Rodent Amyloid-β: Frozen mouse hemi-brains were homogenized (10% w/v) in 5 M guanidine HCl, using a Qiagen TissueLyser. Each sample was homogenized with a 5 mm stainless steel bead, four times, at a shaking rate of 24 times/s for 90 s, then incubated at 25 °C for 3 h, and ultracentrifuged at 125,000 x g for 1 h at 4 °C. The resulting supernatant was removed and stored in a 96-well polypropylene deep well plate at –80 °C. Using solid-phase extraction using Waters Oasis reversed-phase HLB 96-well column plates (60 mg), the Aβ peptides were further purified. Column eluants in 98% MeOH and 2% NH_4OH from 500-800 μL of original brain supernatant were evaporated to complete dryness and stored at –80 °C until assay. For plasma analysis, 140-175 μL of mouse plasma was treated 1:1 with 5 M guanidine HCl and incubated overnight with rotation at 4 ºC. The entire volume was then purified through solid-phase extraction as indicated above.

Samples were analyzed using a dissociation-enhanced lanthanide fluorescent immunoassay (DELFIA) platform enzyme-linked immunosorbent assay (ELISA). Configuration of the antibodies used in determining the level of Aβx-40 and Aβx-42 utilizes a common detect antibody (4G8) in combination with specific C-terminal antibodies for the 40 and 42 cleavage sites. For the Aβx-40 assay, a 384-well black Nunc Maxisorp plate was coated with 15 μL/well (4 μg/mL) capture antibody (Rinat 1219) in 0.1 M sodium bicarbonate coating buffer, pH 8.2. For the Aβx-42 assay, 15 μL/well (8 μg/mL) capture antibody (Rinat 10G3) was used. The

plates were sealed and incubated at 4 °C overnight. Plates were washed with phosphate-buffered saline containing 0.05% Tween-20 (PBS-T), and blocked with 75 μL of blocking buffer (1% BSA in PBS-T) for 2 h at 25 °C.

After the plates had been washed with PBS-T, rodent Aβx-40 (California Peptide) or Aβx-42 (California Peptide) standard was serially diluted in blocking buffer and 15 μL was applied to the plate in quadruplicate. Reconstituted dried brain samples in 120 μL of blocking buffer, which corresponds to a 4.16- to 6.67-fold concentration. Then 15 μL of undiluted brain sample was added to the Aβx-42 assay plate in triplicate, or 15 μL of a 1:2 diluted brain sample was added to the Aβx-40 assay plate in triplicate. Dried plasma samples were reconstituted in 40 μL of blocking buffer, which corresponds to a 3.5- to 4.38-fold concentration, and 15 μL was added to the Aβx-40 assay plate in duplicate. CSF samples were diluted 1:8 in blocking buffer, and 15 μL was added to the Aβx-40 assay plate in duplicate. The plates containing the sample or standards were incubated for 2 h at 25 °C. The plates were washed with PBS-T and 15 μL of detect antibody (4G8-Biotin, Covance), 200 ng/mL in blocking buffer, was added to each well, and incubation was carried out for 2 h at 25 °C. The plates were then washed with PBS-T, and 15 μL of europium-labeled streptavidin (PerkinElmer), 50 ng/mL in blocking buffer, was added for a 1 h incubation in the dark at 25 °C. The plates were washed with PBS-T, and 15 μL of PerkinElmer Enhancement solution was added to each well with 20 minute incubation at RT. Plates were read on an EnVision plate reader using DELFIA time-resolved fluorimetry (Exc340/Em615), and samples were extrapolated against a standard curve using 4-parameter logistics.

Human Melanocyte Cultures. Human primary melanocytes from darkly pigmented neonatal foreskin (HEMn-DP) were obtained from Cascade Biologics (Portland, Oregon),

cultured in Medium 254 (cat# M-254-500) supplemented with Human melanocyte Growth Supplement (HMGS, Cat#S-002-5) in the absence of antibiotics and antimycotics at 37^{o}C under 5% CO_2. All experiments used melanocytes that had been passaged <8 times and were plated at 1,000,000 per well in a 6-well plate. After the initial plating, attached cells were treated with various concentrations (10μM-1nM) of compounds prepared from DMSO stocks that also had a known range of BACE2 selectivity. The final DMSO concentration was 0.1% and DMSO alone served as the control. Following 24 hours of treatment, the media was removed, and the cells were rinsed once with PBS prior to being harvested using a cell scraper into 0.5 mL eppendorff tubes using 75 uL of lysis buffer (1% Triton-X-100 in PBS or RIPA containing protease/phosphatase inhibitors + benzonase nuclease). Samples were incubated with shaking for 30 minutes at 4^{o}C, centrifuged at 5000 RPM for 10 minutes and supernatants and pellets were frozen at -80^{o}C for western blot analysis.

Western Blot analysis. Cell lysates were prepared in NuPAGE® LDS buffer, heated at 80°C for 5 mins and proteins were then separated by gel electrophoresis using the NuPAGE® Novex 4-12% Bis-Tris gel system. Proteins were then transferred onto a nitrocellulose membrane using the iBlot® Dry Blotting system. All the reagents were purchased from ThermoFisher Scientific. The nitrocellulose membranes were then probed with a Rabbit anti-PMEL antibody (Abcam ab137078) or a Mouse anti-PMEL HMB45 (Abcam ab787) and visualized using the corresponding IRDye® anti-species antibody (LI-COR) The membrane was then scanned using the LI-COR Odyssey.

Human BACE1 and BACE2 Enzymatic Activity using a Fluorescence Polarization Assay. Both BACE1 and BACE2 enzymatic activity was measured with the aid of an optimized synthetic peptide substrate Biotin-GLTNIKTEEISEISYEVEFR-C[oregon green]KK-OH. Upon

cleavage of the peptide substrate a decrease in fluorescence polarization was measured. Compounds were diluted by half log in 100% DMSO 11 times with a top concentration of 10 mM in a 384-well polypropylene plate. The 100% DMSO dose response curve was then added to a 384-well black assay plate as 0.150 μL per well. The final working top concentration was 0.1 mM and the DMSO concentration was 1%. A volume of 7.5 μL of BACE substrate was then added in assay buffer (100 mM sodium acetate, pH to 4.5 with glacial acetic acid, 0.001 % Tween 20). The background wells in column 1 of the 384 well assay plate received 7.5 μL of assay buffer. The reaction was started with the addition of 7.5 μL of BACE1 or BACE2 enzyme in assay buffer to all wells except the background wells in column 1. The final concentration of peptide substrate was 150 nM and the final concentration of BACE1 and BACE2 enzyme was 0.15 nM and 2.5 nM, respectively. The assay plate was sealed and incubated at 37°C for 3 hours or 1 hour (BACE1 or BACE2, respectively). After incubation, 15 μL of stop solution (1.5 μM Streptavidin in Dulbecco's Phosphate Buffered Saline) was added to all wells and the plate was read on the Envision Plate Reader (Perkin Elmer, No. 2103) optimized to read fluorescence polarization on the millipolarization scale. Percent effect values for each concentration of compound was calculated based on fluorescence polarization (FP) readings in the 100 % effect control wells containing no enzyme, and the 0% effect control wells containing no compound. Curve-fitting analysis utilyzing concentrations and percent effect values for a given compound were plotted and the concentration for 50 percent effect (IC_{50}) was determined using a sigmoidal four parameter fit algorithm.

Soluble amyloid precursor protein beta (sAPPβ) cellular assay for BACE1 activity. The inhibitory activity of compounds against the BACE1 enzyme is measured in a human neuroglioma cell line. The neuroglioma cell line, H4, was stably transfected with wild type

amyloid precursor protein (APP) which is the substrate for BACE1 enzyme. Upon cleavage by BACE1, a soluble portion of the amyloid precursor protein is released into the cell media which is then measured by an enzyme linked immunosorbent assay (ELISA). Compounds were solubilized in 100% DMSO to a concentration of 30 mM and diluted by half log in 100% DMSO 11 times for a final top concentration of 30 μM and DMSO concentration of 1%.

The neuroglioma cell line H4 cells were grown in Dulbecco's Modified Eagle Medium (DMEM) with 10% Fetal Bovine Serum (FBS) and 200 mM Glutamax. Cells were plated overnight in tissue culture treated Falcon 384 well plates at a cell density of 4,500 cells/well in 50 μL of media. The next day media was removed, and cells were washed once with phosphate buffered saline, after which 25 μL media was placed in all wells, followed by the addition of the diluted compound dose response curve. The highest concentration tested was 30 μM with 1 % DMSO. Cells serving as the background controls received 30 μM of a proprietary compound. Compounds were allowed to incubate with cells overnight in a 37°C incubator. Concurrently, 384 well black Nunc Maxisorp plates were also incubated overnight at 4°C with 10 μL of 4 μg/mL of Aβ antibody available from Pierce (OMA1-03132) in coating buffer (0.1 M sodium bicarbonate, pH 8.8 to 9.0).

The next day, the coated plates were washed 3 times with PBS containing 0.05% Tween 20 (PBST) and blocked with 1% Bovine Serum Albumin (BSA) in PBST for one hour and then washed 3 times with PBST. After which, 10 μL of media from the treated cells was then transferred to the washed plates and incubated for one hour, followed by washing three times. Next, 10 μL of a 1:1000 dilution of sAPPβ antibody (Signet SIG-39138), which is specific for the soluble fragment cleaved n-terminus to the beta secretase cleavage site of

amyloid precursor protein, was added and incubated for one hour. The plates were washed three times and then incubated with 10 μL of a 1:1,000 dilution of anti-rabbit, HRP tagged antibody from GE Healthcare. Plates were washed one last time and then 30 μL chemiluminescent substrate (Pierce 73069) was added to the wells. Signal was then read on an EnVision plate reader using standard luminescent settings. The percent (%) effect at each concentration of compound was calculated based on and relative to the amount of sAPPβ total produced by the positive and negative control wells contained within each assay plate. The positive control wells contained a saturating concentration of a proprietary control compound that produced a maximal level of sAPPβ inhibition. Intrinsic activity values for each compound were calculated relative to the maximal % effect produced by this control compound. The negative control wells did not contain any compound but rather DMSO alone, and the response to DMSO was used to set the baseline (0%) response in the assay. The concentrations and % effect values for each compound were plotted using a four-parameter logistic dose response equation and the concentration that inhibited 50% (IC_{50}) was calculated. The IC_{50} for a control compound was evaluated in each experiment as a quality control measure. If the endpoint value was within 3-fold of the expected value then the experiment was deemed acceptable.

BACE1 and BACE2 radioligand binding assays. The overexpression of human full length BACE1 was completed by transient transfection of HEK-293 cells with the BamMam expression system (invitrogen A24223) followed by zeocin selection and single cell cloning by limiting dilution of the stable transfectant. The resultant clonal HEK293 stable cell line expressing human FL BACE1 was scaled up for production of crude BACE1 cell membrane used for the BACE1 radioligand binding assay. The overexpression of human full length BACE2 was completed by HEK293 cell transfection with human BACE2 (Myc-DDK-tagged)

vector (Origene RC204860) using lipofectamine LTX transfection system (Life Technology #15338100). A stable cell batch was generated by maintaining these cells under geneticin selection. The resultant clonal HEK293 stable cell line expressing human FL BACE2 was scaled up for production of crude BACE2 cell membrane used for the BACE2 radioligand binding assay. Crude cell membrane homogenates were prepared by homogenizing each cell paste at 8 or 24 mg/ml (BACE1 and BACE2 respectively) in 50 mM Tris buffer (pH=7.4) containing 2 mM magnesium chloride on ice for 10 seconds at setting 5 with a Polytron. Aliquots prepared on ice were frozen at -80^{o} C for daily use.

Parallel scintillation proximity assays (SPA) were utilized to quantitate the degree of BACE1 and BACE2 binding by compounds with a radioligand equipotent for BACE1 and BACE2 (^{3}H-PF-6475886, 25 nM). Briefly, the reaction mixture in 50 mM sodium acetate buffer (pH = 6.0) contained 10 nM 3H-ligand, 20 or 440 μgram of cell paste (BACE1 or BACE2 respectively), 66 μ gram SPA bead (PEI-WGA bead, PerkinElmer RPNQ0003) and test compound with a final dimethyl sulfoxide (DMSO) concentration of 1.8% in a final volume of 27.5 μL. Compounds that were solubilized in 100% DMSO were added as a 500 nL spot to the Corning 384-well SPA plates using a non-contact acoustic dispenser and the nonspecific binding was defined by 10 uM of compound **10** (equipotent for BACE1 and BACE2, 27 nM). [31] Binding was carried out at room temperature for 30 minutes after which time the SPA plates were centrifuged and read on a TriLux Microbeta reader to determine the number of counts bound. The percent (%) effect at each concentration of compound was calculated compared to vehicle and the IC_{50} of binding determined with a four-parameter logistic dose response equation.

Phenotypic Pigmentation Assay in Human 3D Reconstructed Skin. Sealed 24 well plates containing individual inserts of the MelanoDerm™ MEL-300 tissues and Medium were purchased from MatTek Corporation and stored unopened at 4°C for 24 hours. On the day that experiments began, the samples were removed from 4°C for one hour and allowed to equilibrate at room temperature before being transferred into 6 well plates under sterile conditions. Pre-warmed maintenance medium was pipetted into each well and placed into a humidified 37°C, 5% CO_2 incubator for 1 hour prior to applying compounds. Following the 1 hour incubation, the media contained within the 6-well plate was removed by aspiration and a culture stand (No MEL-STND) is placed into each well of the 6-well plate. Pre-warmed 5.0 mL of maintenance media containing a final concentration of compound (100 μM to 0.1 nM) was added. The final DMSO concentration is 0.1% which was added to each well. The cell culture insert containing the MelanoDerm™ is placed on top of the culture stand such that the media level touches the bottom of the insert while the surface of the MelanoDerm™ remains dry. Air bubbles that are trapped underneath the cell culture insert are released by tilting the insert with sterile forceps. The 6-well plates were then returned to the incubator for a period of 9 days. Medium was changed every 48-60 hours with the appropriate final concentration of each treatment compound. Care was taken to aspirate all of the media from the well to ensure that exactly 5 mL was delivered for the medium replacement. As controls, 0.1% DMSO was used to represent ZPE. The HPE for the assay was not determined since the degree of pigmentation loss (increasing L∗) varied depending on compound, and often did not demonstrate an upper asymptote.

After 9 days, each MelanoDerm™ was removed from media and washed twice with 0.9 mL of PBS, ensuring that the surface of the MelanoDerm™ remained dry. The insert was blotted on sterile gauze and the sides of the insert were cleaned with sterile cotton-tipped

applicators. AMinolta CR700d spectrophotometer was used to quantitate the level of reflected light represented by the L∗a∗b∗color model system, developed by the Commission Internationale d'Eclairage which was used to objectively describe all colors visible to the human eye. The spectrophotometer was equipped with a retrofitted mask aperture of 1.25 cm, enabling the MelanoDerm™ insert to fit within the reading window of the spectrophotometer where illumination of the surface of the MelanoDerm™ with a pulsed xenon arc lamp was recorded. The instrument was calibrated for both zero and white calibration. The zero calibration was performed by holding the black side of the White Calibration Cap (CM-A177), provided with the instrument, to the mask aperture. The white calibration was performed with the White Calibration Cap locked on to the instrument, with the White Calibration Plate facing the mask aperture. After the MelanoDerm™ insert was rinsed with PBS and dried, it was placed on a Konica Minolta CR-A43 Calibration Plate, which provided a consistent background and even platform during the reading process. The MelanoDerm™ insert was then inserted into the mask aperture of the spectrophotometer and measured using Spectra-Magic NX Software. Each MelanoDerm™ was measured three times with no intervening wait time and measurements were auto-averaged (what does this mean does the instrument do this? If so state that) Readings of L∗ value (brightness spectrum from black to white), a∗ (spectrum from red to green), and b∗ (spectrum from blue to yellow) were taken, as well as absorbance at 470 nm. L∗ values have been previously reported to demonstrate the greatest sensitivity to differences in human facial pigmentation, so this value was used for all quantitation.[41]

Raw L∗ values were converted to delta L∗ by subtracting the DMSO background control L∗ value from each sample L∗ value. The delta L∗ values were plotted in Graph Pad Prism using a log of agonist versus variable response with a 4-parameter nonlinear regression curve fit

(Graph pad reference here) The concentration of any given compound required to give a change in L∗ value of 2.0 was interpolated from the generated curve.

In vivo Hypopigmentation Studies. All procedures were carried out in compliance with the National Institutes of Health Guide for the Care and Use of Laboratory Animals (1985), under approval of an Institutional Animal Care and Use Committee (IACUC). C57BL6 pigmented mice obtained from Jackson Labs were used for all studies. In order to assess oral pharmacokinetic feasibility for chronic dosing studies, mice were acutely dosed via oral gavage with test compound suspended in methylcellulose 0.5% (w/v) / 98.5 % water / 1% tween 80. Blood was collected by cardiac puncture from separate mice at 1, 4, 12, and 24 hours after dosing in order to obtain the free plasma Cave (AUC ng*Hours/mL). Whole blood samples (0.5–1.0 mL) were collected by cardiac puncture into ethylenediaminetetraacetic acid (EDTA)-containing tubes, and plasma was separated by centrifugation (1500 × g for 10 min at 4 °C). The generated plasma was distributed into separate tubes on wet ice for exposure measurements (25 μL).

Only compounds that could achieve free plasma concentrations at adequate exposure multiples above the BACE2 IC50 were selected for chronic dosing. In most cases adequate exposure was obtained with BID (spell out here) dosing. 24 hours prior to the first dose, all mice in the study were depilated with Nair® (Church & Dwight Co., Inc.) in order to synchronize hair growth and provide a more homogenous hypopigmentation response. Briefly mice were anesthetized with 2% isoflurane in oxygen, and all hair removal took place under a hood. A rectangular region of hair on the ventral surface, from the hind legs to the front legs, and on the dorsal surface on the back rear of the mouse was first removed using an electric razor (Norelco

G390, Philips) immediately followed by depilation. Occasional skin lesions were monitored and treated by veterinary care with topical treatment of chlorohexidine and dermal gel.

At weekly time points after initiation of dosing, photographic images were taken under standardized lighting conditions of the initially depilated ventral and dorsal surface areas. A white-light LED floodlight source (30W, IP66, Zitrades) placed atop a white photobox was used as an illumination source. A Canon PowerShot SX20 IS digital camera was subsequently placed at the same distance on the photobox with identical camera settings applied for all photographic sessions (white balanced, ISO400). A CameraTrax 24ColorCard (2x3 with White Balance) card was additionally placed within the photobox followed anesthetized mice centrally positioned for ventral and dorsal surface area capture. The Minolta CR700d spectrophotometer was also used to provide a more quantitative measurement of hair pigmentation. Measurements were taken from the same region of each mouse in the initial depilated area with care taken to avoid any occasional lesions or pre-existing pigmentation patches. The same spectrophotometer and mask aperture of 1.25 cm described above was used to measure mouse hair pigmentation by placing the aperture directly in contact with the mouse to avoid interfering external light. For all photography and spectrophotometric readings, mice were anesthetized with 2% isoflurane in oxygen in order to obtain stable high quality images.

Mice were dosed chronically until the desired phenotypic response was obtained, at which point necropsy was performed at 4 hours post last dose in order to compare with the 4 hour time point assessed in the initial oral PK study. Whole blood samples (0.5–1.0 mL) were collected by cardiac puncture into ethylenediaminetetraacetic acid (EDTA)-containing tubes, and plasma was separated by centrifugation (1500 × g for 10 min at 4 °C). The generated plasma was distributed into separate tubes on wet ice for exposure measurements (25 μL). Skin samples were taken

from both ventral and dorsal surfaces of the mouse and fixed in cold 4% paraformaldehyde for histological evaluation.

Histological Processing and Sectioning. Skin sections and MelanoDerm™ cultures were processed in an automated tissue processor, embedded in paraffin, sectioned at 5 microns and stained with hematoxylin and eosin.

Transmission Electron Microscopy for MelanoDerm™ EM methods. MelanoDerm™ cultures following the standard 9 day treatment were assessed spectrophotometrically as described and fixed in cold 4% paraformaldehyde for processing. The nylon membrane was carefully removed from the wells and then bisected. One half was processed for standard paraffin embedment and H&E staining and the other half was processed for TEM as follows. The MelanoDerms™ were further trimmed and put into EM fixative: 2.5% glutaraldehyde and 2% paraformaldehyde in 0.1M phosphate buffer and fixed for at least 24 hours at 4^0C. Following fixation, MelanoDerms™ were transferred to 0.1M phosphate buffer,rinsed and then post fixed in 1% OsO4 for 2 hours at 4^0C. Following osmication, samples were rinsed in DI water followed by dehydration through a graded alcohol series andtransition through propylene oxide. They were infiltrated in an increasing resin to propylene oxide mixture followed by a change to pure resin prior to embedding. Thick sections were cut on a Leica UCT ultramicrotome and stained with Toluidine blue. Blocks were trimmed for areas of interest and thin sections were picked up on 200 mesh copper palladium grids. These were contrast stained with uranyl acetate and lead citrate prior to evaluation using a Hitachi H-7100 transmission electron microscope. Ten cells per treatment per MelanoDerm™ were photographed at 4000X using a digital CCD camera system (Advanced Microscopy Techniques,

Danvers, MA). Photos were blinded with respect to treatment and evaluated by a veterinary pathologist.

Transmission Electron Microscopy for Mouse skin EM methods. Skin samples were received in 4% methanol free paraformaldehyde. Sections from the ventral and dorsal surfaces were trimmed; one set for standard paraffin embedment and H&E staining and a second set for TEM evaluation. Skin samples were processed for TEM as described above. Thick Toluidine Blue stained sections were evaluated and those containing optimally oriented deep follicular epithelium were further trimmed, thin sectioned, contrast stained and examined using a Hitachi H-7100 transmission electron microscope. Images were captured using a digital CCD camera system (Advanced Microscopy Techniques, Danvers, MA) and evaluated by a veterinary pathologist.

Neuropharmacokinetic Studies in Male CD-1 Mice. The in-life and bioanalytical portions of these studies were conducted at BioDuro, Pharmaceutical Product Development Inc. (Beijing, China). Male CD-1 mice were obtained from PUMC, China. Mice received a 10 mg/kg subcutaneous (sc) dose of compounds **61**, **64**, **65**, or **67**. The doses were prepared in 5% DMSO/95% (0.5% methylcellulose) and delivered in a volume of 5 mL/kg. Animals were sacrificed in a CO_2 chamber. Blood, brain and CSF samples were collected at 1, 4 and 7 hours post-dosing. Plasma was isolated after centrifugation. The plasma, brain and CSF samples were stored at –80 °C prior to analysis.

Measurement of Fraction Unbound in Brain. The unbound fraction of each compound was determined in brain tissue homogenate using a 96-well equilibrium dialysis method as described by Kalvass et al. [42] with the following exceptions. Brain homogenates were prepared from freshly harvested rat brains following dilution with a 4-fold volume of phosphate buffer,

and spiked with 1 μM compound. The homogenates were dialyzed against an equal volume (150 μL) of phosphate buffer at 37 ^{o}C for 6 h. After the incubation, equal volumes (50 μL) of brain homogenate and buffer samples were collected and mixed with 50 μL of buffer or control homogenate, respectively, for preparation of mixed matrix samples. All samples were then precipitated with internal standard in acetonitrile (200 μL), vortexed, and centrifuged. Supernatants were analyzed using an LC-MS/MS assay. A dilution factor of 5 was applied to the calculation of brain fraction unbound.

Generic Liquid Chromatography Tandem Mass Spectrometry (LC-MS/MS) Assay for Exposure Measurements in Plasma, Brain and CSF. Plasma, brain, and CSF were collected as described above and frozen at –80 °C until analysis by LC-MS/MS. Standard curves were prepared in respective matrix via serial dilution at a concentration of 1.0–2000 ng/mL (plasma and CSF) or 0.5–2000 ng/g (brain). For plasma, a 50 μL aliquot of sample was precipitated with 500 μL of MTBE containing an internal standard. Samples were vortexed for 1 min, then centrifuged at 3000 rpm for 10 min. The supernatant was transferred to a 96-well plate. Frozen brain tissue was weighed and an isopropanol:water (60:40) volume equivalent to 4 times the mass was added before homogenization in a bead beater (BioSpec Products Inc., Bartlesville, OK). A 50 μL aliquot of sample was precipitated with 500 μL of MTBE containing an internal standard. Samples were vortexed for 1 min, then centrifuged at 3000 rpm for 10 min. The supernatant was transferred to a 96-well plate. For CSF, a 50 μL aliquot of sample was precipitated with 500 μL of MTBE containing an internal standard. Samples were vortexed for 1 min, then centrifuged at 3000 rpm for 10 min. The supernatant (300 μL) was transferred to a 96-well plate. LC-MS/MS analysis was carried out using a high-performance liquid chromatography system consisting of tertiary Shimadzu LC20AD pumps (Shimadzu Scientific

Instruments, Columbia, MD) with a CTC PAL autosampler (Leap Technologies, Carrboro, NC) interfaced to an API 4000 LC-MS/MS quadrupole tandem mass spectrometer (AB Sciex Inc., Ontario, Canada). The mobile phase consisted of solvent A (water with 0.1% formic acid) and solvent B (acetonitrile with 0.1% formic acid). The gradient was as follows: solvent B was held at 5% for 0.4 min, linearly ramped from 5% to 95% in 0.5 min, held at 90% for 0.6 min and then stepped to 5% over 0.01 min. The mass spectrometer was operated using positive electrospray ionization. All raw data was processed using Analyst Software ver. 1.4.2 (AB Sciex Inc., Ontario, Canada).

hERG Patch Clamp Assay. All testing was carried out in CHO cells transfected with the hERG gene, purchased from Millipore (PrecisION hERG-CHO Recombinant Cell Line CYL3038). The cell line was grown in DMEM/F-12, GlutaMAX with 10% fetal bovine serum, 1% penicillin-streptomycin, 1% genticin and 1% of 1 M HEPES buffer solution, and maintained at approximately 37 °C in a humidified atmosphere containing 5% carbon dioxide. The cells were passaged every 3-5 days based on confluency. On the day of the experiment, 50%-80% confluent cells were harvested from a 175 cm^2 culture flask using Detachin. After 10 minutes of exposure to Detachin at 37 °C, the cells were centrifuged for 1 minute at 1000 rpm. The supernatant was removed and the cell pellet was reconstituted in 5-8 mL of serum-free media with 2.5% of 1 M HEPES, placed on the Qstirrer, and allowed to recover. After a ~30 minute recovery period, experiments were initiated.

hERG Potassium Channel Current Recordings. hERG current was elicited and recorded using the automated Qpatch HT system.[43] The suspended cells in the Qstirrer were transferred to 48 individual recording chambers on a Qplate 48 containing extracellular recording saline composed of (in mM): 132 NaCl, 4 KCl, 1.8 $CaCl_2$, 1.2 $MgCl_2$, 10 HEPES, 11.1 glucose,

and adjusted to pH 7.35 ± 0.1 with NaOH. The intracellular recording saline was composed of (in mM): 70 KF, 60 KCl, 15 NaCl, 5 EGTA, 5 HEPES, and adjusted to pH 7.2 ± 0.1 with KOH. Membrane currents were recorded at room temperature.

hERG current was elicited from a holding potential of –80 mV with a voltage step to +30 mV for 1 second, followed by a ramp back to –80 mV at 0.55 mV/ms. Test pulses were delivered at a frequency of 0.25 Hz. Up to 4 different concentrations were studied for each cell, each exposure lasting 5 minutes or until steady-state effects were observed. In a separate set of experiments, full concentration-response relationships were determined for the positive control, cisapride, and an IC_{50} was reported for this study.

Chemistry General Methods: Solvents and reagents were of reagent grade and were used as supplied by the manufacturer. All reactions were run under a N_2 atmosphere. Organic extracts were routinely dried over anhydrous Na_2SO_4. Concentration refers to rotary evaporation under reduced pressure. Chromatography refers to flash chromatography using disposable RediSepRf 4 to 120 g silica columns or Biotage disposable columns on a CombiFlash Companion or Biotage Horizon automatic purification system. Microwave reactions were carried out in a SmithCreator microwave reactor from Personal Chemistry. Purification by mass-triggered HPLC was carried out using Waters XTerra PrepMS C18 columns, 5 μm, 30 x 100 mm. Compounds were pre-salted as TFA salts and diluted with 1 mL dimethyl sulfoxide. Samples were purified by mass-triggered collection using a mobile phase of 0.1% trifluoroacetic acid in water and acetonitrile, with a gradient of 100% aqueous to 100% acetonitrile over 10 minutes at a flow rate of 20 mL/minute. All target compounds were analyzed using ultra high performance liquid chromatography /ultra violet/ evaporative light scattering detection coupled

to time of flight mass spectrometry (UHPLC/UV/ELSD/TOFMS). LC-MS analyses were performed on a Waters Acquity UPLC-MS system with a Waters Aquity HSS T3, 1.7 μm C18 column (50 mm x 2.1 mm). UPLC conditions: mobile phase A = 0.1% formic acid in water (v/v), mobile phase B = 0.1% formic acid in acetonitrile; flow rate = 1.25 mL/min; compounds were eluted with a gradient of 5% B/A to 95% B/A for 1.1 min. All tested compounds were found to be > 95% pure by UHPLC/UV/ELSD/TOFMS.

UHPLC/MS Analysis. The UHPLC was performed on a Waters ACQUITY UHPLC system (Waters, Milford, MA), which was equipped with a binary solvent delivery manager, column manager, and sample manager coupled to ELSD and UV detectors (Waters, Milford, MA). Detection was performed on a Waters LCT premier XE mass spectrometer (Waters, Milford, MA). The instrument was fitted with an Acquity BEH (Bridged Ethane Hybrid) C18 column (30 mm × 2.1 mm, 1.7 μm particle size, Waters, Milford, MA) operated at 60 °C.

(3aR,5S)-5-Methyl-3,3a,4,5-tetrahydro-7H-pyrano[3,4-c][1,2]oxazole (15)

Step 1. To a suspension of sodium hydride (60% in mineral oil, 13.9 g, 0.348 mol) in tetrahydrofuran (350 mL) was added a solution of (*S*)-pent-4-en-2-ol (10.0 g, 0.116 mol) in tetrahydrofuran (50 mL) at 0 °C. The reaction was warmed to room temperature and stirred for 30 minutes, whereupon 2-bromo-1,1-diethoxyethane (68.6 g, 0.348 mol) was added and the reaction mixture was heated to reflux for 18 hours. The reaction mixture was then cooled to 0 °C, quenched with water (50 mL), and partitioned between ethyl acetate (300 mL) and water (200 mL). The organic layer was washed with saturated aqueous sodium chloride solution (2 x 100 mL), dried, and concentrated *in vacuo*. Silica gel chromatography (Eluent: 30:1 petroleum ether / ethyl acetate) provided the product as a yellow oil. Yield: 17.4 g, 86.0 mmol, 74%. ^{1}H NMR

(400 MHz, $CDCl_3$), δ 5.76-5.85 (m, 1H), 5.02-5.09 (m, 2H), 4.58-4.60 (m, 1H), 3.66-3.74 (m, 2H), 3.43-3.61 (m, 5H), 2.29-2.36 (m, 1H), 2.13-2.20 (m, 1H), 1.21 (t, *J*=7.2 Hz, 6H), 1.14 (d, *J*=6.4 Hz, 3H).

Step 2. To a solution of *(4*S*)-4-(2,2-diethoxyethoxy)pent-1-ene* (17.4 g, 86.0 mmol) in tetrahydrofuran (100 mL) was added aqueous hydrochloric acid (2 M, 51.0 mL, 0.102 mol), and the reaction mixture was heated to 75 °C for 1 hour. After removal of solvent *in vacuo*, ethanol (100 mL) and water (20 mL) were added, followed by sodium acetate (35.17 g, 0.43 mol) and hydroxylamine hydrochloride (17.9 g, 0.257 mol). The reaction mixture was stirred at 60 °C for 18 hours, whereupon it was concentrated *in vacuo*; the residue was then partitioned between water and dichloromethane. The aqueous layer was extracted with dichloromethane (3 x 200 mL) and the combined organic layers were dried over sodium sulfate, filtered, and concentrated under reduced pressure. Silica gel chromatography (Eluent: 10:1 petroleum ether / ethyl acetate) provided the product as a yellow oil, which was used without further purification in the subsequent step. Yield: 8.6 g, 60 mmol, 70%.

Step 3. To a solution of *(1*E*)*-N-*hydroxy-2-[(2*S*)-pent-4-en-2-yloxy]ethanimine* (8.6 g, 60 mmol) and triethylamine (0.455 g, 4.50 mmol) in dichloromethane (150 mL) at room temperature was slowly added an aqueous solution of sodium hypochlorite (6%, 90 mL), at a rate that maintained the internal reaction temperature between 20 °C and 25 °C. After completion of the addition, the organic layer was dried, filtered, and concentrated *in vacuo.* Silica gel chromatography (Eluent: 10:1 petroleum ether / ethyl acetate) provided the product as a yellow oil. Yield: 5.70 g, 40.4 mmol, 67%. LCMS *m/z* 142.1 [$M+H^+$], ^{1}H NMR (400 MHz, $CDCl_3$), δ 4.68 (d, *J* = 13.2 Hz, 1H), 4.59 (dd, *J* = 10, 8 Hz, 1H), 4.18 (d, *J* = 13.2 Hz, 1H), 3.76 (dd, *J* = 12, 8 Hz, 1H), 3.59-3.66 (m, 1H), 3.39-3.50 (m, 1H), 2.14-2.19 (m, 1H). 1.42-1.51 (m, 1H), 1.25 (d, *J*=6 Hz, 3H).

Synthesis of (4aR,6S,8aS)-8a-(2,4-difluorophenyl)-6-methyl-4,4a,5,6,8,8a-hexahydropyrano[3,4-d][1,3]thiazin-2-amine (40)

Step 1: Prepared in similar fashion as **18** but utilized 2,4-difluoro-1-iodobenzene (5.28 g, 22 mmol), $BF_3{\cdot}Et_2O$ (3.12g, 22 mmol), n-BuLi (8.8 mL, 2.5 M in hexane, 22 mmol), **15** (1.55 g, 11 mmol), and 10/1 (v/v) toluene/THF (70 mL total) to afford (3aR,5S,7aS)-7a-(2,4-difluorophenyl)-5-methylhexahydro-1H-pyrano[3,4-c]isoxazole **(16)** (2.24g, 80% yield) as a white solid. ^{1}H NMR (400 MHz, $CDCl_3$) δ 7.92 (td, *J* = 6.9, 9.0, 9.0 Hz, 1H), 6.88 (dddd, *J* = 0.9, 2.5, 8.0, 8.8 Hz, 1H), 6.79 (ddd, *J* = 2.5, 8.6, 11.3 Hz, 1H), 6.30 (s, 1H), 4.10 (dd, *J* = 1.9, 12.6 Hz, 1H), 3.79 (d, *J* = 12.7 Hz, 1H), 3.75 – 3.66 (m, 2H), 3.53 (dd, *J* = 5.0, 7.1 Hz, 1H), 3.06 (dddd, *J* = 1.5, 4.9, 6.4, 11.5 Hz, 1H), 1.90 – 1.80 (m, 1H), 1.51 – 1.38 (m, 1H), 1.26 (d, *J* = 6.2 Hz, 3H).

Step 2: To a solution of **16** (2.6 g, 10.2 mmol) in acetonitrile:water (90 mL: 6 mL) was added molybdenum hexacarbonyl (2.96 g, 11.2 mmol) in one portion at room temperature. The mixture was refluxed for 30 min and cooled down, then sodium borohydride (388 mg, 10.2 mmol) was added slowly. The reaction was refluxed for two hours then the mixture was concentrated. Ethyl acetate (30 mL) was added to the residue then filtered. The filtrate was washed with brine (100 mL x 4). The organic phase was dried and concentrated. The residue was purified by flash column chromatography (Gradient: 10% to 50% ethyl acetate in petroleum ether to afford ((2S,4R,5S)-5-amino-5-(2,4-difluorophenyl)-2-methyltetrahydro-2H-pyran-4-yl)methanol **(24)** (2 g, 76% yield) as yellow oil. LCMS *m/z* 403.0 $[M + H]^+$. ^{1}H NMR (400 MHz, $CDCl_3$) δ 7.64 (td, *J* = 6.4, 8.9, 9.0 Hz, 1H), 6.99 – 6.89 (m, 1H), 6.81 (ddd, *J* = 2.6, 8.6, 12.6 Hz, 1H), 4.18 (dd, *J* = 2.5, 11.3 Hz, 1H), 3.70 (dtt, *J* = 3.0, 3.0, 6.0, 6.0, 12.1 Hz, 1H), 3.52 (dd, *J* = 2.6, 11.4 Hz,

1H), 3.37 – 3.29 (m, 2H), 2.25 (dq, *J* = 2.7, 2.8, 2.8, 12.8 Hz, 1H), 1.98 – 1.84 (m, 1H), 1.68 (ddd, *J* = 2.6, 4.3, 14.2 Hz, 1H), 1.32 (d, *J* = 6.1 Hz, 3H).

Step 3: Prepared in similar fashion as **35** but utilized **24** (450 mg, 1.75 mmol), benzoyl isothiocyanate (0.99 g, 6.12 mmol) and ethyl acetate (20 mL). After stirring at room temperature for 2 hours the reaction was then stirred at 90 ^{o}C for 16 hours. The reaction was cooled to room temperature, left standing overnight which gave way to a white precipitate. The heterogeneous mixture was concentrated to ~ 3 mL and the solid was filtered. The solid was recrystallized twice from ethyl acetate (~10 mL) then lyophilized to afford N-((4aR,6S,8aS)-8a-(2,4-difluorophenyl)-6-methyl-4,4a,5,6,8,8a-hexahydropyrano[3,4-d][1,3]thiazin-2-yl)benzamide **(32)** (290 mg, 41.2%) as a white solid. LCMS *m/z* 403.0 $[M + H]^+$. ^{1}H NMR (400 MHz, $CDCl_3$) δ 12.26 (br s, 1H), 8.23 (d, 2H), 7.54-7.34 (m, 4H), 6.96 – 6.82 (m, 2H), 4.13 (d, 1H), 3.84 – 3.69 (m, 2H), 3.19 – 3.06 (m, 1H), 2.99 (dd, 1H), 2.62 (dd, 1H), 2.00 – 1.84 (m, 1H), 1.68 – 1.60 (m, 1H), 1.28 (d, 3H).

Step 4: To a stirring solution of **32** (304 mg, 0.775 mmol) in methanol (18.9 mL) was added DBU (96.8 mg, 0.604 mmol). The reaction was stirred at 80 °C overnight, cooled to room temperature, concentrated *in vacuo*, then partitioned between ethyl acetate and saturated aqueous sodium bicarbonate solution. The aqueous layer was washed with ethyl acetate then the combined organic extracts were washed with water followed by brine solution. The organic extract was dried over Na_2SO_4, filtered then concentrated *in vacuo* to afford the crude material which was purified by flash column chromatography (silica gel, 100% ethyl acetate isocratic) to afford (188 mg, 83.4%) of (4aR,6S,8aS)-8a-(2,4-difluorophenyl)-6-methyl-4,4a,5,6,8,8a-hexahydropyrano[3,4 d][1,3]thiazin-2-amine **(40)** as a white solid. LCMS *m/z* 299.1 $[M + H]^+$ ^{1}H

NMR (400 MHz, CD_3OD) δ 7.39 – 7.30 (m, 1H), 7.01 – 6.92 (m, 2H), 4.08 (dd, *J* = 2.3, 11.1 Hz, 1H), 3.74 (dqd, *J* = 2.3, 6.1, 6.1, 6.1, 12.2 Hz, 1H), 3.65 (d, *J* = 11.1 Hz, 1H), 2.94 – 2.82 (m, 2H), 2.70 – 2.62 (m, 1H), 1.76 – 1.65 (m, 1H), 1.54 (ddd, *J* = 2.4, 4.1, 13.2 Hz, 1H), 1.22 (d, *J* = 6.2 Hz, 3H). $[\alpha]_D^{28.5}$ = -5.217° (*c* 0.547, CH_3OH).

Synthesis of (4aR,6S,8aS)-6-methyl-8a-(2-(trifluoromethyl)phenyl)-4,4a,5,6,8,8a-hexahydropyrano[3,4-d][1,3]thiazin-2-amine (41)

Step 1: Prepared in similar fashion as **18** but utilized 1-iodo-2-(trifluoromethyl)benzene (2.89 g, 10.6 mmol, 1.2 eq), $BF_3{\cdot}Et_2O$ (1.81 g, 1.6 mL, 12.8 mmol), n-BuLi (5.7 mL, 2.5 M in hexane, 14.2 mmol), **15** (1.5 g, 10.6 mmol), toluene (70 mL) and THF (7 mL) to afford two separate batches of (3aR,5S,7aS)-5-methyl-7a-(2-(trifluoromethyl)phenyl)hexahydro-1H-pyrano[3,4-c]isoxazole **(17)** as white oils after combining different flash column fractions. Combined yield: 62.1%. Batch 1 (293 mg, 99.01% purity by LCMS, 9.6% yield) LCMS *m/z* 287.9 $[M + H]^+$. ^1H NMR (400 MHz, $CDCl_3$) δ 8.46 (d, *J* = 8.2 Hz, 1H), 7.71 (d, *J* = 7.9 Hz, 1H), 7.57 (t, *J* = 7.7, 7.7 Hz, 1H), 7.42 (t, *J* = 7.6, 7.6 Hz, 1H), 6.45 (s, 1H), 4.13 (d, *J* = 12.8 Hz, 1H), 3.81 – 3.69 (m, 3H), 3.50 (dd, *J* = 7.1, 4.8 Hz, 1H), 3.22 (dt, *J* = 11.6, 5.8, 5.8 Hz, 1H), 1.87 (ddd, *J* = 14.2, 7.2, 2.1 Hz, 1H), 1.46 (dt, *J* = 14.2, 11.4, 11.4 Hz, 1H), 1.25 (d, *J* = 6.1 Hz, 3H). Batch 2 (1.60 g, 90.20% purity by LCMS, 52.5% yield) LCMS *m/z* 287.9 $[M + H]^+$.

Step 2: Prepared in similar fashion as **26** but utilized **7** (1.60g, 5.6 mmol), Raney nickel (817mg, 13.9 mmol), isopropanol (40 mL) and THF (40 mL) to afford ((2S,4R,5S)-5-amino-2-methyl-5-(2-(trifluoromethyl)phenyl)tetrahydro-2H-pyran-4-yl)methanol **(25)**, (1.58g, 70% purity by LCMS) as a white oil that was advanced as is without further purification. LCMS *m/z* 289.9 $[M + H]^+$.

Step 3: Prepared in similar fashion as **35** but utilized **25** (1.58 g, 5.46 mmol), benzoyl isothiocyanate (1.96 g, 12.01 mmol) and ethyl acetate (120 mL). After benzoyl isothiocyanate addition, the reaction was stirred at room temperature for 2 hours rather than 1.5 hours before heating to 90°C for 20 hours. Flash column chromatography (40g silica gel, 0% to 35% ethyl acetate in petroleum ether) afforded a white oil (1.2g) which was diluted in methanol (30 mL) and stirred for 30 minutes. Two crops of white solids were filtered to afford N-((4aR,6S,8aS)-6-methyl-8a-(2-(trifluoromethyl)phenyl)-4,4a,5,6,8,8a-hexahydropyrano[3,4-d][1,3]thiazin-2-yl)benzamide **(33)** (620 mg, 26.1% yield). LCMS *m/z* 434.9 $[M + H]^+$. ^{1}H NMR (400 MHz, $CDCl_3$, 50 °C) δ 12.18 (br s, 1H), 8.23 (s, 2H), 7.85 (d, *J* = 7.9 Hz, 1H), 7.75 (br s, 1H), 7.60 (t, *J* = 7.5, 7.5 Hz, 1H), 7.52 – 7.40 (m, 4H), 4.38 – 3.54 (m, 3H), 3.26 (s, 1H), 3.10 (d, *J* = 9.9 Hz, 1H), 2.62 (dd, *J* = 2.6, 12.7 Hz, 1H), 1.94 (q, *J* = 11.8, 12.0, 12.0 Hz, 1H), 1.70 – 1.61 (m, 1H), 1.30 (d, *J* = 6.1 Hz, 3H).

Step 4: To a stirring solution **33** (500 mg, 1.15 mmol) in methanol (25 mL) was added DBU (263 mg, 1.73 mmol). The reaction was stirred at 70 °C for 16 hours, cooled to room temperature, concentrated *in vacuo*, then subjected to preparative reverse-phase HPLC (Column: DuraShell C18 150 x 25mm x 5µm; Gradient: 34% to 54% acetonitrile in aqueous 0.05% (v/v) ammonia hydroxide over 10 minutes then hold 2 minutes; Flow rate: 30 mL/min). Product fractions were lyophilized then re-purified by preparative reverse-phase HPLC (Column: Phenomenex Gemini C18 250 x 50mm x 10µm; Gradient: 13% to 33% acetonitrile in 0.225% aqueous formic acid over 10 minutes then hold 2 minutes; Flow rate: 30 mL/min). Lyophilization afforded the mono formic acid salt of (4aR,6S,8aS)-6-methyl-8a-(2-(trifluoromethyl)phenyl)-4,4a,5,6,8,8a-hexahydropyrano[3,4-d][1,3]thiazin-2-amine **(41)** (66 mg, 15%) as a white solid. LCMS *m/z* 330.8 $[M + H]^+$. ^{1}H NMR (400 MHz, $CDCl_3$) δ 8.59 (s, 1H, formic acid), 7.89 – 7.77 (m, 2H),

7.70 – 7.61 (m, 1H), 7.47 (t, *J* = 7.7, 7.7 Hz, 1H), 4.11 – 3.97 (m, 1H), 3.83 – 3.70 (m, 1H), 3.42 – 3.27 (m, 1H), 3.14 – 3.03 (m, 1H), 2.67 (dd, *J* = 2.8, 12.7 Hz, 1H), 1.79 (q, *J* = 11.6, 11.9, 11.9 Hz, 1H), 1.66 – 1.57 (m, 1H), 1.31 (d, *J* = 6.1 Hz, 3H). $[\alpha]_D^{28.8}$ = -116.8° (*c* 0.518, CH_3OH).

(4aR,6S,8aS)-6-methyl-8a-phenyl-4,4a,5,6,8,8a-hexahydropyrano[3,4-d][1,3]thiazin-2-amine (42)

Step 1: To a colorless solution of iodobenzene (2.25 g, 11.1 mmol, 1.2 eq) in toluene (80 mL) was added $BF_3 \cdot Et_2O$ (1.57 g, 1.39 mL, 11.1 mmol) at -65°C, followed by slowly addition of n-BuLi (4.94 mL, 2.5 M in hexane, 12.3 mmol, 1.34 eq). After stirring for 10 minutes, a solution of **15** (1.30 g, 9.21 mmol, 1 eq) in THF (8 mL) was added dropwise at -65 °C. The resulting colorless solution was stirred for another 50 minutes at the same temperature. Tlc (petroleum ether: ethyl acetate 2:1, Rf~ 0.6, stained by $KMnO_4$) indicated most of the starting material was consumed and a new less polar spot was shown. The mixture was quenched with saturated aqueous NH_4Cl (80 mL) and the temperature quickly warmed up to -10°C. After warming to room temperature, the mixture was diluted with ethyl acetate (50 mL), partitioned and separated. The aqueous layer was extracted with ethyl acetate (80 mL× 2). The combined organic layers were washed with brine (30 mL), dried over anhydrous Na_2SO_4, filtered and concentrated. Flash column chromatography (silica gel, 0→15% ethyl acetate in petroleum ether gradient) of the crude material afforded (*3aR,5S,7aS*)-5-methyl-7a-phenylhexahydro-1H-pyrano[3,4-c]isoxazole **(18)** (1.30 g, 64.4%) as a white solid. LCMS *m/z* 219.8 $[M + H]^+$. ^1H NMR (400 MHz, Chloroform-*d*) δ 7.59 (d, *J* = 7.7 Hz, 2H), 7.32 (t, *J* = 7.6, 7.6 Hz, 2H), 7.26 – 7.20 (m, 1H), 6.24 (s, 1H), 3.84 (d, *J* = 12.9 Hz, 1H), 3.75 (d, *J* = 12.9 Hz, 1H), 3.62 (t, *J* = 7.9, 7.9 Hz, 2H), 3.48 (dd, *J* = 7.0, 4.8 Hz, 1H), 2.92 – 2.81 (m, 1H), 1.81 (ddd, *J* = 14.2, 6.8, 2.1 Hz, 1H), 1.43 (dt, *J* = 14.3, 11.7, 11.7 Hz, 1H), 1.24 (d, *J* = 6.1 Hz, 3H).

Step 2: Raney nickel (0.603g, 13.7 mmol) was added to a solution of **18** (1.2 g, 5.472 mmol, 1eq) in isopropanol (20 mL) and THF (20 mL) at room temperature while under Ar. The resulting black mixture was degassed three times with hydrogen and stirred at 50 ^{o}C under a hydrogen balloon (~15 psi) for 2 hours. TLC (petroleum ether: ethyl acetate 2: 1, Rf ~0.03, UV) showed the starting material was consumed completely. The mixture was cooled to room temperature and filtered through a pad of Celite® pad. The filter cake was washed with ethyl acetate (40 mL). The combined filtrates were concentrated *in vacuo* to afford ((2S,4R,5S)-5-amino-2-methyl-5-phenyltetrahydro-2H-pyran-4-yl)methanol **(26)** (1.32 g) as a crude yellow oil that was advanced as is without further purification.

Step 3: Benzoyl isothiocyanate (2.14 g, 13.1 mmol) was added in one portion to a stirring solution **26** (1.32 g, 5.965 mmol) in ethyl acetate (30 mL) at room temperature. The resulting yellow solution was stirred at room temperature for 20 hours then at 90 ^{o}C for an additional 20 hours. The reaction mixture was filtered, the filter cake was washed with ethyl acetate (10 mL) and the solid was dried *in vacuo* to afford N-((4aR,6S,8aS)-6-methyl-8a-phenyl-4,4a,5,6,8,8a-hexahydropyrano[3,4-d][1,3]thiazin-2-yl)benzamide **(34)** (1.28 g, 58.6% yield) as a yellow solid. LCMS *m/z* 366.9 $[M + H]^{+}$. ^{1}H NMR (400 MHz, $CDCl_3$) δ 12.13 (br s, 1H), 8.29 – 8.22 (m, 2H), 7.53 – 7.30 (m, 8H), 3.83 – 3.72 (m, 3H), 3.02 (dd, *J* = 12.6, 4.1 Hz, 1H), 2.80 – 2.72 (m, 1H), 2.53 (dd, *J* = 12.7, 2.9 Hz, 1H), 2.04 – 1.92 (m, 1H), 1.66 (ddd, *J* = 13.7, 4.3, 2.3 Hz, 1H), 1.30 (d, *J* = 6.1 Hz, 3H).

Step 4: DBU (218mg, 1.43 mmol) was added to a solution of **34** (350mg, 0.955 mmol) in methanol (15mL) at room temperature. The reaction was stirred at 70^{o}C for 16 hours, concentrated *in vacuo* then the crude material was purified by preparative reverse-phase HPLC

(Column: DuraShell 150x25mmx5µm; Gradient: 24% to 44% acetonitrile in aqueous 0.05% (v/v) ammonia hydroxide over 10 minutes then hold 2 minutes; Flow rate: 30 mL/min). After concentration and lyophilization, compound **42** (184 mg, 73.4% yield) was obtained as a white solid. LCMS *m/z* 262.8 $[M + H]^+$. ^{1}H NMR (400 MHz, Chloroform-*d*) δ 7.37 – 7.29 (m, 4H), 7.27 – 7.21 (m, 1H), 4.54 (s, 2H), 3.85 (d, *J* = 11.2 Hz, 1H), 3.77 – 3.67 (m, 2H), 2.98 (dd, *J* = 4.1, 12.0 Hz, 1H), 2.49 (dd, *J* = 2.7, 12.1 Hz, 1H), 2.44 (dt, *J* = 3.5, 3.5, 12.2 Hz, 1H), 1.80 (q, *J* = 12.0, 12.3, 12.3 Hz, 1H), 1.48 (ddd, *J* = 2.4, 3.8, 13.2 Hz, 1H), 1.29 (d, *J* = 6.1 Hz, 3H). ^{13}C NMR (100 MHz, $CDCl_3$) δ 151.00, 143.35, 128.62, 127.07, 126.53, 79.24, 73.76, 58.75, 33.47, 32.01, 28.86, 21.85. $[\alpha]_D^{28.8}$ = +0.844° (*c* 0.533, CH_3OH). For 2D-NMR experiments (HSQC, NOESY) see SI, Table 1.

Synthesis of (4aR,6S,8aS)-8a-(2-methoxyphenyl)-6-methyl-4,4a,5,6,8,8a-hexahydropyrano[3,4-d][1,3]thiazin-2-amine (43)

Step 1: Prepared in similar fashion as **18** but utilized 2-bromoanisole (2.38 g, 12.8 mmol), $BF_3{\cdot}Et_2O$ (1.81 g, 1.6 mL, 12.8 mmol), n-BuLi (5.7 mL, 2.5 M in hexane, 14.2 mmol), **15** (1.5 g, 10.6 mmol), toluene (80mL) and THF (8mL) to afford (3aR,5S,7aS)-7a-(2-methoxyphenyl)-5-methylhexahydro-1H-pyrano[3,4-c]isoxazole **(19)** (718mg, 27.1% yield) as a colorless gum. LCMS *m/z* 249.8 $[M + H]^+$. ^{1}H NMR (400 MHz, $CDCl_3$) δ 7.81 (d, *J* = 7.6 Hz, 1H), 7.19 – 7.13 (m, 1H), 6.88 (t, *J* = 7.5, 7.5 Hz, 1H), 6.78 (d, *J* = 8.2 Hz, 1H), 6.21 (s, 1H), 4.27 (d, *J* = 12.4 Hz, 1H), 3.77 (s, 3H), 3.69 – 3.55 (m, 2H), 3.53 (d, *J* = 6.9 Hz, 1H), 3.44 – 3.38 (m, 1H), 3.22 (ddd, *J* = 11.8, 7.0, 4.9 Hz, 1H), 1.71 (ddd, *J* = 14.0, 7.0, 2.0 Hz, 1H), 1.32 (dt, *J* = 14.1, 11.5, 11.5 Hz, 1H), 1.14 (d, *J* = 6.2 Hz, 3H).

Step 2: Prepared in similar fashion as **26** but utilized **19** (250mg, 1mmol), Raney nickel (147mg, 2.51 mmol), isopropanol (10mL) and THF (10mL) to afford ((2S,4R,5S)-5-amino-5-(2-

methoxyphenyl)-2-methyltetrahydro-2H-pyran-4-yl)methanol **(27)** (245mg, 97.9% yield) as a yellow oil that was advanced as is. LCMS *m/z* 252.0 $[M + H]^+$.

Step 3: Benzoyl isothiocyanate (525 mg, 3.22 mmol) was added in one portion to a stirring solution **27** (245 mg, 0.975 mmol) in ethyl acetate (15 mL) at room temperature. The resulting yellow solution was stirred at room temperature for 1.5 hours then at 90 ^oC for an additional 20 hours. The reaction mixture was concentrated and the crude was purified by flash column chromatography (silica gel, 10→30% ethyl acetate in petroleum ether) to afford 345mg of yellow solid which was triturated with petroleum ether : ethyl acetate (6 mL, 5: 1) to yield (174mg, 45% yield) of N-((4aR,6S,8aS)-8a-(2-methoxyphenyl)-6-methyl-4,4a,5,6,8,8a-hexahydropyrano[3,4-d][1,3]thiazin-2-yl)benzamide **(35)** as as a white solid after filtration. LCMS *m/z* 396.9 $[M + H]^+$. ^1H NMR (400 MHz, $CDCl_3$, 50 °C) δ 12.05 (br s, 1H), 8.27 (d, 2H), 7.51 – 7.35 (m, 4H), 7.31 (td, 1H), 6.99 (t, 1H), 6.95 (d, 1H), 4.38 (d, 1H), 3.88 (s, 3H), 3.81 – 3.68 (m, 2H), 3.55 (d, 1H), 3.11 – 2.94 (m, 1H), 2.53 (dd, 1H), 1.94 (d, 1H), 1.60 (ddd, 1H), 1.28 (d, 3H).

Step 4: DBU (20 µL, 20.4 mg, 0.127 mmol) was added to a stirring suspension of **35** (55 mg, 0.139 mmol) in methanol (2.0 mL). The initial heterogeneous mixture was heated to 70 °C and the resulting solution was heated at that temperature for 16h. The reaction mixture was cooled to room temperature, concentrated, dissolved in dichloromethane (10mL) and washed with brine (2x5mL). The aqueous layers were back- extracted with additional dichloromethane (5 mL) and the combined organic extracts were dried over Na_2SO_4, filtered and concentrated in vacuo. Preparative reverse-phase HPLC purification (Column: XBridge C18 19×100mm 5µm; A=water; B=acetonitrile; Gradient: 95.0% water/5.0% acetonitrile linear to 5.0% water/95.0%

acetonitrile in 8.5min, HOLD at 0% water/100% acetonitrile to 10.0min. Flow Rate: 25mL/min) followed by lyophilization afforded (29.6 mg, 72.9%) of (4aR,6S,8aS)-8a-(2-methoxyphenyl)-6-methyl-4,4a,5,6,8,8a-hexahydropyrano[3,4-d][1,3]thiazin-2-amine **(43)** as a white solid. LCMS *m/z* 293.3 $[M + H]^+$. ^{1}H NMR (400 MHz, Acetonitrile-*d3*) δ 7.28 – 7.20 (m, 2H), 7.01 – 6.97 (m, 1H), 6.92 (td, 1H), 4.83 (br s, 2H), 4.33 (d, 1H), 3.82 (s, 3H), 3.68 (dqd, 1H), 3.43 (d, 1H), 3.31 (dq, 1H), 2.74 (dd, 1H), 2.52 (dd, 1H), 1.62 – 1.51 (m, 1H), 1.45 (dd, 1H), 1.15 (d, 3H). $[\alpha]_D^{29.1}$ = -50.4° (*c* 0.522, CH_3OH).

Synthesis of (4aR,6S,8aS)-8a-(3-fluoropyridin-2-yl)-6-methyl-4,4a,5,6,8,8a-hexahydropyrano[3,4-d][1,3]thiazin-2-amine (44)

Step 1: To a solution of 2-bromo-3-fluoropyridine (3.12g, 17.7 mmol) in toluene (80 mL) and THF (40 mL) was added n-BuLi (7.5 mL, 2.5 M in hexane, 19 mmol,) dropwise at -70 ^{o}C. After stirring for 40 min, a solution of **15** (1 g, 7.084 mmol) in toluene (20 mL) and THF (10 mL) was added dropwise at -70 ^{o}C. The mixture was stirred for 60 minutes at the same temperature. Tlc (petroleum ether: ethyl acetate 2:1, Rf~0.15, stained by $KMnO_4$) showed the reaction was complete. The reaction solution was quenched with saturated aqueous NH_4Cl (50 mL). The mixture was separated and the aqueous layer was extracted with additional ethyl acetate (50 mL× 3). The combined organic layers were dried over anhydrous Na_2SO_4, filtered and concentrated to afford the crude product (3.85 g, yellow oil). Flash column chromatography (silica gel, Gradient: 0 to 60% ethyl acetate in petroleum ether) afforded (3aR,5S,7aS)-7a-(3-fluoropyridin-2-yl)-5-methylhexahydro-1H-pyrano[3,4-c]isoxazole **(20)** (1.15g, 68.1% yield) as a white solid. LCMS *m/z* 238.8 $[M + H]^+$. ^{1}H NMR (400 MHz, $CDCl_3$) δ 8.39 (d, *J* = 4.5 Hz, 1H), 7.41 (dd, *J* = 11.1, 8.3 Hz, 1H), 7.31 – 7.26 (m, 1H), 6.41 (s, 1H), 4.18 (s, 1H), 3.84 (d, *J* = 12.3 Hz, 1H), 3.65 (dt, *J*

= 18.7, 6.2, 6.2 Hz, 4H), 1.88 (dd, *J* = 13.9, 6.8 Hz, 1H), 1.79 – 1.54 (m, 1H), 1.27 (d, *J* = 6.1 Hz, 3H).

Step 2: Prepared in similar fashion as **26** but utilized **20** (780mg, 3.27 mmol), Raney nickel (576mg, 9.82 mmol), isopropanol (20mL) and THF (20mL) to afford crude ((2S,4R,5S)-5-amino-5-(3-fluoropyridin-2-yl)-2-methyltetrahydro-2H-pyran-4-yl)methanol **(20)** (780mg) as a white oil that was advanced as is without further purification.

Step 3: Prepared in similar fashion as **35** but utilized **20** (0.78 g, 3.25 mmol), benzoyl isothiocyanate (1.32 g, 8.12 mmol) and ethyl acetate (30 mL). After stirring at room temperature for 1.5 hours the reaction was then stirred at 90 ^{o}C for 16 hours. Flash column chromatography (12g silica gel, 10% to 100% ethyl acetate in petroleum ether) of the crude material afforded N-((4aR,6S,8aS)-8a-(3-fluoropyridin-2-yl)-6-methyl-4,4a,5,6,8,8a-hexahydropyrano[3,4-d][1,3]thiazin-2-yl)benzamide **(28)** (560 mg, 44.7% yield) as a yellow solid. LCMS *m/z* 385.9 $[M + H]^+$. ^{1}H NMR (400 MHz, $CDCl_3$) δ 12.45 (br s, 1H), 8.40 (dt, *J* = 4.4, 1.4, 1.4 Hz, 1H), 8.23 (dd, *J* = 8.3, 1.3 Hz, 2H), 7.49 – 7.36 (m, 4H), 7.31 (dt, *J* = 8.3, 3.9, 3.9 Hz, 1H), 4.18 (d, *J* = 12.1 Hz, 1H), 3.76 – 3.65 (m, 2H), 3.52 (dd, *J* = 12.8, 4.3 Hz, 1H), 3.44 (dq, *J* = 11.3, 4.2, 4.1, 4.1 Hz, 1H), 2.64 (dd, *J* = 12.8, 2.6 Hz, 1H), 1.98 (q, *J* = 12.9, 12.9, 12.8 Hz, 1H), 1.66 (ddd, *J* = 13.5, 4.2, 2.3 Hz, 1H), 1.28 (d, *J* = 6.1 Hz, 3H).

Step 4: To a stirring solution **28** (480 mg, 1.25 mmol) in methanol (10 mL) was added DBU (190 mg, 1.25 mmol). The reaction was stirred at 70 °C for 16 hours, cooled to room temperature, concentrated *in vacuo*, then purified by flash column chromatography (silica gel, Gradient: 0→10% methanol in dichloromethane) to afford (4aR,6S,8aS)-8a-(3-fluoropyridin-2-yl)-6-

methyl-4,4a,5,6,8,8a-hexahydropyrano[3,4-d][1,3]thiazin-2-amine **(36)** (105 mg, white solid, contaminated with DBU). The solid was suspended in water (10 mL), stirred for 1 hour, filtered and lyophilized to afford pure **(36)** (52 mg, 14.8% yield) as a white solid. LCMS *m/z* 281.8 [M + H]$^+$ ^{1}H NMR (400 MHz, $CDCl_3$) δ 8.36 (d, *J* = 4.0 Hz, 1H), 7.41 – 7.29 (m, 1H), 7.20 (dt, *J* = 3.8, 3.8, 7.8 Hz, 1H), 4.38 (br s, 2H), 4.16 (d, *J* = 11.0 Hz, 1H), 3.76 (d, *J* = 11.0 Hz, 1H), 3.72 – 3.61 (m, 1H), 3.39 (dd, *J* = 4.6, 12.3 Hz, 1H), 3.09 – 2.96 (m, 1H), 2.66 – 2.56 (m, 1H), 1.77 (q, *J* = 12.5, 12.6, 12.6 Hz, 1H), 1.53 – 1.42 (m, 1H), 1.26 (d, *J* = 6.1 Hz, 3H). $[\alpha]_D^{29.0}$ = -19.0° (*c* 0.524, CH_3OH).

Synthesis of (4aR,6S,8aS)-6-methyl-8a-(thiophen-3-yl)-4,4a,5,6,8,8a-hexahydropyrano[3,4-d][1,3]thiazin-2-amine (45)

Step 1: To a solution of 3-bromothiophene (2.6 g, 15.9 mmol) in toluene (50 mL) and THF (5 mL) was added $BF_3{\cdot}Et_2O$ (2.11 g, 14.9 mmol) at -70 ^{o}C, followed by slow addition of n-BuLi (2.5M in hexane, 5.12 mL, 12.8 mmol). After stirring for 30 min, a solution of **15** (1.5 g, 10.6 mmol) in toluene (10 mL) and THF (1 mL) was added dropwise at -78 ^{o}C. The mixture was stirred for 60 min at the same temperature. TLC (petroleum ether : ethyl acetate = 3: 1, Rf~0.5, stained by I2) showed the reaction was complete. The reaction solution was quenched with saturated aqueous ammonium chloride (50 mL) and the temperature warmed up to 15 ^{o}C rapidly. The mixture was separated and the aqueous layer was extracted with ethyl acetate (50 mL× 3). The combined organic layers were dried over anhydrous sodium sulfate, filtered and concentrated. The crude product was purified by flash column chromatography (silica gel, 0→20% ethyl acetate in petroleum ether) to afford ~90% pure product (1.25g). This was combined with similarly-enriched material from another reaction (same otherwise but 1/3 the

scale; via 0.5g of **15**) and re-purified as above to afford pure (3aR,5S,7aS)-5-methyl-7a-(thiophen-3-yl)hexahydro-1H-pyrano[3,4-c]isoxazole **(21)** (1.12g, 35.2% averaged yield) as an off-white solid. LCMS *m/z* 225.8 $[M + H]^+$. ^{1}H NMR (400 MHz, $CDCl_3$) δ 7.43 (d, *J* = 2.6 Hz, 1H), 7.30 (dd, *J* = 5.0, 3.0 Hz, 1H), 7.13 (d, *J* = 5.1 Hz, 1H), 6.29 (s, 1H), 3.93 (d, *J* = 12.9 Hz, 1H), 3.79 (d, *J* = 12.8 Hz, 1H), 2.81 (ddd, *J* = 11.5, 6.7, 4.6 Hz, 1H), 1.82 (ddd, *J* = 14.2, 6.7, 2.1 Hz, 1H), 1.44 (dt, *J* = 14.3, 11.6, 11.6 Hz, 1H), 1.26 (d, *J* = 6.1 Hz, 3H).

Step 2: Prepared in similar fashion as **26** but utilized **21** (550mg, 2.44 mmol), Raney nickel (500mg, 8.52 mmol) and ethanol (20mL, in lieu of 1:1 THF:isopropanol) to afford ((2S,4R,5S)-5-amino-2-methyl-5-(thiophen-3-yl)tetrahydro-2H-pyran-4-yl)methanol **(29)** (550mg) as a colorless oil that was advanced as is without further purification.

Step 3: Prepared in similar fashion as **35** but utilized **29** (550 mg, 2.42 mmol), benzoyl isothiocyanate (1g, 6.1 mmol) and ethyl acetate (20 mL). After stirring at room temperature for 1.5 hours the reaction was then stirred at 90 ^{o}C for 16 hours. Two identical flash column chromatographies (12g silica gel, Gradient: 5% to 30% ethyl acetate in petroleum ether) afforded N-((4aR,6S,8aS)-6-methyl-8a-(thiophen-3-yl)-4,4a,5,6,8,8a-hexahydropyrano[3,4-d][1,3]thiazin-2-yl)benzamide **(29)** (240 mg, 66.6% yield) as an off-white solid. LCMS *m/z* 372.8 $[M + H]^+$. ^{1}H NMR (400 MHz, $CDCl_3$) δ 12.40 (br s, 1H), 8.22 (d, *J* = 6.6 Hz, 2H), 7.51 – 7.38 (m, 4H), 7.25 – 7.23 (m, 1H), 6.98 (dd, *J* = 5.1, 1.5 Hz, 1H), 3.87 (d, *J* = 12.4 Hz, 1H), 3.82 – 3.69 (m, 2H), 3.14 (dd, *J* = 12.4, 3.9 Hz, 1H), 2.66 – 2.52 (m, 2H), 2.03 – 1.90 (m, 1H), 1.68 – 1.61 (m, 1H), 1.29 (d, *J* = 6.1 Hz, 3H).

Step 4: To a stirring solution of **29** (170 mg, 0.456 mmol) in methanol (10 mL) was added DBU (69.5 mg, 0.456 mmol). The reaction was stirred at 70 °C for 16 hours, cooled to room

temperature, concentrated *in vacuo*, then subjected to preparative reverse-phase HPLC (Column: DuraShell C18 150 x 25mm x 5µm; Gradient: 24% to 44% acetonitrile in aqueous 0.05% (v/v) ammonium hydroxide over 10 minutes then hold 2 minutes; Flow rate: 30 mL/min). Product fractions were lyophilized to afford (4aR,6S,8aS)-6-methyl-8a-(thiophen-3-yl)-4,4a,5,6,8,8a-hexahydropyrano[3,4-d][1,3]thiazin-2-amine **(45)** (58 mg, 47.4% yield) as a white solid. LCMS *m/z* 268.8 $[M + H]^+$. ^{1}H NMR (400 MHz, $CDCl_3$) δ 7.30 (dd, *J* = 3.1, 5.0 Hz, 1H), 7.08 (dd, *J* = 1.3, 3.1 Hz, 1H), 6.96 (dd, *J* = 1.3, 5.1 Hz, 1H), 4.43 (br s, 2H), 3.88 (d, *J* = 11.2 Hz, 1H), 3.76 – 3.64 (m, 2H), 3.07 (dd, *J* = 4.1, 12.1 Hz, 1H), 2.52 (dd, *J* = 2.8, 12.2 Hz, 1H), 2.33 – 2.25 (m, 1H), 1.83 – 1.71 (m, 1H), 1.46 (ddd, *J* = 2.2, 4.0, 13.3 Hz, 1H), 1.27 (d, *J* = 6.2 Hz, 3H). $[\alpha]_D^{29.0}$ = +46.0° (*c* 0.524, CH_3OH).

(4aR,6S,8aR)-6-methyl-8a-(thiophen-2-yl)-4,4a,5,6,8,8a-hexahydropyrano[3,4-d][1,3]thiazin-2-amine (46)

Step 1: Prepared in similar fashion to **18** but utilized 2-bromothiophene (1.91 g, 11.7 mmol), $BF_3 . Et_2O$ (1.7 g, 1.5 mL, 12 mmol), n-BuLi (2.5M in hexane, 5.1 mL, 12.8 mmol), **15** (1.5g, 10.6 mmol), toluene (80 mL) and THF (8 mL) at -70 ^{o}C rather than at -65 ^{o}C. Purification of the crude compound by flash column chromatography (silica gel, 0 to 25% ethyl acetate in petroleum ether) afforded an off-white solid (1.78g) which was dissolved in ethyl acetate (30cmL), concentrated to ~10mL causing a precipitate then filtered to obtain pure (3aR,5S,7aR)-5-methyl-7a-(thiophen-2-yl)hexahydro-1H-pyrano[3,4-c]isoxazole **(22)** (995mg, 41.6% yield) as a white solid. LCMS *m/z* 225.7 $[M + H]^+$. ^{1}H NMR (400 MHz, $CDCl_3$) δ 7.22 (d, *J* = 5.0 Hz, 1H), 7.03 (dd, *J* = 3.6, 1.1 Hz, 1H), 6.99 (dd, *J* = 5.0, 3.6 Hz, 1H), 6.37 (s, 1H), 3.99 (d, *J* = 12.8 Hz, 1H), 3.84 – 3.69 (m, 3H), 3.64 (dqd, *J* = 12.1, 6.2, 6.1, 6.1, 2.1 Hz, 1H), 2.89 (ddd, *J* = 11.5, 6.7, 4.6

Hz, 1H), 1.84 (ddd, *J* = 14.2, 6.8, 2.1 Hz, 1H), 1.45 (dt, *J* = 14.2, 11.6, 11.6 Hz, 1H), 1.26 (d, *J* = 6.2 Hz, 3H). Concentration of the mother liquor afforded additional **22** as a pale yellow solid (780mg, 32.6% yield) of slightly lower purity by 1H-NMR as compared to the precipitated batch. Combined yield is 74.2%.

Step 2: Prepared in similar fashion as **26** but utilized **22** (780 mg, 3.46 mmol), Raney nickel (508 mg, 8.66 mmol), isopropanol (10 mL) and THF (10 mL) to afford ((2S,4R,5R)-5-amino-2-methyl-5-(thiophen-2-yl)tetrahydro-2H-pyran-4-yl)methanol **(30)** (740 mg, 94% yield) as a yellow oil that was advanced as is without further purification. LCMS *m/z* 227.8 $[M + H]^+$

Step 3: Prepared in similar fashion as **35** but utilized **30** (700 mg, 2.35 mmol), benzoyl isothiocyanate (1.34g , 8.22 mmol, 3.3 eq) and ethyl acetate (25 mL). Two sequential flash column chromatographies (Gradient: 0% to 12-13% ethyl acetate in petroleum ether) afforded N-((4aR,6S,8aR)-6-methyl-8a-(thiophen-2-yl)-4,4a,5,6,8,8a-hexahydropyrano[3,4-d][1,3]thiazin-2-yl)benzamide **(38)** (390 mg, 44.6%) as white solid. LCMS *m/z* 372.9 $[M + H]^+$. ^{1}H NMR (400 MHz, $CDCl_3$) δ 12.28 (br s, 1H), 8.19 (d, *J* = 7.6 Hz, 2H), 7.50 (t, *J* = 7.2, 7.2 Hz, 1H), 7.43 (t, *J* = 7.5, 7.5 Hz, 2H), 7.29 (d, *J* = 5.3 Hz, 1H), 7.04 – 6.97 (m, 2H), 3.95 (d, *J* = 12.2 Hz, 1H), 3.82 – 3.70 (m, 2H), 3.27 (dd, *J* = 12.9, 4.1 Hz, 1H), 2.57 (t, *J* = 10.8, 10.8 Hz, 2H), 1.94 (q, *J* = 12.5, 12.5, 12.5 Hz, 1H), 1.70 – 1.64 (m, 1H), 1.28 (d, *J* = 6.1 Hz, 3H).

Step 4: To a stirring solution **38** (175 mg, 0.470 mmol) in methanol (10 mL) was added DBU (107 mg, 0.705 mmol). The reaction was stirred at 70 °C for 16 hours, concentrated *in vacuo*, dissolved in dichloromethane (20 mL) and washed with brine (2x15 mL). The aqueous layers were back- extracted dichloromethane (30mL) and the combined organic extracts were dried

over Na_2SO_4, filtered and concentrated. The crude residue was first purified by silica gel chromatography (gradient: 0→4% methanol in dichloromethane) then twice by preparative reverse-phase HPLC (Column: Diamonsil C18 150x20mmx5µm; Gradient: 22% →42% acetonitrile in aqueous 0.05% (v/v) ammonia hydroxide over 10 minutes then hold 2 minutes; Flow rate: 30 mL/min). Lyophilization afforded (4aR,6S,8aR)-6-methyl-8a-(thiophen-2-yl)-4,4a,5,6,8,8a-hexahydropyrano[3,4-d][1,3]thiazin-2-amine **(46)** (53mg, 42% yield). LCMS *m/z* 268.8 $[M + H]^+$. ^{1}H NMR (400 MHz, $CDCl_3$) δ 7.20 (dd, *J* = 1.1, 5.1 Hz, 1H), 6.98 (dd, *J* = 3.6, 5.1 Hz, 1H), 6.83 (dd, *J* = 1.1, 3.6 Hz, 1H), 4.46 (br s, 2H), 3.96 (d, *J* = 11.2 Hz, 1H), 3.75 – 3.64 (m, 2H), 3.24 (dd, *J* = 4.1, 12.2 Hz, 1H), 2.56 (dd, *J* = 2.8, 12.3 Hz, 1H), 2.37 – 2.28 (m, 1H), 1.84 – 1.73 (m, 1H), 1.49 (ddd, *J* = 2.3, 4.1, 13.4 Hz, 1H), 1.27 (d, *J* = 6.2 Hz, 3H). $[\alpha]_D^{29.1}$ = +10.0° (*c* 0.549, CH_3OH).

Synthesis of (4aR,6S,8aR)-6-methyl-8a-(thiazol-2-yl)-4,4a,5,6,8,8a-hexahydropyrano[3,4-d][1,3]thiazin-2-amine (47)

Step 1: Prepared in similar fashion as **18**, but utilized 2-bromothiazole (2.09 g, 12.8 mmol), $BF_3{\cdot}Et_2O$ (1.81 g, 1.6 mL, 12.8 mmol), n-BuLi (5.7 mL, 2.5 M in hexane, 14.2 mmol), **15** (1.5 g, 10.6 mmol), toluene (80 mL) and THF (8 mL). Flash column chromatography (silica gel, 0→35% ethyl acetate in petroleum ether gradient) on the crude product afforded enriched (3aR,5S,7aR)-5-methyl-7a-(thiazol-2-yl)hexahydro-1H-pyrano[3,4-c]isoxazole **(23)** (630mg) as a yellow solid. This solid was triturated with petroleum ether : ethyl acetate (5:1, 6 mL) to afford pure **23** (456 mg, 19% yield, 100% purity by LCMS) as a white solid. LCMS *m/z* 226.8 $[M + H]^+$. ^{1}H NMR (400 MHz, $CDCl_3$) δ 7.75 (d, *J* = 3.2 Hz, 1H), 7.29 (d, *J* = 3.3 Hz, 1H), 6.45 (s, 1H), 3.97 (d, *J* = 3.1 Hz, 2H), 3.75 – 3.62 (m, 3H), 3.36 (dt, *J* = 12.1, 5.5, 5.5 Hz, 1H), 1.25 (d, *J*

= 6.0 Hz, 3H), 4.03 – 3.91 (m, 2H), 1.88 (ddd, *J* = 13.8, 6.6, 1.8 Hz, 1H), 1.50 – 1.35 (m, 1H). Note: Concentration of the mother liquor afforded additional **23** (153 mg, 6% yield, 94% purity by LCMS) as a pale yellow solid. Combined yield: 25%.

Step 2: Prepared in similar fashion as **26** but utilized **23** (187mg, 0.826 mmol), Raney nickel (121mg, 2.07 mmol), isopropanol (10mL) and THF (10mL) to afford ((2S,4R,5R)-5-amino-2-methyl-5-(thiazol-2-yl)tetrahydro-2H-pyran-4-yl)methanol **(31)** (169mg) as a yellow oil that was advanced as is without further purification.

Step 3: Prepared in similar fashion as **35** but utilized **31** (169 mg, 0.740 mmol), benzoyl isothiocyanate (399 mg, 2.44 mmol) and ethyl acetate (15mL). Flash column chromatography (20g silica gel, 10% to 70% ethyl acetate in petroleum ether) of the crude sample afforded 378mg of a yellow oil that was resubjected to an additional flash column chromatography (12g silica gel, 30% to 50% ethyl acetate in petroleum ether). Two separate batches of N-((4aR,6S,8aR)-6-methyl-8a-(thiazol-2-yl)-4,4a,5,6,8,8a-hexahydropyrano[3,4-d][1,3]thiazin-2-yl)benzamide **(39)** were isolated after combining different flash column fractions. Combined yield: 160mg, 57.9%. Batch 1 (60mg, 21.7% yield, pale yellow solid after lyophilization, 98.9% purity by LCMS). LCMS *m/z* 373.9 $[M + H]^+$. ^{1}H NMR (400 MHz, $CDCl_3$, 50 °C) δ 11.52 (s, 1H), 8.23 – 8.06 (m, 2H), 7.56 – 7.48 (m, 1H), 7.48 – 7.40 (m, 2H), 7.32 (d, *J* = 3.2 Hz, 1H), 4.03 – 3.92 (m, 2H), 3.78 (dq, *J* = 2.3, 6.1, 6.1, 6.1, 12.3 Hz, 1H), 3.20 – 3.07 (m, 2H), 2.59 (dd, *J* = 1.8, 12.4 Hz, 1H), 1.91 (d, *J* = 12.4 Hz, 1H), 1.70 – 1.62 (m, 1H), 1.29 (d, *J* = 6.1 Hz, 3H). Batch 2 (100mg, 36.2% yield, pale yellow oil, 89.2% purity by LCMS). LCMS *m/z* 373.8 $[M + H]^+$.

Step 4: To a stirring mixture of **39** (100 mg, 0.668 mmol) in methanol (10 mL) was added DBU (61.1mg, 0.268 mmol). The reaction was stirred at 70 ^{o}C for 16 hours, concentrated *in vacuo* then the residue dissolved in dichloromethane (20 mL) and washed with brine (2 x 15 mL). The aqueous layers were back- extracted dichloromethane (30 mL) and the combined organic extracts (~50 mL) were dried over Na_2SO_4, filtered and concentrated. Purification of the crude residue by preparative reverse-phase HPLC (Column: Diamonsil C18 150 x 20 mm x 5µm; Gradient: 12% to 32% acetonitrile in aqueous 0.05% (v/v) ammonia hydroxide over 10 minutes then hold 2 minutes; Flow rate: 30 mL/min) followed by concentration and lyophilization of the product fractions afforded (47mg, 65% yield) of (4aR,6S,8aR)-6-methyl-8a-(thiazol-2-yl)-4,4a,5,6,8,8a-hexahydropyrano[3,4-d][1,3]thiazin-2-amine **(47)**. LCMS *m/z* 269.8 $[M + H]^+$. ^{1}H NMR (400 MHz, $CDCl_3$) δ 7.77 (d, *J* = 3.2 Hz, 1H), 7.26 (d, *J* = 2.6 Hz, 1H), 4.71 (s, 2H), 3.95 (d, *J* = 11.1 Hz, 1H), 3.87 (d, *J* = 11.1 Hz, 1H), 3.75 (tdd, *J* = 12.3, 10.6, 6.0, 3.1 Hz, 1H), 3.12 (dd, *J* = 12.5, 3.9 Hz, 1H), 2.90 (dq, *J* = 11.3, 3.5, 3.5, 3.2 Hz, 1H), 2.58 (dd, *J* = 12.5, 2.5 Hz, 1H), 1.80 (q, *J* = 12.8, 12.8, 12.7 Hz, 1H), 1.54 (dt, *J* = 13.5, 3.7, 3.7 Hz, 1H), 1.28 (d, *J* = 6.1 Hz, 3H). $[\alpha]_D^{29.1}$ = -32.7° (*c* 0.554, CH_3OH).

N-(2-((4aR,6S,8aR)-2-amino-6-methyl-4,4a,5,6-tetrahydropyrano[3,4-d][1,3]thiazin-8a(8H)-yl)thiazol-4-yl)-4-methoxybenzamide (56)

Step 1. Synthesis of N-(2-((4aR,6S,8aR)-2-benzamido-6-methyl-4,4a,5,6-tetrahydropyrano[3,4-d][1,3]thiazin-8a(8H)-yl)thiazol-4-yl)-4-methoxybenzamide. To a solution of 4-methoxybenzoic acid (62.0 mg, 0.405 mmol), N,N-diisopropylethylamine (0.080 mL, 0.463 mmol) in DMF (3mL, 0.1M) was added O-(7-azabenzotriazol-1-yl)-N,N,N',N'-tetramethyluronium hexafluorophosphate (HATU, 97%, 154 mg, 0.405 mmol) in one portion at 15 ^{o}C. The resulting mixture was stirred for 30min., followed by addition of **72** (150 mg, 0386 mmol) in one portion.

The resulting mixture was stirred at RT over 16h. The reaction mixture was then partitioned between ethyl acetate (10 mL) and water (10 mL). The aqueous layer was extracted twice with ethyl acetate, and the combined organic layers were washed with saturated aqueous sodium chloride solution (50 mL), dried over sodium sulfate, filtered, and concentrated in vacuo. Silica gel chromatography (Gradient: 10% to 40% ethyl acetate in petroleum ether) afforded the product, N-(2-((4aR,6S,8aR)-2-benzamido-6-methyl-4,4a,5,6-tetrahydropyrano[3,4-d][1,3]thiazin-8a(8H)-yl)thiazol-4-yl)-4-methoxybenzamide, as a solid. Yield: 110 mg, 0.210 mmol, 55%. LC/MS M+z 523.1, M + H). ^{1}H NMR (400 MHz, $CDCl_3$) δ ppm 8.65 (s, 1H), 8.10 (d, *J* = 7.6 Hz, 2H), 8.01 (s, 1H), 7.92 – 7.85 (m, 2H), 7.73 (s, 1H), 7.58 – 7.50 (m, 1H), 7.46 (dd, *J* = 8.2, 6.7 Hz, 2H), 7.01 – 6.95 (m, 2H), 3.88 (s, 3H), 3.81 – 3.69 (m, 1H), 3.17 (dd, *J* = 13.0, 4.0 Hz, 1H), 2.95 (m, 2H), 2.59 (dd, *J* = 12.9, 2.8 Hz, 1H), 1.90 (q, *J* = 12.6 Hz, 1H), 1.71 – 1.62 (m, 2H), 1.33 – 1.27 (d, 3H).

Step 2. Synthesis of N-(2-((4aR,6S,8aR)-2-amino-6-methyl-4,4a,5,6-tetrahydropyrano[3,4-d][1,3]thiazin-8a(8H)-yl)thiazol-4-yl)-4-methoxybenzamide (**56**). To an EtOH solution (10mL) of N-(2-((4aR,6S,8aR)-2-benzamido-6-methyl-4,4a,5,6-tetrahydropyrano[3,4-d][1,3]thiazin-8a(8H)-yl)thiazol-4-yl)-4-methoxybenzamide (110mg, 0.210mmol) at rt, was added Pyridine (anhydrous, 1.66g, 21mmol, 100eq.) and Methoxyamine hydrochloride (176mg, 2.10mmol, 10eq.). The resulting solution was heated to 35 ^{o}C until complete consumption of starting material. The reaction mixture was then concentrated under reduced pressure and purified by preparative HPLC purification (Column: DuraShell 150 x 25mm x 5um; Mobile phase: from 28% MeCN in H_2O (0.05% ammonia) to 48% MeCN in H_2O (0.05% ammonia); Gradient Time: 10 min; 100% B Hold Time: 2 min; Flow rate: 30 mL/min), the eluents were concentrated and lyophilized to afford compound **56** (75mg, 0.179mmol, 85%). LC/MS M+z 418.9 M+. $[\alpha]^{23}_D$ -

89.1 (c=0.63, MeOH). ^{1}H NMR (400 MHz, $CDCl_3$) δ ppm 8.60 (s, 1H), 7.88 (dd, *J* = 9.5, 2.8 Hz, 2H), 7.68 (s, 1H), 7.07 – 6.91 (m, 2H), 4.87 – 4.50 (b, 2H), 4.06 – 3.77 (m, 5H), 3.74 (m, 1H), 3.16 (dd, *J* = 12.5, 4.3 Hz, 1H), 2.76 (d, *J* = 12.3 Hz, 1H), 2.66 – 2.52 (m, 1H), 1.81 (q, *J* = 12.9 Hz, 1H), 1.54 (d, *J* = 13.9 Hz, 1H), 1.29 (d, *J* = 7.8 Hz, 3H).

N-(2-((4aR,6S,8aR)-2-amino-6-methyl-4,4a,5,6-tetrahydropyrano[3,4-d][1,3]thiazin-8a(8H)-yl)thiazol-4-yl)-5-methoxypicolinamide (57).

Step 1. Synthesis of N-(2-((4aR,6S,8aR)-2-benzamido-6-methyl-4,4a,5,6-tetrahydropyrano[3,4-d][1,3]thiazin-8a(8H)-yl)thiazol-4-yl)-5-methoxypicolinamide. To a solution of 4-methoxybenzoic acid (62.0 mg, 0.405 mmol), N,N-diisopropylethylamine (0.080 mL, 0.463 mmol) in DMF (3mL, 0.1M) was added O-(7-azabenzotriazol-1-yl)-N,N,N',N'-tetramethyluronium hexafluorophosphate (HATU, 97%, 154 mg, 0.405 mmol) in one portion at 15 ^{o}C. The resulting mixture was stirred for 30min., followed by addition of **72** (150 mg, 0386 mmol) in one portion. The resulting mixture was stirred at RT over 32h. The reaction mixture was then partitioned between ethyl acetate (10 mL) and water (10 mL). The aqueous layer was extracted twice with ethyl acetate, and the combined organic layers were washed with saturated aqueous sodium chloride solution (50 mL), dried over sodium sulfate, filtered, and concentrated in vacuo. Silica gel chromatography (Gradient: 10% to 40% ethyl acetate in petroleum ether) afforded the product as a solid. Yield: 150 mg, 0.286 mmol, 85%. LC/MS M+z 524.1, M + H). ^{1}H NMR (400 MHz, $CDCl_3$) δ ppm 10.43 (s, 1H), 8.28 (d, *J* = 2.8 Hz, 1H), 8.23 (d, *J* = 8.6 Hz, 1H), 8.12 (m, 2H), 7.75 (s, 1H), 7.54 (m, 1H), 7.46 (m, 2H), 7.35 (dd, *J* = 8.7, 2.8 Hz, 1H), 3.96 (m, 5H), 3.78 (m, 1H), 3.19 (dd, *J* = 13.0, 4.1 Hz, 1H), 3.10 – 3.00 (m, 1H), 2.61 (dd, *J* = 13.0, 2.8 Hz, 1H), 1.91 (m, 1H), 1.67 (m, 1H), 1.30 (d, *J* = 6.1 Hz, 3H).

Step 2. Synthesis of N-(2-((4aR,6S,8aR)-2-amino-6-methyl-4,4a,5,6-tetrahydropyrano[3,4-d][1,3]thiazin-8a(8H)-yl)thiazol-4-yl)-5-methoxypicolinamide (**57**). To an EtOH solution (10mL) of N-(2-((4aR,6S,8aR)-2-benzamido-6-methyl-4,4a,5,6-tetrahydropyrano[3,4-d][1,3]thiazin-8a(8H)-yl)thiazol-4-yl)-5-methoxypicolinamide (150mg, 0.286mmol) at rt, was added pyridine (anhydrous, 2.27g, 28.6 mmol) and methoxyamine hydrochloride (239 mg, 2.86 mmol). The resulting solution was heated to 35 ^{o}C until complete consumption of starting material. The reaction mixture was then concentrated under reduced pressure and purified by preparative HPLC purification (Column: DuraShell 150 x 25mm x 5um; Mobile phase: from 28% MeCN in H_2O (0.05% ammonia) to 48% MeCN in H_2O (0.05% ammonia); Gradient Time: 10 min; 100%B Hold Time: 2 min; Flow rate: 30 mL/min), the eluents were concentrated and lyophilized to afford compound **57** (7mg, 0.017mmol, 6%). LC/MS M+z 441.9, M + Na. $[\alpha]^{22}_{D}$ -107.1 (c=0.32, MeOH). ^{1}H NMR (400 MHz, $CDCl_3$) δ ppm 10.39 (s, 1H), 8.27 (d, *J* = 2.8 Hz, 1H), 8.23 (d, *J* = 8.7 Hz, 1H), 7.68 (s, 1H), 7.34 (dd, *J* = 8.7, 2.9 Hz, 1H), 4.58 (b, 2H), 3.94 (s, 4H), 3.87 (d, *J* = 11.1 Hz, 1H), 3.80 – 3.67 (m, 1H), 3.18 (dd, *J* = 12.5, 4.0 Hz, 1H), 2.84 (dd, *J* = 12.9, 3.6 Hz, 1H), 2.64 – 2.53 (m, 1H), 1.80 (m, 1H), 1.57 – 1.48 (m, 1H), 1.29 (d, *J* = 6.1 Hz, 3H).

N-{2-[(4aR,6S,8aR)-2-Amino-6-methyl-4,4a,5,6-tetrahydropyrano[3,4-d][1,3]thiazin-8a(8H)-yl]-1,3-thiazol-4-yl}-5-chloropyridine-2-carboxamide (61)

Step 1. Synthesis of N-{2-[(4aR,6S,8aR)-2-(benzoylamino)-6-methyl-4,4a,5,6-tetrahydropyrano[3,4-d][1,3]thiazin-8a(8H)-yl]-1,3-thiazol-4-yl}-5-chloropyridine-2-carboxamide. To a solution of 5-chloropyridine-2-carboxylic acid (38.9 mg, 0.247 mmol) in DMF (2 mL) was added DIPEA (133 mg, 1.03 mmol) at r.t, followed by addition of HATU (235 mg, 0.618 mmol). The resulting orange solution was stirred for 30 min at r.t. Then **72** (80 mg,

0.21 mmol) in DMF (3 mL) was added via syringe, the mixture was stirred at r.t for 2 h. LCMS showed that the reaction was done. The mixture was poured into ice-water (50 mL), extracted with EA (20 mLx2). The combined organic layers were washed with water (20 mL×2), brine (20 mLx2), dried over anhydrous Na2SO4, concentrated to give crude product as yellow oil. The crude product was purified by prep. TLC (pet ether/EtOAc 2:1). The product was obtained as a colorless oil and used directly in the next transformation. Yield: 80 mg, 0.15 mmol, 71%. LCMS *m/z* 527.9 $[M+H]^+$.

Step 2. Synthesis of N-{2-[(4aR,6S,8aR)-2-amino-6-methyl-4,4a,5,6-tetrahydropyrano[3,4-d][1,3]thiazin-8a(8H)-yl]-1,3-thiazol-4-yl}-5-chloropyridine-2-carboxamide (**61**).

Methoxylamine hydrochloride (94.9 mg, 1.14 mmol) and pyridine (899 mg, 11.4 mmol) were added to a solution of the above thioamide (60 mg, 0.11 mmol) in ethanol (5 mL), and the reaction mixture was heated at reflux for 72 hours. Volatiles were removed under reduced pressure, and the residue was purified by reversed phase HPLC (Column: Phenomenex Gemini C18, 8 μm; Mobile phase A: aqueous ammonia, pH 10; Mobile phase B: acetonitrile; Gradient: 45% to 65% B) to afford the product as a white solid. Yield: 12.7 mg, 30.0 μmol, 27%. LCMS *m/z* 423.8 $[M+H]^+$. ^{1}H NMR (400 MHz, $CDCl_3$) δ 10.40 (br s, 1H), 8.58 (d, *J* = 2.3 Hz, 1H), 8.24 (d, *J* = 8.3 Hz, 1H), 7.90 (dd, *J* = 8.4, 2.4 Hz, 1H), 7.73 (s, 1H), 4.5-4.8 (br s, 2H), 3.92 (AB quartet, J_{AB} = 11.1 Hz, $\Delta\nu_{AB}$=40.2 Hz, 2H), 3.71-3.80 (m, 1H), 3.18 (dd, *J* = 12.6, 4.2 Hz, 1H), 2.81-2.89 (m, 1H), 2.60 (dd, *J* = 12, 3 Hz, 1H), 1.75-1.87 (m, 1H), 1.51-1.59 (m, 1H), 1.30 (d, *J* = 6.2 Hz, 3H). ^{13}C NMR (101 MHz, $CDCl_3$) Shift 173.4, 160.9, 153.8, 147.31, 147.29, 146.8, 137.4, 135.6, 123.4, 103.5, 78.6, 73.5, 60.0, 33.1, 30.7, 29.1, 21.6

Generation of Crystalline Compound 61, hydrochloride salt

A sample of compound **61** (15 mg, 0.035 mmol) was dissolved in ethanol (5 mL) at 60 °C. Concentrated hydrochloric acid (5.9 μL, 0.0708 mmol) was added, and the slurry was allowed to slowly cool to room temperature with stirring. The resulting crystals were collected via filtration to afford the product as a white solid, which was crystalline by powder X-ray diffraction analysis. Yield: 14.7 mg, 0.0319 mmol, 91%. LCMS *m/z* 424.3, 426.3 $[M+H]^+$. $[\alpha]^{22}_D$ -83.4 (c = 0.75, DMSO), ^{1}H NMR (400 MHz, CD_3OD) δ 8.71 (dd, *J* = 2.4, 0.7 Hz, 1H), 8.22 (dd, half of ABX pattern, *J* = 8.4, 0.7 Hz, 1H), 8.09 (dd, half of ABX pattern, *J* = 8.4, 2.4 Hz, 1H), 7.90 (s, 1H), 4.06 (s, 2H), 3.82-3.92 (m, 1H), 3.19-3.26 (m, 2H), 2.97-3.04 (m, 1H), 1.83 (ddd, *J* = 14, 4, 2.5 Hz, 1H), 1.62 (ddd, *J* = 14, 11.5, 11.5 Hz, 1H), 1.29 (d, *J* = 6.2 Hz, 3H).

N-{2-[(4aR,6S,8aR)-2-Amino-6-methyl-4,4a,5,6-tetrahydropyrano[3,4-d][1,3]thiazin-8a(8H)-yl]-1,3-thiazol-4-yl}-5-cyanopyridine-2-carboxamide (63)

Step 1. Synthesis of N-{2-[(4aR,6S,8aR)-2-(benzoylamino)-6-methyl-4,4a,5,6-tetrahydro-pyrano[3,4-d][1,3]thiazin-8a(8H)-yl]-1,3-thiazol-4-yl}-5-cyanopyridine-2-carboxamide. To a solution of 5-cyanopyridine-2-carboxylic acid (236 mg, 1.54 mmol) in DMF (4 mL) was added HATU (1.47 g, 3.86 mmol) at r.t, followed by addition of DIPEA (832 mg, 6.43mmol). The resulting solution was stirred for 30 min at r.t. Then a solution of **72** (500 mg, 1.29 mmol) in DMF (6 mL) was added via syringe, the mixture was stirred at rt for 1 h. LCMS showed the reaction was done. The mixture was poured into ice-water (100 mL), extracted with EA (100 mLx2). The combined organic layers were washed with water (50 mLx2) , brine (50 mLx2), dried over anhydrous Na_2SO_4, concentrated to give crude product as yellow oil. The crude product was purified by prep. TLC (Pet Ether/EtOAC 2:1).The product was obtained as a yellow oil and was directly in the next transformation. Yield: 300 mg, 0.58 mmol, 45%. LCMS *m/z* 519.1 $[M+H]^+$.

Step 2. Synthesis of N-{2-[(4aR,6S,8aR)-2-amino-6-methyl-4,4a,5,6-tetrahydropyrano[3,4-d][1,3]thiazin-8a(8H)-yl]-1,3-thiazol-4-yl}-5-cyanopyridine-2-carboxamide (**63**). Methoxylamine hydrochloride (483 mg, 5.78 mmol) and pyridine (4.58 g, 57.9 mmol) were added to a solution of the above thioamide (300 mg, 0.58 mmol) in ethanol (4 mL), and the reaction mixture was stirred at 50 °C for 16 hours. After removal of solvent under reduced pressure, the residue was purified via reversed phase HPLC (Column: Kromasil Eternity XT C18, 10 μm; Mobile phase A: aqueous ammonia, pH 10; Mobile phase B: acetonitrile; Gradient: 22% to 42% B) to afford the product as a white solid. Yield: 69 mg, 0.17 mmol, 29%. LCMS *m/z* 414.8 $[M+H]^+$. $[\alpha]^{22}{}_D$ -142 (0.29, Acetonitrile), ^{1}H NMR (400 MHz, $CDCl_3$) δ 10.44 (br s, 1H), 8.90-8.94 (m, 1H), 8.43 (br d, *J* = 8.3 Hz, 1H), 8.22 (dd, *J* = 8, 2 Hz, 1H), 7.77 (s, 1H), 4.5-4.9 (br s, 2H), 3.92 (AB quartet, J_{AB} = 11 Hz, $\Delta\nu_{AB}$=44 Hz, 2H), 3.70-3.80 (m, 1H), 3.17 (dd, *J* = 12, 4 Hz, 1H), 2.81-2.89 (m, 1H), 2.61 (dd, *J* = 13, 3 Hz, 1H), 1.75-1.87 (m, 1H), 1.52-1.60 (m, 1H), 1.30 (d, *J* = 6.2 Hz, 3H).

N-{2-[(4aR,6S,8aR)-2-Amino-6-methyl-4,4a,5,6-tetrahydropyrano[3,4-d][1,3]thiazin-8a(8H)yl]-1,3-thiazol-4-yl}-5-(difluoromethoxy)pyridine-2-carboxamide (64).

Step 1. Potassium carbonate (45.1 g, 326 mmol) was added to a solution of methyl 5-hydroxypyridine-2-carboxylate (20 g, 130 mmol) in N,N-dimethylformamide (500 mL), and the reaction mixture was stirred at room temperature for 0.5 hours. Sodium chloro(difluoro)acetate (63.7 g, 418 mmol) was introduced, and the resulting mixture was heated at 100 °C for 5 hours, whereupon it was partitioned between saturated aqueous sodium chloride solution (300 mL) and ethyl acetate (300 mL). The aqueous layer was extracted with ethyl acetate (3 x 200 mL), and the combined organic layers were washed with saturated aqueous sodium chloride solution (2 x 200 mL), dried, filtered, and concentrated in vacuo. Silica gel chromatography (Eluent: 5:1 petroleum

ether / ethyl acetate) afforded the product as a pale yellow oil. Yield: 17 g, 84 mmol, 65%. LCMS m/z 204.1 [M+H+]; GCMS m/z 203 (M+). ^{1}H NMR (400 MHz, CDCl3) δ 8.56 (s, 1H), 8.17 (d, J=8.7 Hz, 1H), 7.59 (br d, J=8.7 Hz, 1H), 6.64 (t, JHF=71.9 Hz, 1H), 4.00 (s, 3H).

Step 2. A solution of methyl 5-(difluoromethoxy)pyridine-2-carboxylate (17 g, 84 mmol) in tetrahydrofuran (100 mL) and water (50 mL) was cooled to 0 °C and treated with lithium hydroxide (6.0 g, 250 mmol). After the reaction mixture had stirred at room temperature for 2 hours, it was acidified to a pH of 3 with 1 M aqueous hydrochloric acid. The aqueous layer was extracted with ethyl acetate (3 x 100 mL), and the combined organic layers were washed with saturated aqueous sodium chloride solution (100 mL), dried, filtered, and concentrated under reduced pressure to provide the product as a white solid. Yield: 13 g, 69 mmol, 82%. LCMS m/z 189.8 [M+H]+. ^{1}H NMR (400 MHz, CDCl3) δ 8.52 (d, J = 2.4 Hz, 1H), 8.29 (d, J = 8.5 Hz, 1H), 7.73 (dd, J = 8.6, 2.4 Hz, 1H), 6.68 (t, J_{HF} = 71.5 Hz, 1H).

Step 3. Synthesis of N-{2-[(4aR,6S,8aR)-2-(benzoylamino)-6-methyl-4,4a,5,6-tetrahydropyrano[3,4-d][1,3]thiazin-8a(8H)-yl]-1,3-thiazol-4-yl}-5-(difluoromethoxy)pyridine-2-carboxamide (**73**). To a solution of **72** (350 mg, 0.901 mmol) and 5-(difluoromethoxy)pyridine-2-carboxylic acid (204 mg, 1.08 mmol) in acetonitrile (9 mL) was added N,N-diisopropylethylamine (0.314 mL, 1.80 mmol), followed by O-(7-azabenzotriazol-1-yl)-N,N,N',N'-tetramethyluronium hexafluorophosphate (HATU, 97%, 424 mg, 1.08 mmol). After the reaction mixture had stirred for 4 hours, it was partitioned between ethyl acetate (10 mL) and water (10 mL). The aqueous layer was extracted twice with ethyl acetate, and the combined organic layers were washed with saturated aqueous sodium chloride solution (50 mL), dried over sodium sulfate, filtered, and concentrated in vacuo. Silica gel chromatography (Gradient: 0% to 80% ethyl acetate in heptane) afforded the product as a solid. Yield: 410 mg, 0.733 mmol, 81%.

LCMS m/z 560.3 [M+H]+. ^{1}H NMR (400 MHz, $CDCl_3$) δ 10.45 (s, 1H), 8.33 (d, *J* = 8.59 Hz, 1H), 8.14 (d, *J* = 7.41 Hz, 2H), 7.79 (s, 1H), 7.70 (dd, *J* = 2.34, 8.59 Hz, 1H), 7.45-7.60 (m, 3H), 6.48-6.89 (m, 1H), 3.94-4.06 (m, 2H), 3.80 (dd, *J* = 6.05, 9.17 Hz, 1H), 3.21 (dd, *J* = 3.90, 12.88 Hz, 1H), 3.01-3.11 (m, 1H), 2.63 (dd, *J* = 2.73, 12.88 Hz, 1H), 1.92 (q, *J* = 12.62 Hz, 1H), 1.65-1.75 (m, 1H), 1.32 (d, *J* = 6.24 Hz, 3H).

Step 4. Synthesis of N-{2-[(4aR,6S,8aR)-2-amino-6-methyl-4,4a,5,6-tetrahydropyrano[3,4-d][1,3]thiazin-8a(8H)-yl]-1,3-thiazol-4-yl}-5-(difluoromethoxy)pyridine-2-carboxamide (**39**). A solution of **73** (390 mg, 0.762 mmol) and 1,8-diazabicyclo[5.4.0]undec-7-ene (DBU, 95%, 132 μL, 0.838 mmol) in methanol (15 mL) was heated at 70 °C for 90 minutes. After removal of solvent in vacuo, the residue was purified via silica gel chromatography (Gradient: 0% to 8% methanol in dichloromethane) to provide the product **64** as a solid. Yield: 191 mg, 0.419 mmol, 55%. $[\alpha]^{22}_D$ = -102.82 (c 1.3, $CHCl_3$) , LCMS m/z 456.2 [M+H]+. ^{1}H NMR (400 MHz, $CDCl_3$) δ 10.40 (br s, 1H), 8.48 (br dd, *J* = 2.7, 0.6 Hz, 1H), 8.31 (dd, *J* = 8.6, 0.6 Hz, 1H), 7.72 (s, 1H), 7.68 (ddt, *J* = 8.6, 2.7, 0.7 Hz, 1H), 6.65 (t, *J*HF = 72.0 Hz, 1H), 3.93 (AB quartet, downfield doublet is broadened, *J*AB = 11.2 Hz, ΔνAB=45.8 Hz, 2H), 3.75 (dqd, J=11.2, 6.1, 2.3 Hz, 1H), 3.19 (dd, *J* = 12.6, 4.0 Hz, 1H), 2.83-2.90 (m, 1H), 2.61 (dd, *J* = 12.6, 2.8 Hz, 1H), 1.81 (ddd, *J* = 13.2, 12.9, 11.4 Hz, 1H), 1.56 (ddd, *J* = 13.4, 4.2, 2.3 Hz, 1H), 1.30 (d, *J* = 6.1 Hz, 3H).

Generation of crystalline compound 64, hydrochloride salt. A sample of compound **64** (224 mg, 0.492 mmol) was dissolved in ethyl acetate (1 mL) at 60 °C. Hydrogen chloride (2 M in diethyl ether, 0.49 mL, 0.98 mmol) was added, and the slurry was allowed to cool to room temperature with stirring. Solvents were removed in vacuo, and the residue was dissolved in hot ethanol. The resulting solution was allowed to cool to room temperature and stand for 3 days;

single crystals were observed, one of which was subjected to the X-ray crystal structure determination described below. This confirmed the indicated stereochemistry of the hydrochloride salt of **64**. The ethanol was blown down to a minimum, and the solid was collected via filtration. This sample was crystalline by powder X-ray diffraction analysis. Yield: 200 mg, 0.41 mmol, 83%. LCMS m/z 457.1 [M+H+]. ^{1}H NMR (400 MHz, $CDCl_3$) δ 10.41 (s, 1H), 8.49 (d, *J* = 2.34 Hz, 1H), 8.33 (d, *J* = 8.59 Hz, 1H), 7.74 (s, 1H), 7.69 (dd, *J* = 2.34, 8.59 Hz, 1H), 6.46-6.88 (m, 1H), 3.96-4.03 (m, 1H), 3.85-3.92 (m, 1H), 3.71-3.82 (m, 1H), 3.20 (dd, *J* = 3.90, 12.88 Hz, 1H), 2.83-2.93 (m, 1H), 2.62 (dd, *J* = 2.54, 12.68 Hz, 1H), 1.76-1.90 (m, 1H), 1.53-1.61 (m, 1H), 1.31 (d, *J* = 6.24 Hz, 3H). ^{13}C NMR (151 MHz, $CDCl_3$) δ 173.3, 160.8, 153.8, 149.6, 146.8, 146.1, 140.3, 127.9, 123.6, 115.0, 103.3, 78.6, 73.4, 60.0, 33.1, 30.7, 29.0, 21.6

The procedure above was repeated as follows: 10.6 g (1 equiv, 23.3 mmol) of 1 was dissolved in ethanol (0.1 M, 115 mL) at 65 ^{o}C. Once the material was dissolved, concentrated HCl (2 equiv, 3.9 mL, 12M) was added. The slurry was stirred at room temperature for 2 hours. The crystals were collected by vacuum filtration. A single crystal x-ray analysis of **64** · HCl was obtained (see Supplmental Figure 9).

Direct Amide coupling in the preparation of Compound 64.

Step 1. To a suspension of 5-(difluoromethoxy)picolinic acid (1 g, 5.29 mmol) in dichloromethane (10 mL) was added oxalyl chloride (944 mg, 7.93 mmol) and a catalytic amount of dimethylformamide in room temperature. After the addition, the reaction was stirred at 30 ^{o}C for 2 h. The reaction was concentrated in vacuo. The residue was taken up in dry dichloromethane (10 mL) and ammonia gas was bubble through at -20 ^{o}C for 5 min followed by stirring for 30min at room temperature. The reaction mixture was diluted with water (20 mL)

and extracted with dichloromethane (20 mL). The organic layer was concentrated in vacuo to give desired product, which was triturated with 10 mL of diethyl ether to give product as a white solid. (667mg, 66.9%). LCMS *m/z* 189.0 [M+H$^+$]. ^{1}H NMR (400 MHz, $CDCl_3$) δ ppm 5.77 (br. s., 1 H) 6.61 (t, *J* = 71.80 Hz, 1 H) 7.62 (dd, *J* = 8.53, 2.51 Hz, 1 H) 7.73 (br. s., 1 H) 8.25 (d, *J* = 8.53 Hz, 1 H) 8.43 (d, *J* = 2.51 Hz, 1 H).

Step 2. Synthesis of N-(2-((4aR,6S,8aR)-2-benzamido-6-methyl-4,4a,5,6-tetrahydropyrano[3,4-d][1,3]thiazin-8a(8H)-yl)thiazol-4-yl)-5-(difluoromethoxy)picolinamide (**64**). To a vial charged with tris(dibenzylideneacetone)dipalladium(0) (5.5mg, 0.006mmol), 2-(Di-tert-butylphosphino)-2',4',6'-triisopropyl-3,6-dimethoxy-1,1'-biphenyl (8.2mg, 0.017mmol) and lithium tertbutoxide (22.3mg, 0.278mmol) was added 2-methyl-2-butanol (0.3ml, degassed). The vial was purged with nitrogen and heated at 95 oC for 3min. Compound **54**, N-((4aR,6S,8aR)-8a-(4-bromothiazol-2-yl)-6-methyl-4,4a,5,6,8,8a-hexahydropyrano[3,4-d][1,3]thiazin-2-yl)benzamide (50mg, 0.11 mmol) and 5-(difluoromethoxy)picolinamide (25mg 0.133 mmol) in 2:1 mixture of 2-methyl-2-butanol and 1,4-dioxane (0.15ml, degassed) was added and stirred at 95 ^{o}C for 1hr. Solvent was removed and residue was purified via silica gel chromatography (Heptane/EtOAc 0-50% gradient) to give product as a white solid (38mg, 61%). LCMS *m/z* 560.0 [M+H$^+$], ^{1}H NMR (400 MHz, $CDCl_3$) δ ppm 1.30 (d, *J* = 6.24 Hz, 3 H), 1.68 (ddd, *J* = 13.46, 3.90, 2.15 Hz, 1 H), 1.83 - 2.00 (m, 1 H), 2.61 (dd, *J* = 13.27, 2.73 Hz, 1 H), 3.04 (dd, *J* = 12.49, 2.73 Hz, 1 H), 3.19 (dd, *J* = 13.07, 4.10 Hz, 1 H), 3.72 - 3.85 (m, 1 H), 3.91 - 4.03 (m, 2 H), 6.66 (t, *J* = 7.81, 1 H), 7.42 - 7.50 (m, 2 H), 7.50 - 7.57 (m, 1 H), 7.68 (dd, *J* = 8.59, 2.73 Hz, 1 H), 7.78 (s, 1 H), 8.12 (br. s., 2 H), 8.32 (d, *J* = 8.59 Hz, 1 H), 8.48 (d, *J* = 2.34 Hz, 1 H) 10.43 (s, 1 H).

N-{2-[(4aR,6S,8aR)-2-Amino-6-methyl-4,4a,5,6-tetrahydropyrano[3,4-d][1,3]thiazin-8a(8H)-yl]-1,3-thiazol-4-yl}-5-(difluoromethoxy)-3-methylpyridine-2-carboxamide (65)

Step 1. A mixture of 3-methylpyridine-2-carbonitrile (128 g, 1.08 mol) and tetrabutylammonium nitrate (363 g, 1.19 mol) in *tert*-butyl methyl ether (1.3 L) was cooled to 4 °C. Trifluoroacetic anhydride (171 mL, 1.21 mol) was added, and the reaction mixture was allowed to stir at room temperature for 60 hours. It was then adjusted to a pH of approximately 7 by addition of 20% aqueous sodium hydroxide solution, and extracted with dichloromethane (3 x 1 L). The combined organic layers were dried, filtered, and concentrated *in vacuo*; purification via silica gel chromatography (Gradient: 0% to 10% ethyl acetate in petroleum ether) afforded 3-methyl-5-nitropyridine-2-carbonitrile as a yellow solid. Yield: 70 g, 0.43 mmol, 40%. ^{1}H NMR (400 MHz, $CDCl_3$) δ 9.31-9.36 (m, 1H), 8.47-8.52 (m, 1H), 2.74 (s, 3H).

Step 2. To a solution of *3-methyl-5-nitropyridine-2-carbonitrile* (40.0 g, 245 mmol) in ethanol (630 mL) and water (70 mL) was added calcium chloride (13.6 g, 123 mmol), followed by iron powder (123 g, 2.20 mol), and the reaction mixture was stirred overnight at room temperature. After filtration of the reaction mixture, the filtrate was concentrated *in vacuo*, and the residue was purified by chromatography on silica gel (Gradient: 10% to 50% ethyl acetate in petroleum ether). 5-amino-3-methylpyridine-2-carbonitrile was obtained as a yellow solid. Yield: 20.0 g, 150 mmol, 61%. ^{1}H NMR (400 MHz, $CDCl_3$) δ 7.94 (d, J = 2.5 Hz, 1H), 6.81 (d, J = 2.5 Hz, 1H), 4.07-4.19 (br s, 2H), 2.45 (s, 3H).

Step 3. Sodium nitrite (1.6 M aqueous solution containing 10.3 g of sodium nitrite, 149 mmol) was slowly added to a 0 °C solution of *5-amino-3-methylpyridine-2-carbonitrile* (18.0 g, 135 mmol) in water (243 mL) and concentrated sulfuric acid (67.5 mL). The reaction mixture was warmed to room temperature and then stirred at 100 °C for 3 hours, whereupon it was cooled and extracted with ethyl acetate (3 x 75 mL). The combined organic layers were washed with water (2 x 75 mL) and with saturated aqueous sodium chloride solution (2 x 75 mL), dried, filtered,

and concentrated under reduced pressure to afford 5-hydroxy-3-methylpyridine-2-carbonitrile as a yellow solid. Yield: 16 g, 120 mmol, 89%. ^{1}H NMR (400 MHz, DMSO-d_6) δ 11.07 (br s, 1H), 8.08 (d, J = 2.6 Hz, 1H), 7.20 (d, J = 2.3 Hz, 1H), 2.40 (s, 3H).

Step 4. A mixture of *5-hydroxy-3-methylpyridine-2-carbonitrile* (5.70 g, 42.5 mmol), sodium chlorodifluoroacetate (13.0 g, 85.3 mmol), and potassium carbonate (17.6 g, 127 mmol) in *N*,*N*-dimethylformamide (175 mL) was stirred for 30 minutes at 100 °C. The reaction mixture was then diluted with ethyl acetate (400 mL), and sequentially washed with saturated aqueous ammonium chloride solution (3 x 200 mL) and saturated aqueous sodium chloride solution (3 x 200 mL). The combined aqueous layers were extracted with ethyl acetate (200 mL), and the combined organic layers were dried over sodium sulfate, filtered, and concentrated *in vacuo*. Silica gel chromatography (Gradient: 5% to 15% ethyl acetate in petroleum ether) provided 5-(difluoromethoxy)-3-methylpyridine-2-carbonitrile as a colorless oil. Yield: 3.9 g, 21 mmol, 49%. ^{1}H NMR (400 MHz, $CDCl_3$) δ 8.39 (br d, J = 2.1 Hz, 1H), 7.43-7.47 (m, 1H), 6.64 (t, J_{HF} = 71.5 Hz, 1H), 2.59 (s, 3H).

Step 5. Aqueous sodium hydroxide solution (1 M, 124 mL, 124 mmol) was added to a solution of *5-(difluoromethoxy)-3-methylpyridine-2-carbonitrile* (7.60 g, 41.3 mmol) in ethanol (200 mL), and the reaction mixture was stirred for 16 hours at 70 °C. It was then diluted with *tert*-butyl methyl ether (200 mL) and extracted with water (2 x 100 mL). The combined aqueous layers were washed with *tert*-butyl methyl ether (100 mL), acidified to pH 2 with 1 M aqueous hydrochloric acid, and extracted with *tert*-butyl methyl ether (2 x 200 mL). The combined organic extracts were dried over sodium sulfate, filtered, and concentrated *in vacuo* to afford 5-(difluoromethoxy)-3-methylpyridine-2-carboxylic acid as a white solid. Yield: 6.6 g, 32 mmol,

77%. LCMS *m/z* 203.7 $[M+H]^+$. ^{1}H NMR (400 MHz, CD_3OD) δ 8.32 (br d, J = 2.1 Hz, 1H), 7.58-7.62 (m, 1H), 7.06 (t, J_{HF} = 72.7 Hz, 1H), 2.64 (s, 3H).

Step 6. A flask charged with tris(dibenzylideneacetone)dipalladium(0) (0.35g, 0.39 mmol), di-*tert*-butyl[2',4',6'-tri(propan-2-yl)biphenyl-2-yl]phosphane (0.49 g, 1.16 mmol), and sodium *tert*-butoxide (1.86 g,19.4 mmol) was purged twice with nitrogen. 1,4-Dioxane (15 mL) was added, and the reaction mixture was heated at 85 °C (internal reaction temperature) for 5 minutes, whereupon a solution of **72** (3.5 g, 7.74 mmol) and 1-(2,4-dimethoxyphenyl)methanamine (1.98 mL, 13.2 mmol) in 1,4-dioxane (14 mL) was concurrently added via syringe. After the addition had been completed, stirring was continued for 15 minutes at 85 °C (internal reaction temperature); the reaction mixture was then removed from the oil bath and quickly cooled to room temperature via immersion in a water bath. Diatomaceous earth and water (60 mL) were added, and the mixture was filtered through a pad of diatomaceous earth. The pad was washed with dichloromethane (3 x 30 mL). The organic layer of the combined filtrates was washed with water (3 x 30 mL) until the pH of the resulting aqueous layer was found to be neutral. The organic layer was then washed sequentially with an aqueous solution of citric acid (5%, 2 x 50 mL), saturated aqueous sodium bicarbonate solution (2 x 30 mL), and saturated aqueous sodium chloride solution (50 mL), dried over sodium sulfate, and filtered. The filtrate was adsorbed onto silica gel and chromatographed [Gradient: 10% to 100% (5% triethylamine in ethyl acetate) in heptane]; the orange solid obtained from chromatography was triturated with diethyl ether (10 mL) to afford N-[(4aR,6S,8aR)-8a-{4-[(2,4-dimethoxybenzyl)amino]-1,3-thiazol-2-yl}-6-methyl-4,4a,5,6,8,8a-hexahydropyrano[3,4-d][1,3]thiazin-2-yl]benzamide as a white solid (1.78 g). The filtrate from the trituration was concentrated *in vacuo*, and the residue was triturated with diethyl ether (5 mL) to provide additional product as a brown solid (1.15 g). Combined yield:

2.93 g, 5.44 mmol, 70%. LCMS *m/z* 539.2 $[M+H]^+$. ^1H NMR (400 MHz, $CDCl_3$) δ 8.04-8.27 (br s, 2H), 7.39-7.58 (m, 3H), 7.20 (d, *J* = 8.3 Hz, 1H), 6.48 (d, half of AB quartet, *J* = 2.4 Hz, 1H), 6.44 (dd, half of ABX pattern, *J* = 8.3, 2.4 Hz, 1H), 5.74 (s, 1H), 4.21 (br s, 2H), 3.94 (br s, 2H), 3.84 (s, 3H), 3.81 (s, 3H), 3.7-3.8 (m, 1H), 3.23 (dd, *J* = 13, 4 Hz, 1H), 2.95-3.06 (m, 1H), 2.52-2.62 (m, 1H), 1.80-1.95 (m, 1H), 1.6-1.69 (m, 1H, assumed; partially obscured by water peak), 1.28 (d, *J* = 6.0 Hz, 3H).

Step 7. Synthesis of N-{2-[(4aR,6S,8aR)-2-(benzoylamino)-6-methyl-4,4a,5,6-tetrahydropyrano[3,4-d][1,3]thiazin-8a(8H)-yl]-1,3-thiazol-4-yl}-5-(difluoromethoxy)-3-methylpyridine-2-carboxamide. 2,4,6-Tripropyl-1,3,5,2,4,6-trioxatriphosphinane 2,4,6-trioxide (50% solution by weight in ethyl acetate, 8.84 mL, 14.8 mmol) was added to a mixture of *5-(difluoromethoxy)-3-methylpyridine-2-carboxylic acid* (1.21 g, 5.96 mmol) and triethylamine (2.06 mL, 14.8 mmol) in ethyl acetate (8 mL), and the reaction mixture was heated at 65 °C for 20 minutes. Amine **37** (2.0 g, 3.71 mmol) was introduced, and stirring was continued at 65 °C for 1 hour. The reaction mixture was then cooled to room temperature and diluted with ethyl acetate (10 mL); the resulting solution was washed sequentially with water (2 x 15 mL), saturated aqueous sodium bicarbonate solution (25 mL), and saturated aqueous sodium chloride solution (25 mL), dried over sodium sulfate, filtered, and concentrated under reduced pressure. The resulting solid was dissolved in dichloromethane (150 ml) and treated with trifluoroacetic acid (14 mL); the reaction mixture was allowed to stir at room temperature for 16 hours, whereupon it was basified to pH 8 with saturated aqueous sodium bicarbonate solution (100 mL). The aqueous layer was extracted with dichloromethane (2 x 25 mL), and the combined organic layers were washed with saturated aqueous sodium chloride solution (100 mL), dried over sodium sulfate, filtered, and concentrated *in vacuo*. The residue was purified using

chromatography on silica gel (Gradient: 0% to 5% methanol in dichloromethane) to afford a solid (2.4 g), which was triturated with ethyl acetate (10 mL) to provide the product as a white solid (2.13 g). By ^{1}H NMR analysis, this material contained ethyl acetate. Yield, corrected for solvent: 1.93 g, 3.36 mmol, 91%. LCMS *m/z* 574.2 M+H, ^{1}H NMR (400 MHz, $CDCl_3$) δ 10.62 (s, 1H), 8.34 (br d, *J* = 2.6 Hz, 1H), 8.00-8.26 (v br s, 2H), 7.75 (s, 1H), 7.51-7.58 (m, 1H), 7.41-7.51 (m, 3H), 6.64 (t, J_{HF} = 72.1 Hz, 1H), 3.93-4.02 (m, 2H), 3.74-3.84 (m, 1H), 3.20 (br dd, *J* = 13, 4 Hz, 1H), 3.00-3.10 (m, 1H), 2.84 (s, 3H), 2.61 (br dd, *J* = 13, 2.6 Hz, 1H), 1.84-1.98 (m, 1H), 1.64-1.72 (m, 1H), 1.31 (d, *J* = 6.1 Hz, 3H).

Step 8. Synthesis of N-{2-[(4aR,6S,8aR)-2-amino-6-methyl-4,4a,5,6-tetrahydropyrano[3,4-d][1,3]thiazin-8a(8H)-yl]-1,3-thiazol-4-yl}-5-(difluoromethoxy)-3-methylpyridine-2-carboxamide (**65**). A solution of the above thioamide (2.10 g, 3.66 mmol) in xylenes (11 mL) was placed in a pressure tube and treated with SiliCycle, SiliaMetS® diamine (7.0 g, 11.0 mmol); the tube was sealed and stirred at room temperature for 5 minutes before being placed in a 135 °C oil bath. After stirring for 16 hours, the reaction mixture was cooled to room temperature over 20 minutes. Dichloromethane (5 mL) was added, and the mixture was filtered through diatomaceous earth, followed by rinsing of the filter pad with dichloromethane (3 x 10 mL). Concentration of the combined filtrates under reduced pressure provided a clear oil, which was seeded with a crystal of the product. The mixture immediately became heterogeneous, and the solid was collected via filtration, washed with toluene (2 x 5 mL), and stirred in diethyl ether (10 mL) for 30 minutes. Filtration and washing of the collected solid with cold diethyl ether (2 x 10 mL) afforded the product as a white solid (1.28 g). The combined filtrates were concentrated *in vacuo*, and the residue was filtered; the isolated solid was stirred with diethyl ether (5 mL) for 30 minutes, then filtered and washed with cold diethyl ether (2 x 10 mL). This provided

additional product, as an off-white solid (0.33 g). Combined yield: 1.61 g, 3.43 mmol, 94%. $[\alpha]^{22}_{D}$ = -102.27 (c 0.555, $CHCl_3$), LCMS *m/z* 470.5 $[M+H]^+$. ^{1}H NMR (400 MHz, $CDCl_3$) δ 10.57 (br s, 1H), 8.32 (br d, *J* = 2 Hz, 1H), 7.68 (s, 1H), 7.42 (br d, *J* = 2 Hz, 1H), 6.63 (t, J_{HF} = 72.2 Hz, 1H), 4.51-4.59 (br s, 2H), 3.91 (AB quartet, J_{AB} = 11.0 Hz, $\Delta\nu_{AB}$=32.5 Hz, 2H), 3.70-3.80 (m, 1H), 3.18 (dd, *J* = 12.5, 4.0 Hz, 1H), 2.84 (s, 3H), 2.80-2.88 (m, 1H), 2.59 (dd, *J* = 12.6, 2.8 Hz, 1H), 1.75-1.86 (m, 1H), 1.54 (ddd, *J* = 13, 4, 2 Hz, 1H), 1.29 (d, *J* = 6.2 Hz, 3H).

Generation of Crystalline Compound 65. A sample of compound **65** (94.0 mg, 0.200 mmol) was mixed with propan-2-yl acetate (1.0 mL) and heated to 55 °C. The fine suspension was stirred at 55 °C to 60 °C for 2 hours, then allowed to cool to room temperature and stir for 1 hour. Filtration, followed by washing of the filter cake with propan-2-yl acetate, provided Example 45 as an off-white solid. This material was crystalline by powder X-ray diffraction analysis. Yield: 60 mg, 0.13 mmol, 64%. ^{1}H NMR (400 MHz, DMSO-d_6) δ 10.81 (s, 1H), 8.42 (d, *J* = 2.2 Hz, 1H), 7.72 (d, *J* = 2 Hz, 1H), 7.62 (s, 1H), 7.44 (t, J_{HF} = 73.0 Hz, 1H), 6.25 (br s, 2H), 3.68 (s, 2H), 3.57-3.66 (m, 1H), 2.85-2.94 (m, 1H), 2.60-2.70 (m, 5H), 1.49-1.66 (m, 2H), 1.14 (d, *J* = 6.0 Hz, 3H). ^{13}C NMR (101 MHz, $CDCl_3$) δ 173.1, 162.3, 153.7, 148.9, 147.3, 143.2, 138.1, 137.3, 130.9, 115.0, 102.6, 78.7, 73.5, 60.0, 33.1, 30.7, 29.1, 21.6, 20.8

N-{2-[(4aR,6S,8aR)-2-Amino-6-methyl-4,4a,5,6-tetrahydropyrano[3,4-d][1,3]thiazin-8a(8H)-yl]-1,3-thiazol-4-yl}-5-(difluoromethoxy)pyrazine-2-carboxamide (67)

Step 1. To a solution of methyl 5-hydroxypyrazine-2-carboxylate (9.25 g, 60.0 mmol) in *N*,*N*-dimethylformamide (120 mL) were added potassium carbonate (24.8 g, 179 mmol) and sodium chloro(difluoro)acetate (18.3 g, 120 mmol). The mixture was heated to 100 °C for 15 minutes, whereupon it was filtered, and the filter cake was washed with ethyl acetate (2 x 50 mL). The

combined filtrates were poured into saturated aqueous ammonium chloride solution (200 mL) and extracted with ethyl acetate (3 x 200 mL); the combined organic layers were washed sequentially with saturated aqueous sodium bicarbonate solution (2 x 300 mL) and with saturated aqueous sodium chloride solution (2 x 300 mL), dried, filtered, and concentrated *in vacuo*. Chromatography on silica gel (Gradient: 0% to 15% ethyl acetate in petroleum ether) afforded methyl 5-(difluoromethoxy)pyrazine-2-carboxylate as a yellow solid. Yield: 1.7 g, 8.3 mmol, 14%. ^{1}H NMR (400 MHz, $CDCl_3$) δ 8.92 (d, J = 1.2 Hz, 1H), 8.47 (d, J = 1.2 Hz, 1H), 7.49 (t, J_{HF} = 71.3 Hz, 1H), 4.04 (s, 3H).

Step 2. Aqueous sodium hydroxide solution (5 M, 4.10 mL, 20.5 mmol) was added to a solution of *methyl 5-(difluoromethoxy)pyrazine-2-carboxylate* (2.10 g, 10.3 mmol) in tetrahydrofuran (25 mL) and water (12 mL). The reaction mixture was stirred at room temperature for 5 minutes, whereupon it was treated with aqueous hydrochloric acid (2 M, 11 mL). The mixture was extracted with ethyl acetate (2 x 150 mL), and the combined organic layers were washed with saturated aqueous sodium chloride solution (2 x 100 mL), dried, filtered, and concentrated under reduced pressure to provide 5-(difluoromethoxy)pyrazine-2-carboxylic acid as a yellow solid. Yield: 1.8 g, 9.5 mmol, 92%. LCMS *m/z* 189.0 [M-H$^+$]. ^{1}H NMR (400 MHz, $CDCl_3$) δ 9.05 (d, J = 1.3 Hz, 1H), 8.43 (d, J = 1.4 Hz, 1H), 7.52 (t, J_{HF} = 71.0 Hz, 1H).

Step 3. Amine **72** (5.0 g, 13.0 mmol, 1 equiv), 5-(difluoromethoxy)pyrazine-2-carboxylic acid (2.52 g, 13.3 mmol, 1.03 equiv) and ethyl acetate (25.7 mL, 0.5 M) were added to a round bottom flask. To this solution was added triethylamine (7.16 mL, 51.5 mmol, 4 equiv). This solution was cooled to 0^{o}C followed by the slow addition of 50% T_3P in DMF (18.8 mL, 32.2 mmol, 2.5 equiv). After 5 mins the reaction was warmed to rt and stirred for 1 hour. The reaction was then diluted with DCM and quenched with 1N HCl. The layers were stirred and

separated. The organic layer was then washed with sat. aqueous bicarbonate, and the aqueous layer was back extracted with DCM (3x). The combined organic layers were concentrated to 1/4 the volume, then diluted with isopropyl alcohol. The solution is heated to 80 ^{o}C to get precipitate back into solution. The solution was then cooled to 0^{o}C and stirred for 30 mins. The mixture was filtered and washed with cold isopropyl alcohol N-{2-[(4aR,6S,8aR)-2-(benzoylamino)-6-methyl-4,4a,5,6-tetrahydropyrano[3,4-d][1,3]thiazin-8a(8H)-yl]-1,3-thiazol-4-yl}-5-(difluoromethoxy)-pyrazine-2-carboxamide was isolated as a solid. Yield: 3.8 g, 8.45 mmol, 65%. LCMS *m/z* 561.3 $[M+H]^+$. 1H NMR (400 MHz, $CDCl_3$) δ 10.12 (s, 1H), 9.06 (d, *J* = 1.37 Hz, 1H), 8.35 (d, *J* = 1.17 Hz, 1H), 7.99-8.20 (m, 2H), 7.77 (s, 1H), 7.31-7.71 (m, 4H), 3.89-4.02 (m, 2H), 3.70-3.81 (m, 1H), 3.16 (dd, *J* = 3.72, 12.91 Hz, 1H), 2.93-3.05 (m, 1H), 2.60 (dd, *J* = 2.64, 13.01 Hz, 1H), 1.82-1.96 (m, 1H), 1.62-1.71 (m, 1H), 1.29 (d, *J* = 6.06 Hz, 3H).

Step 4. Synthesis of N-{2-[(4aR,6S,8aR)-2-amino-6-methyl-4,4a,5,6-tetrahydropyrano[3,4-d][1,3]thiazin-8a(8H)-yl]-1,3-thiazol-4-yl}-5-(difluoromethoxy)pyrazine-2-carboxamide (**67**). Pyridine (0.96 mL, 12 mmol) and methoxylamine hydrochloride (96.9 mg, 1.16 mmol) were added to a solution of N-{2-[(4aR,6S,8aR)-2-(benzoylamino)-6-methyl-4,4a,5,6-tetrahydropyrano[3,4-d][1,3]thiazin-8a(8H)-yl]-1,3-thiazol-4-yl}-5-(difluoromethoxy)pyrazine-2-carboxamide (65 mg, 0.12 mmol) in ethanol (1.2 mL). The reaction mixture was stirred at 50 °C for 5 hours, whereupon it was cooled to room temperature and concentrated *in vacuo*. The residue was diluted with dichloromethane and washed sequentially with aqueous sodium bicarbonate solution (3 times), with water, and with saturated aqueous sodium chloride solution. After being dried over sodium sulfate and filtered, the solution was concentrated under reduced pressure and purified via silica gel chromatography (Gradient: 0% to 4% methanol in dichloromethane) to provide the product as a solid. Yield: 41 mg, 90 μmol, 75%. LCMS *m/z*

457.1 $[M+H]^+$. $[\alpha]^{20}_D$ -55.5 (c 0.765, CH_2Cl_2). ^{1}H NMR (400 MHz, $CDCl_3$) δ 10.09 (br s, 1H), 9.06 (d, *J* = 1.3 Hz, 1H), 8.34 (d, *J* = 1.3 Hz, 1H), 7.71 (s, 1H), 7.51 (t, J_{HF} = 71.4 Hz, 1H), 3.89 (AB quartet, J_{AB} = 11.1 Hz, $\Delta\nu_{AB}$ =4 0.8 Hz, 2H), 3.73 (dqd, *J* = 11.2, 6.1, 2.2 Hz, 1H), 3.16 (dd, *J* = 12.5, 4.0 Hz, 1H), 2.77-2.84 (m, 1H), 2.58 (dd, *J* = 12.5, 2.8 Hz, 1H), 1.80 (ddd, *J* = 13.1, 12.9, 11.4 Hz, 1H), 1.53 (ddd, *J* = 13.4, 4.2, 2.3 Hz, 1H), 1.28 (d, *J* = 6.1 Hz, 3H). ^{13}C NMR (151 MHz, CD_3OD) δ 168.8, 160.9, 147.7, 141.25, 141.19, 140.4, 133.5, 114.3, 103.9, 100.0, 74.5, 73.4, 59.8, 33.6, 31.9, 28.1, 20.2.

Synthesis of N-{2-[(4aR,6S,8aR)-2-amino-6-methyl-4,4a,5,6-tetrahydropyrano[3,4-d][1,3]thiazin-8a(8H)-yl]-1,3-thiazol-4-yl}amides via *N*-acylation of 37 followed by selective hydrolysis

Method A. A solution of **72** (25.2 mg, 64.9 μmol) in ethyl acetate (0.5 mL) was added to the appropriate carboxylic acid (78 μmol). 2,4,6-Tripropyl-1,3,5,2,4,6-trioxatriphosphinane 2,4,6-trioxide (50% weight solution in ethyl acetate, 0.26 mL, 0.13 mmol) and pyridine (21 uL, 0.26 mmol) were added, and the reaction mixture was shaken at room temperature for 16 hours. It was then partitioned between water (1.5 mL) and ethyl acetate (2.4 mL) with vortexing. The organic layer was passed through a solid-phase extraction cartridge (6 mL) charged with sodium sulfate (~1 g); this extraction procedure was repeated twice. The combined eluents were concentrated *in vacuo*, dissolved in ethanol (0.75 mL), treated with hydrazine monohydrate (51 μL, 1.0 mmol) and shaken at room temperature for 6 hours. After removal of solvent *in vacuo*, the product was purified via reversed phase HPLC using one of the following methods: 1) Column: Waters XBridge C18, 5 μm; Mobile phase A: 0.03% ammonium hydroxide in water (v/v); Mobile phase B: 0.03% ammonium hydroxide in acetonitrile (v/v); Gradient: [5% or 10%] to

100% B. 2) Waters Sunfire C18, 5 μm; Mobile phase A: 0.05% trifluoroacetic acid in water (v/v); Mobile phase B: 0.05% trifluoroacetic acid in acetonitrile (v/v); Gradient: 5% to 100% B.

Method B. A solution of **72** (46.6 mg, 0.120 mmol) in ethyl acetate (1.5 mL) was added to the appropriate carboxylic acid (0.12 mmol), and the mixture was cooled in a dry ice box. Triethylamine (70 μL, 0.50 mmol) and 2,4,6-tripropyl-1,3,5,2,4,6-trioxatriphosphinane 2,4,6-trioxide (50% weight solution in ethyl acetate, 0.14 mL, 0.24 mmol) were added, and the reaction mixture was allowed to warm to ambient temperature, then shaken at room temperature for 3 to 6 hours. It was then partitioned between half-saturated aqueous sodium bicarbonate solution (1.5 mL) and ethyl acetate (2.4 mL) with vortexing. The organic layer was passed through a solid-phase extraction cartridge (6 mL) charged with sodium sulfate (~1 g); this extraction procedure was repeated twice. The combined eluents were concentrated *in vacuo*, dissolved in ethanol (0.5 mL), treated with a solution of methylamine in ethanol (33% by weight, 0.5 mL, 4 mmol), and shaken at room temperature for 3 hours. After removal of solvent *in vacuo*, the product was purified via reversed phase HPLC (Column: Waters XBridge C18, 5 μm; Mobile phase A: 0.03% ammonium hydroxide in water (v/v); Mobile phase B: 0.03% ammonium hydroxide in acetonitrile (v/v); Gradient: 5% to [40% or 100%] B).

Table 1. Method of Preparation, Structure, and Physicochemical Data for Examples **58**-**60**, **62**, **66**, **68**

Example Number	Structure	^{1}H NMR (400 MHz, $CDCl_3$) δ (ppm); Mass spectrum, observed ion *m/z* ($M+H^+$) or HPLC retention time; Mass spectrum *m/z* $[M+H]^+$ (unless otherwise indicated)

58	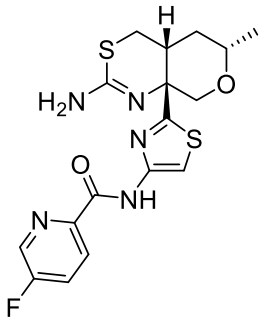	10.37 (br s, 1H), 8.47 (br d, *J*=2.8 Hz, 1H), 8.32 (ddd, *J*=8.7, 4.6, 0.5 Hz, 1H), 7.71 (s, 1H), 7.60 (ddd, *J*=8.7, 8.0, 2.8 Hz, 1H), 3.91 (AB quartet, J_{AB}=11.1 Hz, $\Delta\nu_{AB}$=38.0 Hz, 2H), 3.75 (dqd, *J*=11.2, 6.1, 2.3 Hz, 1H), 3.17 (dd, *J*=12.5, 4.0 Hz, 1H), 2.80-2.88 (m, 1H), 2.59 (dd, *J*=12.5, 2.8 Hz, 1H), 1.81 (ddd, *J*=13, 13, 11.4 Hz, 1H), 1.54 (ddd, *J*=13.4, 4.2, 2.4 Hz, 1H), 1.29 (d, *J*=6.2 Hz, 3H); LCMS m/z 408.3 (M+1), $[\alpha]^{22}{}_{D}$: -97.6 (c = 0.77, DMSO).
66	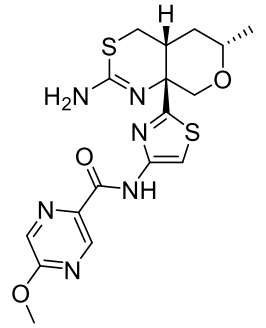	10.11 (br s, 1H), 9.01 (s, 1H), 8.17 (s, 1H), 7.71 (s, 1H), 4.07 (s, 3H), 3.92 (AB quartet, J_{AB}=11.2 Hz, $\Delta\nu_{AB}$=46.6 Hz, 2H), 3.69-3.79 (m, 1H), 3.18 (dd, *J*=12.5, 3.7 Hz, 1H), 2.80-2.89 (m, 1H), 2.60 (br dd, *J*=12.6, 2 Hz, 1H), 1.74-1.87 (m, 1H), 1.51-1.59 (m, 1H), 1.29 (d, *J*=6.1 Hz, 3H); LCMS m/z 421.3 (M+1). $[\alpha]^{22}{}_{D}$ -102.3 (c 0.770, CH_3OH).
59	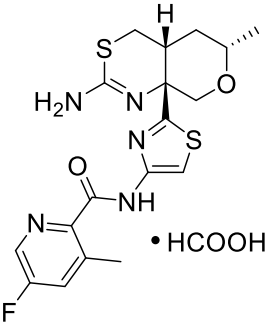	10.55 (br s, 1H), 8.32 (d, *J*=2.5 Hz, 1H), 7.71 (s, 1H), 7.35-7.41 (m, 1H), 4.11 (d, *J*=11.7 Hz, 1H), 3.86 (d, *J*=11.7 Hz, 1H), 3.71-3.81 (m, 1H), 3.21 (dd, *J*=13, 4 Hz, 1H), 2.91-2.99 (m, 1H), 2.84 (s, 3H), 2.63 (dd, *J*=13, 2 Hz, 1H), 1.74-1.86 (m, 1H), 1.55-1.63 (m, 1H), 1.31 (d, *J*=6.0 Hz, 3H); LCMS m/z 422.0 (M+1), $[\alpha]^{23}{}_{D}$: -69.2 (c = 0.76, DMSO).
60	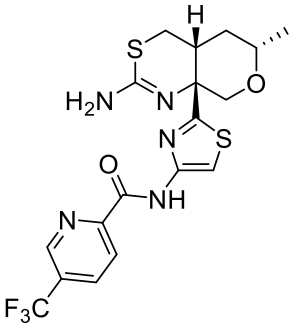	10.49 (br s, 1H), 8.90 (br s, 1H), 8.43 (d, *J*=8.3 Hz, 1H), 8.18 (br d, *J*=8 Hz, 1H), 7.76 (s, 1H), 4.46-4.82 (br s, 2H), 3.92 (AB quartet, J_{AB}=11.2 Hz, $\Delta\nu_{AB}$=36.1 Hz, 2H), 3.71-3.81 (m, 1H), 3.18 (dd, *J*=12.7, 4.1 Hz, 1H), 2.81-2.89 (m, 1H), 2.57-2.64 (m, 1H), 1.76-1.87 (m, 1H), 1.52-1.59 (m, 1H), 1.30 (d, *J*=6.0 Hz, 3H); LCMS *m/z* 458.0 (M+1), $[\alpha]^{22}{}_{D}$: -68.3 (c = 1.01, DMSO).

62	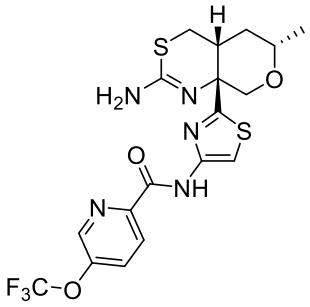	10.40 (br s, 1H), 8.52-8.57 (m, 1H), 8.36 (d, *J*=8.8 Hz, 1H), 7.77 (br d, *J*=9 Hz, 1H), 7.72 (s, 1H), 4.45-4.85 (br s, 2H), 3.91 (AB quartet, J_{AB}=11.1 Hz, $\Delta\nu_{AB}$=38.1 Hz, 2H), 3.70-3.80 (m, 1H), 3.17 (dd, *J*=12.6, 4.0 Hz, 1H), 2.80-2.88 (m, 1H), 2.60 (dd, *J*=12.6, 2.3 Hz, 1H), 1.75-1.87 (m, 1H), 1.51-1.59 (m, 1H), 1.30 (d, *J*=6.2 Hz, 3H); LCMS *m/z* 474.0 (M+1), $[\alpha]^{22}{}_{D}$ -78.3 (0.49, MeOH).
68	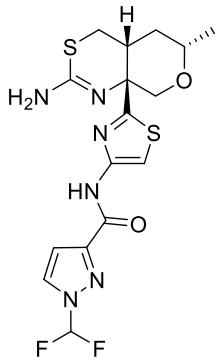	1H NMR (400 MHz, CHLOROFORM-d) Shift 9.37 (br. s., 1H), 7.91 (s, 1H), 7.68 (s, 1H), 7.07-7.41 (m, 2H), 4.02 (d, J=11.32 Hz, 1H), 3.87 (d, J=11.32 Hz, 1H), 3.71-3.81 (m, J=5.90, 10.90 Hz, 1H), 3.19 (dd, J=3.71, 12.68 Hz, 1H), 2.82-2.90 (m, J=12.90 Hz, 1H), 2.63 (d, J=12.88 Hz, 1H), 1.82 (q, J=12.62 Hz, 1H), 1.54-1.62 (m, J=13.30 Hz, 1H), 1.31 (d, J=5.85 Hz, 3H). LCMS *m/z* 429.1 (M+1), $[\alpha]^{22}{}_{D}$ -59.0 (0.69, MeOH).

Synthesis of 2-((4aR,6S,8aR)-2-amino-6-methyl-4,4a,5,6-tetrahydropyrano[3,4-d][1,3]thiazin-8a(8H)-yl)-N-(3-methoxyphenyl)thiazole-5-carboxamide (70)

Step 1. 2-((4aR,6S,8aR)-2-benzamido-6-methyl-4,4a,5,6-tetrahydropyrano[3,4-d][1,3]thiazin-8a(8H)-yl)-N-(3-methoxyphenyl)thiazole-5-carboxamide. To a stirring mixture of 2-((4aR,6S,8aR)-2-benzamido-6-methyl-4,4a,5,6-tetrahydropyrano[3,4-d][1,3]thiazin-8a(8H)-yl)thiazole-5-carboxylic acid (92 mg, 0.22 mmol) and *m*-anisidine (137mg, 1.11 mmol) in ethyl acetate (4 mL) was added trimethylamine (0.135 mL, 0.969 mmol) followed by T_3P (0.285 mL, 0.479 mmol, 50 wt % solution in ethyl acetate). The resulting solution was stirred cold for 0.5

hours then allowed to warm to r.t. overnight as the cooling bath expired. The reaction was diluted with saturated aqueous sodium bicarbonate solution (7.5 mL) and extracted with ethyl acetate (3 x 10 mL). The combined organic extracts were dried (Na_2SO_4), filtered and concentrated in vacuo to give a crude residue. Purification via flash column chromatography (silica gel, Gradient: 0 to 100% ethyl acetate in heptanes) afforded 2-((4aR,6S,8aR)-2-benzamido-6-methyl-4,4a,5,6-tetrahydropyrano[3,4-d][1,3]thiazin-8a(8H)-yl)-N-(3-methoxyphenyl)thiazole-5-carboxamide (98 mg, 85% yield) as a solid. LCMS *m/z* 523.3 $[M + H]^+$. ^{1}H NMR (400 MHz, $CDCl_3$) δ 8.29 (s, 1H), 8.05 (br s., 2H), 7.61 (s, 1H), 7.55-7.60 (m, *J* = 7.20, 7.20 Hz, 1H), 7.46-7.52 (m, *J* = 7.50, 7.50 Hz, 2H), 7.32 (t, *J* = 2.25 Hz, 1H), 7.22-7.26 (m, 1H), 7.06 (dd, *J* = 1.96, 8.02 Hz, 1H), 6.72 (dd, *J* = 2.45, 8.31 Hz, 1H), 3.97-4.02 (m, 1H), 3.90-3.96 (m, 1H), 3.81 (s, 3H), 3.78 (ddd, *J* = 1.96, 6.21, 11.20 Hz, 1H), 3.10-3.16 (m, 1H), 3.04-3.10 (m, 1H), 2.63 (dd, *J* = 2.35, 12.91 Hz, 1H), 1.82-1.94 (m, 1H), 1.65-1.71 (m, 1H), 1.30 (d, *J* =.26 Hz, 3H).

Step 2. Synthesis of 2-((4aR,6S,8aR)-2-amino-6-methyl-4,4a,5,6-tetrahydropyrano[3,4-d][1,3]thiazin-8a(8H)-yl)-N-(3-methoxyphenyl)thiazole-5-carboxamide (**70**). Methylamine (2 mL, 16 mmol, 33 wt % solution in ethanol) was added to a stirring solution of the above thioamide (94 mg, 0.18 mmol) in absolute ethanol (1.5 mL). The reaction was stirred at room temperature for 3.5 hours, concentrated *in vacuo*, then purified via flash column chromatography (silica gel, Gradient: 30→100% ethyl acetate in heptanes) to afford 2-((4aR,6S,8aR)-2-amino-6-methyl-4,4a,5,6-tetrahydropyrano[3,4-d][1,3]thiazin-8a(8H)-yl)-N-(3-methoxyphenyl)thiazole-5-carboxamide **(70)** (71 mg, 94% yield) as a solid. LCMS *m/z* 419.4 $[M + H]^+$. $[\alpha]^{22}_D$ + 36.1 (c=0.63, CH_3OH). ^{1}H NMR (400 MHz, $CDCl_3$) δ 8.25 (s, 1H), 7.58 (s, 1H), 7.32 (t, *J* = 2.2, 2.2 Hz, 1H), 7.23 (t, *J* = 8.2, 8.2 Hz, 1H), 7.03 (ddd, *J* = 0.8, 2.0, 8.0 Hz, 1H), 6.70 (ddd, *J* = 0.8, 2.5,

8.3 Hz, 1H), 4.71 (br s, 2H), 3.95 (d, *J* = 11.0 Hz, 1H), 3.85 (d, *J* = 11.0 Hz, 1H), 3.81 (s, 3H), 3.73 (dqd, *J* = 2.1, 6.0, 6.1, 6.1, 12.2 Hz, 1H), 3.13 (dd, *J* = 4.0, 12.6 Hz, 1H), 2.89 (ddq, *J* = 2.0, 2.0, 2.9, 4.0, 11.0 Hz, 1H), 2.61 (dd, *J* = 2.8, 12.6 Hz, 1H), 1.80 (td, *J* = 11.4, 12.9, 13.0 Hz, 1H), 1.55 (ddd, *J* = 2.4, 4.2, 13.4 Hz, 1H), 1.28 (d, *J* = 6.1 Hz, 3H).

2-((4aR,6S,8aR)-2-amino-6-methyl-4,4a,5,6-tetrahydropyrano[3,4-d][1,3]thiazin-8a(8H)-yl)-N-(6-methoxypyridin-2-yl)thiazole-5-carboxamide (71)

Step 1. N-((4aR,6S,8aR)-6-methyl-8a-(thiazol-2-yl)-4,4a,5,6,8,8a-hexahydropyrano[3,4-d][1,3]thiazin-2-yl)benzamide. Sodium hydroxide (35 mL, 1M) was added to a suspension of compound **54** (3.02 g, 6.68 mmol), and zinc dust (2400 mg), in THF (35 mL) . The mixture was stirred at 40 ^{o}C for 16 hours then at 50 ^{o}C for 2.5 hours prior to allowing the mixture to cool back to room temperature. The suspension was filtered over celite. The celite was washed with THF. The combined filtrates were washed with brine (50 mL), and separated. The aqueous phase was extracted with ethyl acetate (2 x 50 mL). The pooled organic layers were dried over sodium sulfate, filtered and concentrated in vacuo to a colorless foam that was purified by flash column chromatography [Gradient: 0 to 100% ethyl acetate in heptane] to afford the title compound as a white solid (2.15 g, 5.76 mmol, 86%). LC/MS M+z 374.4 M + H. ^{1}H NMR (400 MHz, $CDCl_3$) δ ppm 8.00-8.40 (br m, 2 H) 7.85 (d, *J* = 3.12 Hz, 1 H) 7.44 - 7.62 (m, 3 H) 7.35 (d, *J* = 2.73 Hz, 1 H) 3.99 (br. s., 2 H) 3.74 - 3.91 (m, 1 H) 3.09-3.21 (m, 2 H) 2.63 (d, *J* = 11.32 Hz, 1 H) 1.86-2.00 (m, 1 H) 1.69 (d, *J* = 13.27 Hz, 1 H) 1.32 (d, *J* = 5.85 Hz, 3 H).

Step 2. 2-((4aR,6S,8aR)-2-benzamido-6-methyl-4,4a,5,6-tetrahydropyrano[3,4-d][1,3]thiazin-8a(8H)-yl)thiazole-5-carboxylic acid. *n*-Butyllithium (394 uL, 2.5M in hexanes) was added dropwise to a pre-argon-sparged solution of N-((4aR,6S,8aR)-6-methyl-8a-(thiazol-2-yl)-

4,4a,5,6,8,8a-hexahydropyrano[3,4-d][1,3]thiazin-2-yl)benzamide (153 mg, 0.41 mmol), in tetrahydrofuran (10 mL) at -78 ^{o}C. The mixture was stirred cold for one hour prior to bubbling carbon dioxide through the mixture for ten minutes. After stirring this mixture at – 78 ^{o}C for one hour, argon was bubbled through the mixture for 5 minutes. Sodium hydroxide was added (20 mL, 0.25M) and the mixture removed from the dry-ice bath and allowed to warm to near room temperature. The mixture was extracted with dichloromethane (2 x 15 mL). The aqueous phase was brought to an approximate pH of 2 by addition of 1M hydrochloric acid, and extracted w/ ethyl actetate (3 x 25 mL). The pooled ethyl acetate layers were dried over sodium sulfate, filtered and concentrated in vacuo to afford the title compound as a yellow-white solid (162 mg, 0.39 mmol, 95%). LC/MS M+z 418.1 M + H. ^{1}H NMR (400 MHz, CD_3OD) δ ppm 8.39 (s, 1 H) 8.06 (d, *J* = 7.41 Hz, 2 H) 7.58 - 7.67 (m, 1 H) 7.49 - 7.55 (m, 2 H) 3.94 - 4.08 (m, 2 H) 3.75 - 3.89 (m, 1 H) 2.99 - 3.14 (m, 2 H) 2.75 (d, *J* = 10.54 Hz, 1 H) 1.73 - 1.83 (m, 2 H) 1.29 (d, *J* = 6.24 Hz, 3 H).

Step 3. 2-((4aR,6S,8aR)-2-benzamido-6-methyl-4,4a,5,6-tetrahydropyrano[3,4-d][1,3]thiazin-8a(8H)-yl)-N-(6-methoxypyridin-2-yl)thiazole-5-carboxamide. To O-(2-Oxo-1(2H)pyridyl)-N,N,N′,N′-tetramethyluronium tetrafluoroborate (29 mg) was added to a mixture of 2-((4aR,6S,8aR)-2-benzamido-6-methyl-4,4a,5,6-tetrahydropyrano[3,4-d][1,3]thiazin-8a(8H)-yl)thiazole-5-carboxylic acid (41 mg, 0.098 mmol), and N,N-diisopropylethylamine (34 uL) in DMF (2.5 mL). The mixture was stirred at RT for 45 min prior to addition of 6-methoxypyridin-2-amine (48.7 mg in 0.3 mL DMF). The mixture was stirred at RT for 1h then stirred at 45 ^{o}C for 16 hours prior to addition of more 6-methoxypyridin-2-amine (35 uL). This mixture was stirred at 45 ^{o}C for another seven hours prior to allowing to cool back to near room temperature. The mixture was diluted with saturated aqueous sodium bicarbonate (25 mL) and

extracted with ethyl acetate (3 x 35 mL). The pooled ethyl acetate layers were dried over sodium sulfate, filtered and concentrated in vacuo to an amber oil that was purified by flash column chromatography [Gradient: 0 to 100% ethyl acetate in heptane] to afford the title compound as a white solid (23.6 mg, 0.045 mmol, 46%). LC/MS M+z 524.1 M + H. ^{1}H NMR (400 MHz, $CDCl_3$) δ ppm 8.36 (s, 1 H) 7.96-8.20 (br. m., 3 H) 7.81 (d, *J* = 7.81 Hz, 1 H) 7.65 (t, *J* = 8.00 Hz, 1 H) 7.60 (d, *J* = 6.24 Hz, 1 H) 7.49 - 7.56 (m, 2 H) 6.57 (d, *J* = 8.20 Hz, 1 H) 3.94 - 4.07 (m, 2 H) 3.91 (s, 3 H) 3.76 - 3.86 (m, 1 H) 3.05 - 3.21 (m, 2 H) 2.67 (d, *J* = 12.10 Hz, 1 H) 1.83 - 1.98 (m, 1 H) 1.72 (d, *J* = 14.05 Hz, 1 H) 1.33 (d, *J* = 6.24 Hz, 3 H).

Step 4. 2-((4aR,6S,8aR)-2-amino-6-methyl-4,4a,5,6-tetrahydropyrano[3,4-d][1,3]thiazin-8a(8H)-yl)-N-(6-methoxypyridin-2-yl)thiazole-5-carboxamide. Methylamine (0.5 mL, 33% in ethanol) was added to a solution of 2-((4aR,6S,8aR)-2-benzamido-6-methyl-4,4a,5,6-tetrahydropyrano[3,4-d][1,3]thiazin-8a(8H)-yl)-N-(6-methoxypyridin-2-yl)thiazole-5-carboxamide (23.5 mg, 0.045 mmol) in ethanol (0.5 mL) and stirred at room temperature. After stirring for 16 hours the mixture was concentrated in vacuo to a colorless oil that was purified by flash column chromatography [Gradient: 25-100% ethyl acetate in heptane) to afford the title compound **71** as a white solid (14 mg, 0.033 mmol, 74%). LC/MS M+z 420.1 M + H). $[\alpha]^{22}_D$ + 18.0 (c=0.76, MeOH). ^{1}H NMR (400 MHz, $CDCl_3$) δ ppm 8.30 (s, 1 H) 8.02 (br. s., 1 H) 7.78 (d, *J* = 7.83 Hz, 1 H) 7.62 (t, *J* = 7.92 Hz, 1 H) 6.53 (d, *J* = 8.41 Hz, 1 H) 3.96 - 4.03 (m, 1 H) 3.84-3.90 (m, 4 H) 3.69 - 3.78 (m, 1 H) 3.14 (d, *J* = 12.62 Hz, 1 H) 2.94 (d, *J* = 12.91 Hz, 1 H) 2.64 (d, *J* = 12.91 Hz, 1 H) 1.73 - 1.88 (m, 1 H) 1.54 - 1.62 (m, 1 H) 1.29 (d, *J* = 6.16 Hz, 3 H).

N-[(4aR,6S,8aR)-8a-(4-Amino-1,3-thiazol-2-yl)-6-methyl-4,4a,5,6,8,8a-hexahydropyrano[3,4-d][1,3]thiazin-2-yl]benzamide (72)

Step 1. Synthesis of (3aR,5S,7aR)-7a-(4-bromo-1,3-thiazol-2-yl)-5-methylhexahydro-1H-pyrano[3,4-c][1,2]oxazole (**51**). 2,4-Dibromo-1,3-thiazole (44.7 g, 184 mmol) was dissolved in a mixture of toluene and tetrahydrofuran (10:1, 900 mL) and cooled to −78 °C. To this solution was added boron trifluoride diethyl etherate (21.9 mL, 177 mmol), followed by drop-wise addition of *n*-butyllithium (2.5 M solution in hexanes, 68.0 mL, 170 mmol), and the reaction mixture was stirred for 30 minutes. A solution of **15** (20 g, 140 mmol) in a mixture of toluene and tetrahydrofuran (10:1, 22 mL) was then added drop-wise; the reaction temperature was maintained below −72 °C during the course of both additions. Stirring was continued for 1 hour at −78 °C, whereupon the reaction was quenched via addition of saturated aqueous ammonium chloride solution. The aqueous layer was extracted three times with ethyl acetate, and the combined organic layers were washed with water and with saturated aqueous sodium chloride solution, dried over sodium sulfate, filtered, and concentrated *in vacuo*. Silica gel chromatography (Gradient: 0% to 100% ethyl acetate in heptane) afforded the product **51** as a tacky amber oil. Yield: 36.34 g, 119.1 mmol, 85%. LCMS *m/z* 305.0, 307.0 $[M+H]^+$. ^{1}H NMR (400 MHz, $CDCl_3$) δ 7.22 (s, 1H), 3.97 (AB quartet, upfield doublet is broadened, J_{AB} = 12.6 Hz, $\Delta\nu_{AB}$ = 13.4 Hz, 2H), 3.67-3.76 (m, 3H), 3.38 (br ddd, *J* = 11.8, 6.9, 4.6 Hz, 1H), 1.90 (ddd, *J* = 14.1, 6.9, 2.1 Hz, 1H), 1.42 (ddd, *J* = 14.1, 11.7, 11.7 Hz, 1H), 1.27 (d, *J* = 6.2 Hz, 3H).

Step 2. Synthesis of [(2S,4R,5R)-5-amino-5-(4-bromo-1,3-thiazol-2-yl)-2-methyltetrahydro-2H-pyran-4-yl]methanol (**52**). Molybdenum hexacarbonyl (98%, 6.67 g, 24.8 mmol) was added to a solution of **51** (15.12 g, 49.54 mmol) in a mixture of acetonitrile (390 mL) and water (20 mL), and the reaction mixture was heated at reflux for 1 hour. After cooling to room temperature, the reaction mixture was chilled in an ice bath, treated portion-wise with sodium borohydride (7.50 g, 198 mmol), and allowed to stir at 0 °C for 1 hour. The mixture was then filtered through a pad

of diatomaceous earth, and the pad was washed three times with dichloromethane; the organic portion of the combined filtrate and washes was washed with saturated aqueous sodium chloride solution, dried over sodium sulfate, filtered, and concentrated *in vacuo*. Methanol was added to the residue, then removed via concentration under reduced pressure. This methanol treatment was repeated, and the resulting residue was dissolved in dichloromethane, washed twice with 1 M aqueous sodium hydroxide solution, washed once with saturated aqueous sodium chloride solution and concentrated *in vacuo*, affording the product as a brown solid. Yield: 14.48 g, 47.13 mmol, 95%. LCMS *m/z* 307.0, 309.0 $[M+H]^+$. ^{1}H NMR (400 MHz, $CDCl_3$) δ 7.22 (s, 1H), 3.79 (d, half of AB quartet, *J*=11.5 Hz, 1H), 3.64-3.75 (m, 3H), 3.54 (dd, half of ABX pattern, *J* = 11.5, 4.1 Hz, 1H), 2.46-2.54 (m, 1H), 1.82-1.94 (m, 1H), 1.67-1.74 (m, 1H), 1.32 (d, *J* = 6.2 Hz, 3H).

Step 3. Synthesis of N-{[(3R,4R,6S)-3-(4-bromo-1,3-thiazol-2-yl)-4-(hydroxymethyl)-6-methyltetrahydro-2H-pyran-3-yl]carbamothioyl}benzamide (**53**). Benzoyl isothiocyanate (6.92 g, 42.4 mmol) was added in a drop-wise manner to a solution of **52** (14.48 g, 47.13 mmol) in dichloromethane (420 mL), and the reaction mixture was stirred at room temperature for 24 hours. Volatiles were removed *in vacuo*, and the residue was purified via silica gel chromatography (Gradient: 0% to 50% ethyl acetate in heptane), providing the product as a yellow solid. Yield: 14.7 g, 31.2 mmol, 66%. LCMS m/z 472.1 [M+H+]. ^{1}H NMR (400 MHz, $CDCl_3$) δ 11.70 (br s, 1H), 8.93 (br s, 1H), 7.86-7.90 (m, 2H), 7.62-7.67 (m, 1H), 7.51-7.56 (m, 2H), 7.25 (s, 1H), 5.47 (d, *J* = 11.9 Hz, 1H), 3.91 (d, *J* = 12.0 Hz, 1H), 3.83 (d, *J* = 4.4 Hz, 2H), 3.74-3.81 (m, 1H), 2.44-2.52 (m, 1H), 1.80-1.87 (m, 2H), 1.33 (d, *J* = 6.2 Hz, 3H).

Step 4. Synthesis of N-[(4aR,6S,8aR)-8a-(4-bromo-1,3-thiazol-2-yl)-6-methyl-4,4a,5,6,8,8a-hexahydropyrano[3,4-d][1,3]thiazin-2-yl]benzamide (**54**). 1-Chloro-*N*,*N*,2-trimethylprop-1-en-1-

amine (Ghosez's reagent, 7.85 mL, 59.3 mmol) was added drop-wise to a solution of **53** (9.30 g, 19.8 mmol) in dichloromethane (200 mL). After 1 hour at room temperature, the reaction mixture was partitioned between dichloromethane and saturated aqueous sodium bicarbonate solution. The organic layer was washed with saturated aqueous sodium chloride solution, dried over sodium sulfate, filtered, and concentrated *in vacuo*. Silica gel chromatography (Gradient: 0% to 100% ethyl acetate in heptane) provided the product as a solid. Yield: 6.90 g, 15.2 mmol, 77%. LCMS *m/z* 452.1, 454.1 $[M+H]^+$. ^{1}H NMR (400 MHz, $CDCl_3$) δ 13.69 (br s, 1H), 8.38-8.43 (m, 2H), 7.64-7.70 (m, 1H), 7.54-7.60 (m, 2H), 7.34 (s, 1H), 4.45 (d, *J* = 12.5 Hz, 1H), 3.93 (d, *J* = 12.5 Hz, 1H), 3.74-3.83 (m, 1H), 3.28-3.36 (m, 1H), 3.23 (dd, *J* = 13.5, 4.0 Hz, 1H), 2.77 (dd, *J* = 13.5, 2.8 Hz, 1H), 1.66-1.82 (m, 2H), 1.32 (d, *J* = 6.2 Hz, 3H).

Step 5. Synthesis of N-[(4aR,6S,8aR)-8a-(4-amino-1,3-thiazol-2-yl)-6-methyl-4,4a,5,6,8,8a-hexahydropyrano[3,4-d][1,3]thiazin-2-yl]benzamide (**72**). Sodium *tert*-butoxide (19.6 g, 204 mmol), tris(dibenzylideneacetone)dipalladium(0) (3.74 g, 4.09 mmol), and di-*tert*-butyl[2',4',6'-tri(propan-2-yl)biphenyl-2-yl]phosphane (5.21 g, 12.3 mmol) were dissolved in degassed 1,4-dioxane (175 mL), and the reaction flask was purged with nitrogen and placed in an oil bath heated 95 °C. Once the internal temperature reached 90°C a solution of 1-(2,4-dimethoxyphenyl)methanamine (20.9 mL, 139 mmol) and **54** (37.0 g, 81.8 mmol) in 1,4-dioxane (200 mL) was added over 1.5min and the reaction mixture was allowed to heat in a 95 °C oil bath for 13min. The reaction vessel was then placed in an ice water bath to rapidly cool to 25°C and the reaction was filtered through celite. The filter cake was washed with dichlormethane (500 ml) and the filtrate was concentrated in vacuo. The residue was diluted with dichloromethane (300 ml) and the solution cooled to 8°C in an ice bath. Methanesulfonic acid (64 ml, 980 mmol) was added dropwise at such a rate to ensure the internal reaction temperature

does not exceed 21°C. After addition of the methanesulfonic acid the reaction was stirred at 21°C for 25min. The reaction was then washed with aqueous hydrochloric acid (3 x 250ml, 1N). The combined aqueous was filtered through celite and the filter cake washed with water (2 x 250 ml). The filtrate was cooled to 12°C in an ice bath and a mixture of 150g ice in aqueous sodium hydroxide (360 ml, 5N) was added with stirring at such a rate to prevent the internal reaction temperature from exceeding 21°C (final pH = 10). The now heterogenous aqueous mixture was saturated with solid sodium chloride and the aqueous was washed with dichloromethane (4 x 400 ml). The combined organics were washed with aqueous citric acid (500 ml , 5% citric acid in water [w/v]), brine (200 ml), then dried over anhydrous magnesium sulfate, filtered and concentrated to provide title compound containing 16% residual solvent. Yield: 27.1g, 69.6 mmol, 85.1% (69.6% yield corrected for residual solvent). LCMS *m/z* 389.1 $[M+H]^+$. ^{1}H NMR (400 MHz, $CDCl_3$) δ 8.10-8.19 (br m, 2H), 7.49-7.55 (m, 1H), 7.42-7.48 (m, 2H), 5.94 (s, 1H), 3.95 (AB quartet, J_{AB} = 12.1 Hz, $\Delta\nu_{AB}$ = 6.2 Hz, 2H), 3.77 (dqd, *J* = 11.2, 6.1, 2.3 Hz, 1H), 3.22 (dd, *J* = 12.9, 4.1 Hz, 1H), 2.97-3.05 (m, 1H), 2.59 (dd, *J* = 12.9, 2.8 Hz, 1H), 1.83-1.95 (m, 1H), 1.65 (ddd, *J* = 13.7, 4.3, 2.4 Hz, 1H), 1.29 (d, *J* = 6.2 Hz, 3H).

Alternative Step 5. **Synthesis of N-[(4aR,6S,8aR)-8a-(4-amino-1,3-thiazol-2-yl)-6-methyl-4,4a,5,6,8,8a-hexahydropyrano[3,4-d][1,3]thiazin-2-yl]benzamide (72).**

To an ethanol solution (35.0mL, absolute) of N-((4aR,6S,8aR)-8a-(4-bromothiazol-2-yl)-6-methyl-4,4a,5,6,8,8a-hexahydropyrano[3,4-d][1,3]thiazin-2-yl)benzamide **54** (0.44 g, 0.97 mmol) was added *trans*-N,N'-Dimethylcyclohexane-1,2-diamine (0.17g, 1.20 mmol), followed by sodium azide (0.600g, 9.22mmol) and a water solution (10.0 mL) of (+)-sodium-L-ascorbate (0.092g, 0.46 mmol) The resulting solution was purged with nitrogen and vacuum (3x). Then the

reaction mixture was stirred under nitrogen at rt for 15min. Copper (I) Iodide (0.087g, 0.46mmol) was then added and the resulting solution was heated to 70 ^{o}C with a nitrogen inlet for 2h. The reaction mixture was then concentrated under reduced pressure, partitioned between ethyl acetate (50 mL) and hydrogen chloride (1N, 2aq., 100 mL). The resulting organic layer was separated and the aqueous layer was again washed with ethyl acetate (1x50 mL). The aqueous layer was then basified to pH 9 with aq. sodium bicarbonate (250mL). Organics were now extracted with dichloromethane (3x100 mL), washed with brine (1x250 mL), dried over sodium sulfate, filtered and concentrated under reduced pressure to yield N-((4aR,6S,8aR)-8a-(4-aminothiazol-2-yl)-6-methyl-4,4a,5,6,8,8a-hexahydropyrano[3,4-d][1,3]thiazin-2-yl)benzamide as an orange solid (0.177g, 47% yield).

Ancillary Information.

Supporting Information

The effect of compound **64** on brain Aβ following 5-Day sub-chronic dosing; BACE2 inhibition causes accumulation of full length PMEL in primary human melanocytes; BACE1 and BACE2 binding curves; Time course of fur re-growth in control C57Blk mice following depilation with Nair; Dose response effect of compound **3** and compound **4** on pigmentation in C57Blk mice at 3 weeks post depilation; Projected Cavg concentration in mouse studie; Mouse skin epithelial transmission electron microscopic images; 3D skin model delta L quantification for compound **61** and compound **65**; Single crystal x-ray analysis of **64**-HCl; Representative 1H NMR; and molecular formula strings. The supporting information is available free of charge on the ACS Publication website at DOI:…

CCDC1829109 (Single crystal x-ray analysis of **64**-HCl). Authors will release the atomic coordinates and experimental data upon article publication.

Corresponding Author

*Michael A. Brodney; email: michael.a.brodney@hotmail.com

Acknowledgements

The authors would like to thank Leslie Pustilnik, Stephen Noell, Shawn Hallowell, Carol Menard, Eric Benvenuti for screening support along with Katherine McGrath, Theresa Dickinson, Tracy Brown Phillips for reagent production. Peter Mikochik contributed experiments for the optimization of the Buchwald coupling of bromide **54.**

Abbreviations

β-secretase, BACE1; drug drug interaction, DDI; Alzheimer's disease, AD; amyloid-β, Aβ; Alzheimer's disease, AD; N-terminal ectodomain of APP, sAPPβ; C-terminal fragment, C99; cathepsin D, CatD; whole cell assay, WCA; cell free assay, CFA; P-glycoprotein, P-gp; human liver microsomes, HLM; transmembrane protein 27, TMEM27; pigment cell-specific melanocyte protein, PMEL17; hydrogen bond donor, HBD; National Institue of Health, NIH; breast cancer resistant protein, BCRP; below limit of quantitation, BLQ; cerebrospinal fluid, CSF; central nervous system (CNS); hour, h; milligram per kilogram, mg/kg; standard error of the mean, three-dimensional, 3D; SEM; ethylenediaminetetraacetic acid, EDTA; dissociation-enhanced lanthanide fluorescent immunoassay, DELFIA; platform enzyme-linked immunosorbent assay, ELISA; tetrahydropyran; THP;

REFERENCES

1. Vassar, R.; Kovacs, D. M.; Yan, R.; Wong, P. C. The β-secretase enzyme BACE in health and Alzheimer's disease: regulation, cell biology, function, and therapeutic potential. *J. Neurosci.* **2009,** *29* (41), 12787-12794.

2. Marks, N.; Berg, M. J. BACE and γ-secretase characterization and their sorting as therapeutic targets to reduce amyloidogenesis. *Neurochem. Res.* **2010,** *35* (2), 181-210.

3. Citron, M.; Eckman, C. B.; Diehl, T. S.; Corcoran, C.; Ostaszewski, B. L.; Xia, W.; Levesque, G.; St. George Hyslop, P.; Younkin, S. G.; Selkoe, D. J. Additive effects of PS1 and APP mutations on secretion of the 42-residue amyloid β-protein. *Neurobiol. Dis.* **1998,** *5* (2), 107-116.

4. Jonsson, T.; Atwal, J. K.; Steinberg, S.; Snaedal, J.; Jonsson, P. V.; Bjornsson, S.; Stefansson, H.; Sulem, P.; Gudbjartsson, D.; Maloney, J.; Hoyte, K.; Gustafson, A.; Liu, Y.; Lu, Y.; Bhangale, T.; Graham, R. R.; Huttenlocher, J.; Bjornsdottir, G.; Andreassen, O. A.; Joensson, E. G.; Palotie, A.; Behrens, T. W.; Magnusson, O. T.; Kong, A.; Thorsteinsdottir, U.; Watts, R. J.; Stefansson, K. A mutation in APP protects against Alzheimer's disease and age-related cognitive decline. *Nature (London, U. K.)* **2012,** *488* (7409), 96-99.

5. Hardy, J.; Allsop, D., Amyloid deposition as the central event in the etiology of Alzheimer's disease. *Trends Pharmacol. Sci.* **1991,** *12* (10), 383-388.

6. Walsh, D. M.; Minogue, A. M.; Sala Frigerio, C.; Fadeeva, J. V.; Wasco, W.; Selkoe, D. J. The APP family of proteins: similarities and differences. *Biochem. Soc. Trans.* **2007,** *35* (2), 416-420.

7. Bennett, B. D.; Babu-Khan, S.; Loeloff, R.; Louis, J. C.; Curran, E.; Citron, M.; Vassar, R., Expression analysis of BACE2 in brain and peripheral tissues. *The Journal of Biological Chemistry* **2000,** *275* (27), 20647-20651.

8. Esterhazy, D.; Stuetzer, I.; Wang, H.; Rechsteiner, M. P.; Beauchamp, J.; Doebeli, H.; Hilpert, H.; Matile, H.; Prummer, M.; Schmidt, A.; Lieske, N.; Boehm, B.; Marselli, L.; Bosco, D.; Kerr-Conte, J.; Aebersold, R.; Spinas, G. A.; Moch, H.; Migliorini, C.; Stoffel, M. Bace2 Is a β cell-enriched protease that regulates pancreatic β cell function and mass. *Cell Metab.* **2011,** *14* (3), 365-377.

9. Fowler, D. M.; Koulov, A. V.; Alory-Jost, C.; Marks, M. S.; Balch, W. E.; Kelly, J. W. Functional amyloid formation within mammalian tissue. *PLoS Biology* **2006,** *4* (1), e6.

10. Watt, B.; van Niel, G.; Fowler, D. M.; Hurbain, I.; Luk, K. C.; Stayrook, S. E.; Lemmon, M. A.; Raposo, G.; Shorter, J.; Kelly, J. W.; Marks, M. S. N-terminal domains elicit formation of functional Pmel17 amyloid fibrils. *The Journal of Biological Chemistry* **2009,** *284* (51), 35543-35555.

11. Rochin, L.; Hurbain, I.; Serneels, L.; Fort, C.; Watt, B.; Leblanc, P.; Marks, M. S.; De Strooper, B.; Raposo, G.; van Niel, G. BACE2 processes PMEL to form the melanosome amyloid matrix in pigment cells. *Proceedings of the National Academy of Sciences* **2013,** *110* (26), 10658-10663.

12. van Bebber, F.; Hruscha, A.; Willem, M.; Schmid, B.; Haass, C. Loss of Bace2 in zebrafish affects melanocyte migration and is distinct from Bace1 knock out phenotypes. *Journal of Neurochemistry* **2013,** *127* (4), 471-481.

13. Burgoyne, T.; O'Connor, M. N.; Seabra, M. C.; Cutler, D. F.; Futter, C. E. Regulation of melanosome number, shape and movement in the zebrafish retinal pigment epithelium by OA1 and PMEL. *Journal of Cell Science* **2015,** *128* (7), 1400-1407.

14. Cebers, G.; Lejeune, T.; Attalla, B.; Soderberg, M.; Alexander, R. C.; Budd Haeberlein, S.; Kugler, A. R.; Ingersoll, E. W.; Platz, S.; Scott, C. W. Reversible and species-specific

depigmentation effects of AZD3293, a BACE inhibitor for the treatment of Alzheimer's Disease, are related to BACE2 inhibition and confined to epidermis and hair. *The Journal of Prevention of Alzheimer's Disease* **2016,** *3* (4), 202-218.

15. Neumann, U.; Rueeger, H.; Machauer, R.; Veenstra, S. J.; Lueoend, R. M.; Tintelnot-Blomley, M.; Laue, G.; Beltz, K.; Vogg, B.; Schmid, P.; Frieauff, W.; Shimshek, D. R.; Staufenbiel, M.; Jacobson, L. H. A novel BACE inhibitor NB-360 shows a superior pharmacological profile and robust reduction of amyloid-beta and neuroinflammation in APP transgenic mice. *Molecular Neurodegeneration* **2015,** *10*, 44.

16. Filser, S.; Ovsepian, S. V.; Masana, M.; Blazquez-Llorca, L.; Brandt Elvang, A.; Volbracht, C.; Mueller, M. B.; Jung, C. K. E.; Herms, J. Pharmacological inhibition of BACE1 impairs synaptic plasticity and cognitive functions. *Biol. Psychiatry* **2015,** *77* (8), 729-739.

17. Kennedy, M. E.; Stamford, A. W.; Chen, X.; Cox, K.; Cumming, J. N.; Dockendorf, M. F.; Egan, M.; Ereshefsky, L.; Hodgson, R. A.; Hyde, L. A.; Jhee, S.; Kleijn, H. J.; Kuvelkar, R.; Li, W.; Mattson, B. A.; Mei, H.; Palcza, J.; Scott, J. D.; Tanen, M.; Troyer, M. D.; Tseng, J. L.; Stone, J. A.; Parker, E. M.; Forman, M. S. The BACE1 inhibitor verubecestat (MK-8931) reduces CNS β-amyloid in animal models and in Alzheimer's disease patients. *Sci. Transl. Med.* **2016,** *8* (363), 363ra150/1-363ra150/14.

18. Ghosh, A. K.; Cárdenas, E. L.; Osswald, H. L. The design, development, and evaluation of BACE1 inhibitors for the treatment of Alzheimer's Disease. *Top. Med. Chem.* **2016,** *24*, 27-85.

19. May, P. C.; Dean, R. A.; Lowe, S. L.; Martenyi, F.; Sheehan, S. M.; Boggs, L. N.; Monk, S. A.; Mathes, B. M.; Mergott, D. J.; Watson, B. M.; Stout, S. L.; Timm, D. E.; LaBell, E. S.; Gonzales, C. R.; Nakano, M.; Jhee, S. S.; Yen, M.; Ereshefsky, L.; Lindstrom, T. D.; Calligaro,

D. O.; Cocke, P. J.; Hall, D. G.; Friedrich, S.; Citron, M.; Audia, J. E. Robust central reduction of amyloid-β in humans with an orally available, non-peptidic β-secretase inhibitor. *J. Neurosci.* **2011,** *31* (46), 16507-16516.

20. Zuhl, A. M.; Nolan, C. E.; Brodney, M. A.; Niessen, S.; Atchison, K.; Houle, C.; Karanian, D. A.; Ambroise, C.; Brulet, J. W.; Beck, E. M.; Doran, S. D.; O'Neill, B. T.; am Ende, C. W.; Chang, C.; Geoghegan, K. F.; West, G. M.; Judkins, J. C.; Hou, X.; Riddell, D. R.; Johnson, D. S. Chemoproteomic profiling reveals that cathepsin D off-target activity drives ocular toxicity of β-secretase inhibitors. *Nat. Commun.* **2016,** *7*, 13042.

21. Scott, J. D.; Li, S. W.; Brunskill, A. P. J.; Chen, X.; Cox, K.; Cumming, J. N.; Forman, M.; Gilbert, E. J.; Hodgson, R. A.; Hyde, L. A.; Jiang, Q.; Iserloh, U.; Kazakevich, I.; Kuvelkar, R.; Mei, H.; Meredith, J.; Misiaszek, J.; Orth, P.; Rossiter, L. M.; Slater, M.; Stone, J.; Strickland, C. O.; Voigt, J. H.; Wang, G.; Wang, H.; Wu, Y.; Greenlee, W. J.; Parker, E. M.; Kennedy, M. E.; Stamford, A. W. Discovery of the 3-imino-1,2,4-thiadiazinane 1,1-dioxide derivative Verubecestat (MK-8931)-a β-site amyloid precursor protein cleaving enzyme 1 inhibitor for the treatment of Alzheimer's Disease. *J. Med. Chem.* **2016,** *59* (23), 10435-10450.

22. May, P. C.; Willis, B. A.; Lowe, S. L.; Dean, R. A.; Monk, S. A.; Cocke, P. J.; Audia, J. E.; Boggs, L. N.; Borders, A. R.; Brier, R. A.; Calligaro, D. O.; Day, T. A.; Ereshefsky, L.; Erickso, J. A.; Gevorkyan, H.; Gonzales, C. R.; James, D. E.; Jhee, S. S.; Komjathy, S. F.; Li, L.; Lindstrom, T. D.; Mathe, B. M.; Martenyi, F.; Sheehan, S. M.; Stout, S. L.; Timm, D. E.; Vaught, G. M.; Watson, B. M.; Winneroski, L. L.; Yang, Z.; Mergott, D. J. The potent BACE1 inhibitor LY2886721 elicits robust central Aβ pharmacodynamic responses in mice, dogs, and humans. *J. Neurosci.* **2015,** *35* (3), 1199-1210.

23. Stepan, A. F.; Walker, D. P.; Bauman, J.; Price, D. A.; Baillie, T. A.; Kalgutkar, A. S.; Aleo, M. D. Structural alert/reactive metabolite concept as applied in medicinal chemistry to mMitigate the risk of idiosyncratic drug toxicity: a perspective based on the critical examination of trends in the top 200 drugs marketed in the United States. *Chem. Res. Toxicol.* **2011,** *24* (9), 1345-1410.

24. Rajapakse, H. A.; Nantermet, P. G.; Selnick, H. G.; Barrow, J. C.; McGaughey, G. B.; Munshi, S.; Lindsley, S. R.; Young, M. B.; Ngo, P. L.; Katherine Holloway, M.; Lai, M.-T.; Espeseth, A. S.; Shi, X.-P.; Colussi, D.; Pietrak, B.; Crouthamel, M.-C.; Tugusheva, K.; Huang, Q.; Xu, M.; Simon, A. J.; Kuo, L.; Hazuda, D. J.; Graham, S.; Vacca, J. P. SAR of tertiary carbinamine derived BACE1 inhibitors: Role of aspartate ligand amine pK a in enzyme inhibition. *Bioorg. Med. Chem. Lett.* **2010,** *20* (6), 1885-1889.

25. Gravenfors, Y.; Viklund, J.; Blid, J.; Ginman, T.; Karlstroem, S.; Kihlstroem, J.; Kolmodin, K.; Lindstroem, J.; von Berg, S.; von Kieseritzky, F.; Bogar, K.; Slivo, C.; Swahn, B.-M.; Olsson, L.-L.; Johansson, P.; Eketjaell, S.; Faelting, J.; Jeppsson, F.; Stroemberg, K.; Janson, J.; Rahm, F. New aminoimidazoles as β-Secretase (BACE-1) inhibitors showing amyloid-β (Aβ) lowering in brain. *J. Med. Chem.* **2012,** *55* (21), 9297-9311.

26. Hitchcock, S. A. Structural modifications that alter the P-Glycoprotein efflux properties of compounds. *J. Med. Chem.* **2012,** *55* (11), 4877-4895.

27. Morgenthaler, M.; Schweizer, E.; Hoffmann-Roder, A.; Benini, F.; Martin, R. E.; Jaeschke, G.; Wagner, B.; Fischer, H.; Bendels, S.; Zimmerli, D.; Schneider, J.; Diederich, F.; Kansy, M.; Muller, K. Predicting and tuning physicochemical properties in lead optimization: amine basicities. *ChemMedChem* **2007,** *2* (8), 1100-1115.

28. Ginman, T.; Viklund, J.; Malmstroem, J.; Blid, J.; Emond, R.; Forsblom, R.; Johansson, A.; Kers, A.; Lake, F.; Sehgelmeble, F.; Sterky, K. J.; Bergh, M.; Lindgren, A.; Johansson, P.; Jeppsson, F.; Faelting, J.; Gravenfors, Y.; Rahm, F. Core refinement toward permeable β-Secretase (BACE-1) inhibitors with low hERG activity. *J. Med. Chem.* **2013,** *56* (11), 4181-4205.

29. Sanguinetti, M. C.; Tristani-Firouzi, M. hERG potassium channels and cardiac arrhythmia. *Nature (London, U. K.)* **2006,** *440* (7083), 463-469.

30. Hilpert, H.; Guba, W.; Woltering, T. J.; Wostl, W.; Pinard, E.; Mauser, H.; Mayweg, A. V.; Rogers-Evans, M.; Humm, R.; Krummenacher, D.; Muser, T.; Schnider, C.; Jacobsen, H.; Ozmen, L.; Bergadano, A.; Banner, D. W.; Hochstrasser, R.; Kuglstatter, A.; David-Pierson, P.; Fischer, H.; Polara, A.; Narquizian, R. β-Secretase (BACE1) inhibitors with high in vivo efficacy suitable for clinical evaluation in Alzheimer's Disease. *J. Med. Chem.* **2013,** *56* (10), 3980-3995.

31. Brodney, M. A.; Beck, E. M.; Butler, C. R.; Barreiro, G.; Johnson, E. F.; Riddell, D.; Parris, K.; Nolan, C. E.; Fan, Y.; Atchison, K.; Gonzales, C.; Robshaw, A. E.; Doran, S. D.; Bundesmann, M. W.; Buzon, L.; Dutra, J.; Henegar, K.; LaChapelle, E.; Hou, X.; Rogers, B. N.; Pandit, J.; Lira, R.; Martinez-Alsina, L.; Mikochik, P.; Murray, J. C.; Ogilvie, K.; Price, L.; Sakya, S. M.; Yu, A.; Zhang, Y.; O'Neill, B. T. Utilizing structures of CYP2D6 and BACE1 complexes to reduce risk of drug-drug interactions with a novel series of centrally efficacious BACE1 inhibitors. *J. Med. Chem.* **2015,** *58* (7), 3223-3252.

32. Rombouts, F. J. R.; Tresadern, G.; Delgado, O.; Martinez-Lamenca, C.; Van Gool, M.; Garcia-Molina, A.; Alonso de Diego, S. A.; Oehlrich, D.; Prokopcova, H.; Alonso, J. M.; Austin, N.; Borghys, H.; Van Brandt, S.; Surkyn, M.; De Cleyn, M.; Vos, A.; Alexander, R.; Macdonald,

G.; Moechars, D.; Gijsen, H.; Trabanco, A. A. 1,4-Oxazine β-Secretase 1 (BACE1) inhibitors: from hit generation to orally bioavailable brain penetrant leads. *J. Med. Chem.* **2015,** *58* (20), 8216-8235.

33. Ghosez, L. α-Chloroenamines. New reagents for organic synthesis. *Angew. Chem., Int. Ed. Engl.* **1972,** *11* (9), 852-853.

34. Ufimtsev, I. S.; Martinez, T. J. Quantum chemistry on graphical processing units. 3. analytical energy gradients, geometry optimization, and first principles molecular dynamics. *J. Chem. Theory Comput.* **2009,** *5* (10), 2619-2628.

35. MacroModel, Schrödinger Release 2017-4: MacroModel, Schrödinger, LLC, New York, NY, 2017.

36. Trapa, P. E.; Belova, E.; Liras, J. L.; Scott, D. O.; Steyn, S. J. Insights from an integrated physiologically based pharmacokinetic model for brain penetration. *J. Pharm. Sci.* **2016,** *105* (2), 965-971.

37. Danilenko, D. M.; Phillips, G. D. L.; Diaz, D. In vitro skin models and their predictability in defining normal and disease biology, pharmacology, and toxicity. *Toxicol. Pathol.* **2016,** *44* (4), 555-563.

38. Takeyama, R.; Takekoshi, S.; Nagata, H.; Osamura, R. Y.; Kawana, S. Quercetin-induced melanogenesis in a reconstituted three-dimensional human epidermal model. *J Mol Histol* **2004,** *35* (2), 157-165.

39. Choi, W.; Wolber, R.; Gerwat, W.; Mann, T.; Batzer, J.; Smuda, C.; Liu, H.; Kolbe, L.; Hearing, V. J. The fibroblast-derived paracrine factor neuregulin-1 has a novel role in regulating the constitutive color and melanocyte function in human skin. *J. Cell Sci.* **2010,** *123* (18), 3102-3111.

40. Qiu, R.; Liu, R.; He, P.; Wills, A.-M.; Tankisheva, E.; Alvey, C.; Buckeridge, C.; Bednar, M.; Alexander, R. C.; Chen, D. Saftey, tolerability, and pharmacokinetic and pharmacodynamic effects of PF-06751979, a potent and selective oral BACE1 inhibitor: results from phase1 single and multiple ascending dose studies in healthy young and older volunteers. *Alzheimer's & Dementia: The Journal of the Alzheimer's Association 13* (7), P575-P576.

41. Lee, J. A.; Osmanovic, S.; Viana, M. A.; Kapur, R.; Meghpara, B.; Edward, D. P. Objective measurement of periocular pigmentation. *Photodermatology, photoimmunology & photomedicine* **2008,** *24* (6), 285-90.

42. Kalvass, J. C.; Maurer, T. S.; Pollack, G. M. Use of plasma and brain unbound fractions to assess the extent of brain distribution of 34 drugs: comparison of unbound concentration ratios to in vivo P-glycoprotein efflux ratios. *Drug Metab. Dispos.* **2007,** *35* (4), 660-666.

43. Kutchinsky, J.; Friis, S.; Asmild, M.; Taboryski, R.; Pedersen, S.; Vestergaard, R. K.; Jacobsen, R. B.; Krzywkowski, K.; Schroder, R. L.; Ljungstrom, T.; Helix, N.; Sorensen, C. B.; Bech, M.; Willumsen, N. J. Characterization of potassium channel modulators with QPatch automated patch-clamp technology: system characteristics and performance. *Assay Drug Dev. Technol.* **2003,** *1* (5), 685-693.

Table of Content Graphics

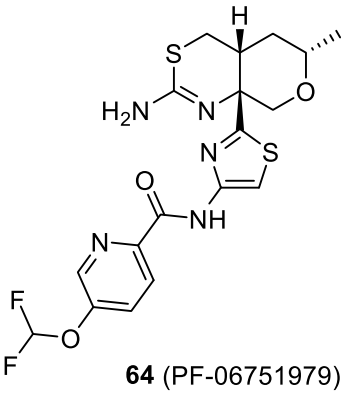

64 (PF-06751979)
BACE1 IC_{50} = 7.3 nM
BACE2 IC_{50} = 193 nM (**27x**)
Completed Ph1 Clinical Trials

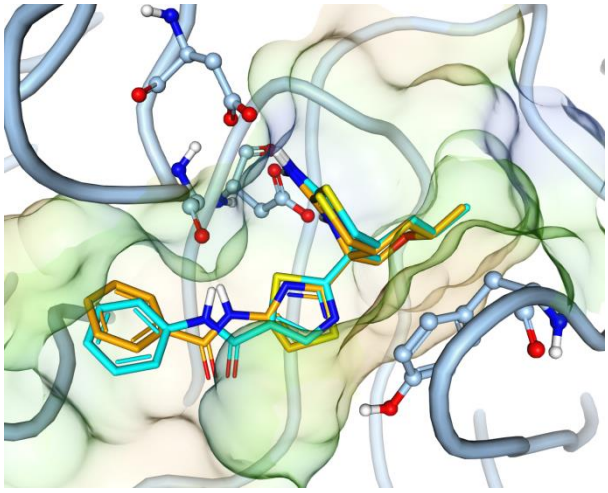

High BACE2 Selectivity of **64**
→ Reduced hypopigmentation

64

3 (non-selective)